OXYANIONS IN INDUSTRIAL WASTE AND WASTEWATER

FORMATION, LEACHING AND ADSORPTION

Bram Verbinnen

Supervisors:
Prof. Dr. Carlo Vandecasteele
Prof. Dr. Chantal Block

Members of the Examination Committee:
Prof. Dr. Ir. Patrick Wollants
Prof. Dr. Ir. Bart Van der Bruggen
Prof. Dr. Ir. Jan Degrève
Prof. Dr. Ir. Christopher Cheeseman
Dr. Ir. Andres Van Brecht

Dissertation presented in partial fulfilment of the requirements for the degree of Doctor in Engineering Science

January 2014

Uitgegeven in eigen beheer, Bram Verbinnen, W. De Croylaan 46, 3001 Leuven, Belgium

ISBN 978-94-6018-786-5
D/2014/7515/10

Dankwoord

Een kleine zeven jaar geleden kreeg ik van mijn toenmalige thesispromotor op Groep T, professor Chantal Block, de vraag of ik na mijn studies geen zin had om projectmedewerker te worden aan de KU Leuven, onder leiding van professor Carlo Vandecasteele. Lang heb ik hier niet over getwijfeld, tijdens mijn thesis was het me immers duidelijk geworden dat het wetenschappelijk onderzoek me wel lag. De volgende drie jaren kon ik me dan ook verdiepen in verschillende bedrijfsprojecten, voornamelijk gericht op het beheersen van zware metalen en/of oxyanionen in vaste afvalstoffen. Gaandeweg ontwikkelde ik mijn praktische en theoretische kennis, tot het moment was gekomen waarop ik besloot om met behulp van deze bagage een doctoraat te behalen. De basis van mijn doctoraatsproject vormden twee industriële projecten, waar ik me verder in kon verdiepen. Uiteraard zijn er tijdens een doctoraat altijd tegenslagen te verwerken en duiken er nieuwe uitdagingen op, maar al bij al verliep alles vrij vlot, zodat ik nu vol trots mijn doctoraat kan presenteren.

Dat alles zo goed verliep was niet mogelijk geweest zonder de steun van mijn promotoren, die ik hierbij dan ook uitdrukkelijk dank: professor Carlo Vandecasteele, altijd gedreven, geïnteresseerd in elk mogelijk klein en groot probleem, en steeds motiverend, zorgde er voor dat dit werk een gefundeerd geheel werd. Professor Chantal Block zag in mij een potentieel wetenschappelijk onderzoeker en bleef mij steeds verder motiveren en mijn werk kritisch bekijken.

De twee andere leden van mijn begeleidingscommissie, professoren Jan Degrève en Bart Van der Bruggen, dank ik voor hun constructieve opmerkingen en commentaren. Jurylid Andres Van Brecht ben ik dankbaar voor de prettige samenwerking doorheen de jaren en de mogelijkheden die hij bood om projecten voor Indaver NV uit te voeren. Ook professor Christopher Cheeseman zou ik willen bedanken

als jurylid; zijn werk omtrent lichtgewicht aggregaten was zeker een voedingsbodem voor dit onderzoek.

Het werkleven is natuurlijk meer dan alleen experimenteren, analyseren, projecten uitvoeren en een doctoraat schrijven. Even belangrijk zijn de collega's met wie je je dagen doorbrengt. Ik zou alle collega's met wie ik gedurende meer dan 6 jaar op CIT heb samengewerkt willen danken voor het draaglijk maken van de lange uren in het labo, voor de toffe babbels tijdens de lunch en de koffiepauzes, en voor de leuke momenten, soms ook buiten het werk.

Enkele mensen zou ik speciaal willen bedanken. Jo Van Caneghem, zes jaar zaten we samen in dezelfde bureau, en je zag me evolueren van de jonge schoolverlater tot de onderzoeker die ik nu ben. Pieter Billen, ik ben er zeker van dat de discussies die we vaak hebben gevoerd mijn, en hopelijk ook jouw werk, naar een hoger niveau hebben getild: een tekening op het bord, erover discussiëren, even laten bezinken en de volgende ochtend met nieuwe ideeën en inzichten komen, bedankt voor de fijne samenwerking. Siavash Darvishmanesh, in ons onderzoek hadden we weinig raakvlakken, maar toch heb je me zeker wat dingen kunnen leren: een fijne selectie van de Iraanse keuken, dansbewegingen of scheldwoorden. Isabel Vermeulen, Michèle Vanroelen, Herman Tollet, Alena Vaes, Marie-Claude Deflem en Beatrice De Geest: bedankt voor de aangename momenten en/of de ondersteuning tijdens het werk.

Een woord van dank is zeker ook passend voor de thesisstudenten die ik heb begeleid: Dries, Stijn, Sander, Lenny, Michiel en Hans. Ik vond het zeer leuk om jullie te ondersteunen, en misschien zien jullie je vele uren in het labo nu ook deels gevaloriseerd in dit werk.

Ik heb ook steeds met minstens evenveel enthousiasme bijgedragen aan de vele industriële projecten die door onze onderzoeksgroep werden uitgevoerd. Enkele industriële partners wil ik speciaal

vermelden voor de uitdagende opdrachten die een basis vormden voor dieper onderzoek in mijn doctoraat. Dankzij Indaver NV (Guido Wauters en Andres Van Brecht) kwam ik in nauw contact met de afvalverwerking, en meer specifiek met de uitdagingen die oxyanionen stellen in vaste afvalresidu's en afvalwater. Het was ook goed samenwerken met Stefan en Etienne, mede door hun vooruitstrevende visie op het aanpakken van de afvalproblematiek. Ook de andere industriële partners en collega's van buitenlandse universiteiten met wie ik heb samengewerkt, voor en tijdens mijn doctoraat, wil ik hier bedanken.

Ik moet er wellicht niemand van overtuigen dat het leven buiten het werk voor mij minstens even belangrijk is als het leven op het werk. Ontspanning na het werk is de ideale manier om de beslommeringen die een doctoraat met zich meebrengt even te vergeten. Met mijn vrienden van op de 501 heb ik gedurende vele jaren lief en leed gedeeld, prachtige momenten die ik nooit zal vergeten! Sport was misschien wel de grootste bron van ontspanning voor mij, dus hulde aan alle Bosgrondjes, en aan alle anderen met wie ik me kon uitleven in de natuur, of het nu fietsen, lopen, klimmen, zwemmen, (toer)skiën of tennissen was! Ook de mooie momenten met mijn studiegenoten in Leuven en daarbuiten zullen mij nog lang bijblijven.

Mijn ouders, zussen en familie wil ik mijn dankbaarheid betuigen om mij zoveel mogelijkheden te bieden en me te maken tot wie ik nu ben.

Maartje, mijn laatste maar zeker belangrijkste woorden van dank zijn voor jou. We hebben samen al zo veel mooie momenten beleefd, zowel hier als op onze reizen, maar het is maar in de momenten dat ik het wat moeilijker heb, dat ik ten volle besef wat je voor mij betekent. Dank je om er altijd voor mij te zijn!

Bram

Januari 2014

Abstract

Oxyanion forming elements like As, Cr, Mo, Sb and Se are toxic and their occurrence and distribution in the environment must therefore be prevented as much as possible. Some industrial projects that were started during the last 6-7 years in our laboratory showed that there was still a lack of knowledge on oxyanion forming elements and of the practical implementation of such knowledge. For some oxyanions, increased concentrations were observed in the leachate when contaminated solid residues were heated in order to obtain a structured product. This could not be explained satisfactorily on the basis of existing results in literature. Furthermore, oxyanions also pose problems when they are present in industrial wastewaters, but the existing literature on removal of oxyanions from water by adsorption is mainly limited to their removal from synthetic solutions. The aim of this thesis is to control the formation and subsequent leaching of oxyanions during high temperature processes and to study the removal of oxyanions from industrial wastewater. Thus, the possibilities to treat and recycle industrial solid residues will be increased and there will be more options available for treating industrial wastewaters.

Experiments with synthetic mixtures were performed to study the influence of process conditions like temperature and residence time on the formation and leaching of Cr and Mo oxyanions. Slightly soluble Cr(III) compounds can be oxidized to mobile and toxic Cr(VI) compounds in the presence of alkali and alkaline earth salts. No spontaneous oxidation was observed in the ambient atmosphere, but when Ca, Na or K salts were added, up to 80 % of Cr(III) was oxidized to Cr(VI) and leached. The leached amount of Cr reached a maximum at around 600 – 800 °C, after which the leaching decreased again. This could be explained by the formation of a binary mixture of

the newly formed chromates with SiO_2, which became amorphous upon cooling and thus prevents the Cr leaching.

To check the plausibility of these findings for real situations, two industrial solid residues that could possibly be valorized by thermal treatment, were heated under the same conditions as the synthetic samples. The leaching of Cr from sludge obtained after cleaning of contaminated soils and from the sand fraction of bottom ash from municipal solid waste incineration showed a similar leaching behavior as a function of temperature as the synthetic samples. The leaching of Mo from contaminated sludge increased as a function of temperature and could be attributed to the initial presence and subsequent oxidation of MoS_2, a solid lubricant that is often used in mineral oils. When pure MoS_2 samples were heated as a function of temperature, the observed leaching behavior was similar to that of the sludge. The leaching of Mo from the sand fraction of bottom ash showed a decrease, similar to that observed for Cr, which could probably also be attributed to the formation of an amorphous phase of the molybdates with SiO_2.

Another aim of this thesis was to develop an adsorbent that can be used for the adsorption of oxyanions from real industrial wastewaters; as an example the method was applied on the scrubber effluent of a waste incinerator for hazardous waste. First, an adsorbent described in literature, zeolite-supported magnetite, was characterized and tested for the simultaneous removal of Mo, Sb and Se oxyanions from a synthetic solution. A lot of attention was paid to elements that can possibly interfere with oxyanion adsorption from industrial wastewaters. Then, the simultaneous adsorption of Mo, Sb and Se from the scrubber effluent was studied, which showed that mainly Mo and Sb can be removed with a high efficiency.

To improve the adsorbent without losing its good adsorption characteristics, efforts were made to improve the coating of magnetite on the support material. As the coating of magnetite on zeolite was not optimal, it was opted to develop a new adsorbent with perlite as support material. Perlite-supported magnetite was characterized first by determining its specific surface area (55.3 m^2/g), magnetite content, and the ideal pH for oxyanion adsorption (pH 3 – 5). Then, the simultaneous removal of As, Cr, Mo, Sb and Se from a synthetic solution was tested, and the adsorption order was determined to be Mo(VI) > As(V) > Sb(V) > Cr(VI) > Se(VI). It could also be concluded that with relatively low adsorbent dosages (1 g/l) most oxyanions could be removed for more than 75 % from an equimolar solution (2 mmol/l) containing all 5 elements. Finally, the adsorption of oxyanions from the scrubber effluent was tested. The presence of interfering compounds changed the adsorption order compared to that of the synthetic water and a higher adsorbent dosage was needed to remove the oxyanions. However, perlite-supported magnetite can still be used to remove oxyanions from industrial wastewater, especially when the main pollutants are Mo and/or Sb.

In this PhD, it was studied how the distribution to the environment of oxyanions from solid residues from high temperature processes and from industrial wastewaters can be avoided or decreased. The mechanism responsible for the formation of oxyanions during high temperature processes was clarified and a new adsorbent material for removal of oxyanions from industrial wastewater was developed.

Samenvatting

Oxyanion vormende elementen zoals As, Cr, Mo, Sb en Se zijn toxisch, en daarom moet hun verspreiding in het milieu zo veel mogelijk voorkomen worden. Enkele industriële projecten die de laatste 6-7 jaar in ons labo werden opgestart, toonden aan dat er nog steeds een gebrek aan kennis bestond over deze elementen, en vooral over praktische toepassing van deze kennis. Voor enkele van deze elementen werden verhoogde uitloogconcentraties waargenomen wanneer gecontamineerde vaste residu's werden verwarmd om ze om te zetten in een bouwstof. Deze verhoogde uitloogconcentraties konden niet worden verklaard aan de hand van de bestaande literatuur. Anderzijds kunnen oxyanionen ook problemen stellen wanneer ze aanwezig zijn in industriële afvalwaters, maar de literatuur over de verwijdering van oxyanionen uit water via adsorptie is voornamelijk gericht op synthetisch water. Het doel van deze thesis is om de vorming van oxyanionen tijdens hoge temperatuursprocessen te begrijpen en te controleren, en om de adsorptie van oxyanionen uit industrieel afvalwater te bestuderen.

Om de invloed van procescondities zoals temperatuur en verblijftijd op de vorming en uitloging van oxyanionen van Cr en Mo te bestuderen, werden experimenten met synthetische stalen uigevoerd. In de aanwezigheid van zouten van alkali- en aardalkalimetalen bleek dat het slecht oplosbare driewaardig Cr kan worden geoxideerd tot het meer mobiele en toxische zeswaardig Cr. De oxidatie gebeurde niet spontaan in de aanwezigheid van omgevingslucht, maar wanneer Ca, Na of K-zouten werden toegevoegd werd tot 80 % van het driewaardige Cr geoxideerd en vervolgens uitgeloogd als zeswaardig Cr. Na het bereiken van een maximum rond 600 – 800 °C, daalde de Cr uitloging uit de synthetische stalen weer. Dit kon verklaard worden door de vorming van een binair mengsel van de gevormde chromaten

met SiO_2, dat amorf wordt na afkoeling en daardoor de uitloging van Cr voorkomt.

Om de juistheid van deze bevindingen te testen voor reële stalen, werden twee industriële vaste residu's, die mogelijk kunnen gevaloriseerd worden door thermische behandeling, verwarmd onder dezelfde omstandigheden als de synthetische stalen. De uitloging van Cr uit slibs van de grondreiniging van verontreinigde bodems en van de zandfractie van bodemas van de verbranding van huishoudelijk vast afval vertoonde een gelijkaardig uitlooggedrag in functie van de temperatuur als de synthetische stalen. De uitloging van Mo uit de verontreinigde slibs verhoogde in functie van de temperatuur en is te wijten aan de aanwezigheid van MoS_2, een smeermiddel dat vaak voorkomt in minerale oliën. Experimenten met puur MoS_2 toonden aan dat het slecht oplosbare Mo(IV) wordt geoxideerd tot mobiele Mo(VI) verbindingen wanneer het verhit wordt en dat het uitlooggedrag in functie van de temperatuur vergelijkbaar is met dat van de slibs. De uitloging van Mo uit de zandfractie van bodemas vertoonde bij hoge temperaturen een daling, net zoals voor Cr, wat waarschijnlijk ook te wijten is aan de vorming van een amorfe fase van molybdaten met SiO_2.

Een ander doel van deze thesis was om een adsorbens te ontwikkelen dat kan gebruikt worden voor de adsorptie van oxyanionen uit reëel afvalwater; als voorbeeld werd hiervoor het effluent van de scrubber van een afvalverbrandingsoven voor gevaarlijk afval gebruikt. Eerst werd een bestaand adsorbens, zeolite-supported magnetite, gekarakteriseerd en getest voor de verwijdering van oxyanionen van Mo, Sb en Se uit een synthetisch water. Daarbij werd veel aandacht geschonken aan de mogelijke interferenties die kunnen optreden in reële afvalwaters. Daarna werd de simultane adsorptie van de drie

elementen uit het effluent van de scrubber onderzocht, waaruit bleek dat voornamelijk Mo en Sb efficiënt konden verwijderd worden.

Vervolgens werd er getracht om het adsorbens verder te verbeteren, zonder de goede adsorptiekarakteristieken te verliezen. De hechting van magnetiet op het dragermateriaal zeoliet was niet optimaal, daarom werd geopteerd om perliet als dragermateriaal te gebruiken. Het nieuw ontwikkelde adsorbens werd eerst grondig gekarakteriseerd door het bepalen van het specifieke oppervlak (55.3 m^2/g), magnetiet gehalte (13%) en de ideale pH voor adsorptie van oxyanionen (pH 3 – 5). Vervolgens werd er getracht om oxyanionen van As, Cr, Mo, Sb en Se simultaan te verwijderen uit een synthetische oplossing, waardoor de adsorptievolgorde kon worden bepaald (Mo(VI) > As(V) > Sb(V) > Cr(VI) > Se(VI)). Er kon worden besloten dat met relatief lage adsorbensconcentraties (1 g/l) de meeste oxyanionen voor meer dan 75 % konden worden verwijderd uit een equimolaire (0.02 mmol/l) oplossing. Tenslotte werd de adsorptie van de oxyanionen uit het effluent van de scrubber getest. Door de aanwezigheid van interferenties werd de adsorptievolgorde gewijzigd t.o.v. het synthetisch water. Ook waren er over het algemeen hogere adsorbensconcentraties nodig om de oxyanionen te verwijderen, maar toch kan worden gesteld dat perlite-supported magnetite in staat is om oxyanionen te verwijderen uit reëel afvalwater, vooral wanneer Mo en/of Sb de voornaamste polluenten zijn.

In deze doctoraatstekst werd onderzocht hoe de verspreiding van oxyanionen uit vaste residu's van hoge temperatuursprocessen en industriële afvalwaters kan tegengegaan of verminderd worden. De mechanismes verantwoordelijk voor de vorming van oxyanionen tijdens hoge temperatuursprocessen werden verklaard en er werd een nieuw adsorbens ontwikkeld dat in staat is oxyanionen te verwijderen uit industrieel afvalwater.

List of abbreviations

ADPC	Ammonium Pyrrolidine Dithiocarbamate
BAT	Best Available Technology
CERCLA	Comprehensive Environmental Response, Compensation, and Liability
EDTA	Ethylenediaminetetraacetic Acid
FGCR	Flue Gas Cleaning Residue
HFO	Hydrous Ferric Oxides
IC	Ion Chomatography
ICP-MS	Inductively Coupled Plasma – Mass Spectroscopy
L/S	Liquid to Solid ratio (l/kg)
LoW	List of Waste
MSW	Municipal Solid Waste
PC	Portland Cement
PAH	Polycyclic Aromatic Hydrocarbons
PCB	Polychlorinated Biphenyls
PE	Polyethylene
pH_{PZC}	pH value at the Point of Zero Charge
PSO	Pseudo-Second Order
SEM	Scanning Electron Microscopy
SOM	Soil Organic Matter
TLM	Triple Layer Model
TMT	Trimercaptotriazine
US EPA	United States Environmental Protection Agency
WHO	World Health Organization
XRD	X-Ray Diffraction

List of symbols

ΔG_r	Reaction Gibbs free energy (kJ/mol)
σ	Surface charge ($\mu C/cm^2$)
ψ	Surface potential (mV)
b	Parameter in the equation of the Langmuir isotherm (l/mg)
C_1	Inner layer capacitance (F/m^2)
C_2	Outer layer capacitance (F/m^2)
C_e	Residual concentration at equilibrium (mg/l)
h	Initial adsorption rate (mg/g·h)
k	Parameter in the equation of the Freundlich isotherm (l/g)
	Rate constant in the pseudo-second order kinetic model (g/mg·h)
1/n	Parameter (Freundlich isotherm) for the adsorption strength (dimensionless)
$t_{1/2}$	Reaction half life (h)
Q_e	Adsorbed amount per gram adsorbent at equilibrium (mg/g)
Q_{max}	Maximum adsorption capacity (mg/g)
Q_t	Adsorbed amount per gram adsorbent at time t (mg/g)

Table of contents

1. Introduction

Since 1991, research on waste treatment and on recycling and energetic valorization of waste streams has been carried out at the Division of Process Engineering for Sustainable Systems (the former Lab of Applied Physical Chemistry and Environmental Technology) at the Department of Chemical Engineering of the KU Leuven. The research focused on the stabilization/solidification of high temperature residues like metallurgical slags and fly and bottom ashes from MSWI incineration. In several residues from high temperature processes, high concentrations of cation forming heavy metals like Zn, Ni, Cu and Pb, and/or oxyanion forming elements like As, Cr, Mo, Sb and Se are found in the leachates. Theoretical knowledge on reducing their leached concentrations to meet the increasingly stringent regulatory limit values was built up through the years.

Some industrial projects that were started during the last 6-7 years in our laboratory showed that there was still a lack of knowledge on oxyanion forming elements and of the practical implementation of such knowledge. For instance, the leachate of contaminated sludge shows high concentrations of Cu, Ni and Zn, and can therefore not be recycled, but should be deposited on a landfill at high cost. A method was developed to treat the sludge, which resulted in both environmental (reduction of the leached concentrations) and economical (reduced costs for landfilling) benefits. After the treatment, which consisted of a heat treatment to produce aggregates, increased concentrations of some oxyanion forming elements were however observed in the leachate, which could not be explained satisfactorily on the basis of existing results in literature. Similar behavior (increased leaching of oxyanions) was observed when the sand fraction of bottom ash was treated thermally in view of recycling.

A better understanding of this leaching could lead to an environmentally more benign process.

Furthermore, oxyanions also pose problems when they are present in industrial wastewaters. These wastewaters are often effluents from high temperature processes, in which the oxyanions end up after leaching from the residues. Here also, some knowledge exists on the removal of oxyanions from synthetic waters, but examples of the removal of oxyanions from real industrial wastewaters are scarce.

The aim of this PhD thesis is to control the formation and subsequent leaching of oxyanions during high temperature processes and to study the removal of oxyanions from industrial wastewater. In this introduction, the research of this PhD thesis will be put in a broader context. First, the regulations concerning oxyanions in waste and wastewater in Europe are given. Then, the state of the art on the two main topics, leaching of oxyanions from residues of high temperature processes and the removal of oxyanions from wastewater by adsorption, is presented. Based on the literature search about this state of the art, the knowledge gaps for these two topics are identified. They form the basis for the research aims and objectives of this thesis. The methods that are used for this research are described briefly.

1.1 General framework

Cr and As oxyanions have since long been recognized as priority pollutants by the US EPA, but other oxyanion forming elements like Sb, Se, Mo, V and W are nowadays also considered ‘emerging pollutants’: compounds that have gained increasing interest during recent years from an environmental point of view due to their moderate to high toxicity (Vandecasteele and Cornelis, 2010). The increased interest for oxyanion forming elements can be demonstrated

by the fact that several legislations have been adapted recently to include or decrease limit values for total or leached concentrations of oxyanion forming elements in or from waste. An overview is presented here on the relevant legislations, focusing on the oxyanion forming elements for which the limit values were lowered recently.

In January 2011, new or lower limit values were included in the Flemish "basic quality standards for surface water", as an implementation of the European Water Framework Directive (2000/60/EC). This regulation stipulates concentrations for toxic elements in industrial wastewaters that are discharged into surface waters (the emission is measured at the point where it leaves the installation, so dilution is disregarded). If these concentrations are exceeded, the wastewater is considered hazardous and the company cannot discharge the wastewater as such, but should try to lower the concentrations and/or apply for an environmental emission permit with appropriate discharge limits. Wastewater with pollutant concentrations higher than those set in the environmental emission permit require treatment prior to discharge. For Se, the concentration in the regulation was lowered from 10 to 3 µg/l (i.e. the limit value for drinking water set by the WHO). For Mo, Sb and V, there were no previous criteria, but in 2011 the concentrations were set at 350, 100 and 5 µg/l, respectively. The concentration for As was lowered from 30 to 5 µg/l and for Cr it remained unchanged at 50 µg/l. The lowered concentrations indicate a growing concern about the distribution of these oxyanion forming elements in the environment, but the specific wastewater considered in this thesis (the scrubber effluent of an incinerator for hazardous waste) is not subjected to this regulation. The scrubber effluent is classified by the European List of Waste (LoW, 2000/532/EC) under the code 19 01 06*. The asterisk indicates that the waste stream is classified as hazardous. As the wastewater is produced by a waste incinerator, it is subject to the European Waste

Incineration Directive (2000/76/EC), and therefore a permit should always be granted by the competent authorities.

In the European Council Decision 2003/33/EC criteria for landfilling hazardous or non-hazardous waste are established. The leaching limit values for the acceptance of granular waste on four types of landfills (i.e. a landfill for inert waste, for non-hazardous waste, for hazardous waste that can be accepted on a landfill for non-hazardous waste and for hazardous waste) calculated for a liquid to solid ratio (L/S) of 10 l/kg are shown in Table 1.1 for the oxyanion forming elements As, Cr, Mo, Sb and Se.

In Flanders, leaching limits with regard to the use of materials in or as building material include two oxyanion forming elements: As and Cr. For As, this value is 0.8 mg/kg and for Cr it is 0.5 mg/kg, comparable to the limit values for the disposal of waste on a landfill for inert waste. These limit values must be met when using solid waste materials like bottom ash or contaminated soils in construction applications.

Table 1.1: Leaching limits (mg/kg dry matter, L/S 10) for As, Cr, Mo, Sb and Se for acceptance of waste on landfills according to the European Council Decision 2003/33/EC.

Element (mg/kg)	As	Cr	Mo	Sb	Se
Inert	0.5	0.5	0.5	0.06	0.1
Non-hazardous	2	10	10	0.7	0.5
Hazardous on non-hazardous	2	10	10	0.7	0.5
Hazardous	25	70	30	5	7

This thesis focuses on the prevention, immobilization and/or treatment of oxyanions occurring in an industrial environment. Oxyanions in solid wastes often occur in residues from high temperature processes

like thermal treatment of waste, fossil fuel combustion and metallurgy; such as bottom ash, fly ashes, and slags. The mechanisms responsible for the formation of mobile Cr and Mo oxyanions during thermal processes are studied in this thesis. These two elements are of special interest, as high leaching concentrations were observed during an industrial project, the thermal treatment of contaminated sludge, which made the sludge unsuitable to be used as a secondary construction material. Based on literature review, it can be stated that elevated Cr and Mo leaching had been often observed after thermal processes, but its origin is not fully understood.

In water, the presence of oxyanions mostly relates to the weathering of natural rocks or the leaching from mining residues or other industrial solid wastes. Oxyanions occurring in natural waters or wastewaters from industrial processes should be removed from the water to prevent them from polluting the environment or because their concentrations exceed discharge limits. Several studies have already been carried out on the removal of oxyanions from water, but most of them mainly focus on synthetic waters containing little or no interferences. In this work, an existing adsorbent will be tested for the removal of oxyanions from a real industrial wastewater: zeolite-supported magnetite, developed by the Institute of Geotechnics (Kosice, Slovakia) and which has already been tested for the removal of As and Cr from synthetic solutions. During the experiments, it became clear that the coating of magnetite onto the zeolite was not optimal. Therefore, several other support materials were tested, and perlite was selected as the best. The newly developed adsorbent, perlite-supported magnetite, was then also tested for the removal of oxyanions from synthetic and industrial wastewaters. The main focus in this thesis is on the removal of Mo, Sb and Se oxyanions. These three elements are present in the scrubber effluent of an incinerator for hazardous waste, and an appropriate treatment to remove them from the effluent should

be developed. When perlite-supported magnetite was tested as adsorbent, the removal of As and Cr oxyanions was also considered.

1.2 State of the art – Literature overview

The main industrial sources of oxyanions are solid residues from high temperature processes and wastewaters from leaching or washing of solid residues. Therefore, treatment of oxyanions should focus on these two types of waste. The state of the art knowledge on these two main industrial sources of oxyanions in the environment is given here. The leaching of oxyanions (i.e. Cr and Mo) after thermal treatment processes is discussed by summarizing relevant data from literature and up-to-date knowledge on the responsible mechanisms. The relevant literature on the removal of oxyanions from (waste)waters by adsorption is also summarized. This will allow discovering the knowledge gaps on these topics.

1.2.1 Leaching of oxyanions from thermally treated waste

Occurrence of oxyanions in solid residues

Cr is used in various industries, such as the metallurgical industry (steel, ferro and non-ferrous alloys), refractories (chrome and chrome-magnesite) and the chemical industry (pigments, electroplating, tanning,…) (Kotas and Stasicka, 2000). Like Cr, Mo is mainly used in metallurgical applications due to its high corrosion resistance and ability to withstand high temperatures. Molybdenum disulfide (MoS_2) is used as a high temperature, high pressure resistant antiwear agent in solid lubricants. An important source for As in solid residues is burning of fossil fuels in power plants, where As mostly ends up in the fly ash (Bissen and Frimmel, 2003). Se is used in glassmaking, in the production of solar cells and in pigments. Sb is mainly used as a fire

retardant, or as an alloy, for instance in bullets or batteries. Typical concentrations of As, Cr, Mo, Sb and Se in MSWI bottom ash, coal bottom ash and steels slag are shown in Table 1.2 (Cornelis et al., 2008).

Table 1.2: Typical concentrations (in mg/kg) of As, Cr, Mo, Sb and Se in MSWI bottom and fly ash, coal bottom and fly ash, and steel slag (adapted from Cornelis et al., 2008).

Element (mg/kg)	MSWI bottom ash	MSWI fly ash	Coal bottom ash	Coal fly ash	Steel slag
As	0.1-200	40-300	0.02-200	2-400	5
Cr	20-3000	100-1000	0.2-6000	4-900	8000-30000
Mo	2-300	15-200	1-500	1-100	20
Sb	10-400	300-1000	NA	NA	NA
Se	0.05-10	0.4-30	0.1-10	0.2-100	NA

NA = not available

Thermal treatment of waste

Waste streams are thermally treated to remove, destroy or immobilize toxic components present in the waste. Organic pollutants, like polycyclic aromatic hydrocarbons (PAHs), solvents, pesticides and PCBs can be removed from contaminated soils by thermal desorption (Zhang and Xu, 2011, Timberlake and Garbaciak, 1995) and are subsequently destroyed. If leaching of heavy metal cations like Cu^{2+}, Ni^{2+}, Pb^{2+} and Zn^{2+} exceeds regulatory limit values, this is often related to the presence of humic substances (mainly humic and fulvic acids) in the waste, as the humic substances form mobile organo-metallic complexes with cations of Cu, Pb, Ni and Zn (Pandey et al., 2000). Removal or destruction of organic substances by thermal treatment decreases the leaching of toxic cations.

Thermal treatment can also be used to obtain a structured product that can be used in or as construction material (Hyks et al., 2011, Van Gerven et al., 2006, Bethanis et al., 2004, Cheeseman et al., 2005, Selinger et al., 1997). Typical examples of waste streams that can be recycled in this way are sewage sludge, dredging sediments, bottom ashes and fly ashes from coal combustion or MSW incineration (Cheeseman et al., 2005, Bethanis et al., 2004, Hyks et al., 2011). Commercial products that can be obtained from such treatment are mainly ceramics: floor and roof tiles, bricks and (lightweight) aggregates. A distinction should be made between sintered and vitrified products, and glass-ceramics. Sintered materials are produced at temperatures below the melting temperature of the material; the individual grains are fused together at their contact points, creating one solid piece. Vitrification occurs at temperatures above the melting point of the material: the material is melted first and then rapidly cooled so that an amorphous material is obtained. As vitrification transforms a material into a glass, the contaminants are trapped into an amorphous glass phase and are thereby prevented from leaching. Vitrification is for instance used to immobilize radioactive waste, but requires substantially more energy than sintering. Glass-ceramics contain both amorphous and crystalline phases, with the amount of crystalline phases typically ranging between 30 and 90 %. They are produced by forming a glass, which is reheated to partially crystallize the glass again.

Leaching of Cr and Mo after thermal treatment of waste streams

After thermal treatment of waste streams that contain organic compounds, leaching of cation forming heavy metals like Cu, Ni, Pb and Zn decreases in most cases due to destruction of the organic compounds that can form soluble organo-metallic complexes with

these cations. However, some authors also observed increased Cr and/or Mo leaching after such thermal treatment.

Leaching of Cr

Chang et al. (2007) produced lightweight aggregates by sintering metal sludge from industrial wastewater treatment plants mixed with mining residues between 850 and 1250 °C. They performed a sequential extraction of the sintered material and observed a maximum concentration of 89.6 mg/kg of water-extractable Cr at 950 °C, compared to 5.4 mg/kg for the untreated material. At temperatures above 950 °C, the water-extractable Cr concentration decreased again, to a value of 2.0 mg/kg at 1250 °C. Xu et al. (2008) produced ceramsite (a type of lightweight aggregate) by using sewage sludge with a high concentration of Cd, Cr, Cu and Pb as an additive in the production process (no information was given on the added percentage or on the other components that make up the mixture). At 850 °C, they observed a maximum in Cr leaching, which decreased at higher temperatures.

Elevated Cr leaching was also observed for residues from other types of thermal processes: the combustion of coal, biomass and municipal solid waste. Abbas et al. (2001) observed elevated Cr(VI) leaching in the bottom ash of a municipal solid waste (MSW) fluidized bed incinerator working at temperatures between 780 and 850 °C; the measured values were 3 orders of magnitude higher than those in the hopper, cyclone and filter ashes. Hyks et al. (2011) performed an additional treatment of bottom ashes from MSW incineration in a rotary kiln at 930 and 1080 °C to improve the leaching quality of the ashes. However, they found an increase in Cr leaching of more than two orders of magnitude compared to the untreated ashes.

To simulate the Cr leaching after thermal treatment of fly ash in view of using it as construction material, Wang et al. (2001) spiked fly ash samples of MSW incineration with 5 % Cr_2O_3 and heated it in various atmospheres at temperatures between 600 and 1000 °C. Cr leaching of the unspiked fly ash was at its maximum value at 900 °C and decreased again at higher temperatures. For the spiked samples, Cr leaching was maximal at 800 °C in ambient atmosphere; heating under N_2 atmosphere did not increase Cr leaching significantly. Hu et al. (2013) also reheated fly ash from MSW incineration and observed higher Cr concentrations in the leachate upon heating. Stam et al. (2011) did a speciation of Cr in coal and biomass (e.g. meat and bone mill, sewage sludge, wood,…) co-combustion products, and found the highest Cr(VI) percentages (up to 16 % of the total Cr amount) after cofiring wood.

Also during the production of cement, leaching of Cr poses problems. Vangelatos et al. (2009) produced Portland Cement (PC) by mixing limestone and sandstone with 1, 3 or 5 % of red mud. After heating at 1450 or 1550 °C, 32 to 35 % of the Cr initially present was converted into water soluble Cr. Sinyoung et al. (2011) studied the Cr behavior during cement production and concluded that Cr containing wastes should not be mixed with raw materials in the cement manufacturing process, as this caused Cr leaching from clinker to exceed the limits set by the US EPA. Chen et al. (2012) also observed limit values exceeding the regulatory limits, when Cr bearing sludge was used to produce clinker under oxidizing atmosphere.

These studies show that in multiple domains, increased Cr leaching is observed after thermal treatment. Several authors suggest that the increase in Cr leaching can be attributed to oxidation of slightly soluble Cr(III) compounds to mobile Cr(VI) compounds, as increased Cr leaching was observed under oxidizing conditions, but not under

inert atmosphere (Wang et al. 2001, Chen et al. 2012). The oxidation of Cr(III) cannot occur in ambient atmosphere alone, as reaction (1) is thermodynamically not feasible (i.e. has a positive ΔG^0 value) at temperatures below 1500 °C.

$$Cr_2O_3 + 3/2\ O_2 \leftrightarrows 2\ CrO_3 \quad (1)$$

Some authors suggest reactions including alkali and alkaline earth salts for the oxidation of Cr(III) to Cr(VI), more specifically in the presence of Ca (Paoletti, 2002, Stam et al., 2011, Hu et al., 2013, Kirk et al., 2002) and K (Wang et al., 2001, Lehmusto et al., 2012, El-Hasan et al., 2011), according to reactions similar to (2) and (3):

$$Cr_2O_3 + 2\ CaO + 3/2\ O_2 \leftrightarrows 2\ CaCrO_4 \quad (2)$$

$$Cr_2O_3 + 4\ KOH + 3/2\ O_2 \leftrightarrows 2\ K_2CrO_4 + 2\ H_2O \quad (3)$$

Little is known about the thermodynamics and kinetics of these reactions, and the papers cited above describe the reactions (2) and (3) as the reactions responsible for increased Cr formation, but do not consider temperature dependency, nor the influence of heating time. They only describe Cr leaching at one fixed temperature, or in a relatively small temperature interval. Furthermore, the reactions with different alkali or alkaline earth salts have not been compared so far.

Several papers cited above also report a decrease in Cr leaching after the maximum value has been reached. Some explanations for this decrease have been hypothesized, but they are sometimes contradictory and no general mechanism was formulated that could be applied for all described cases. Some authors suggest that the formed Cr(VI) can be reduced to Cr(III), either by more reducing conditions at higher temperatures (Sorensen et al., 2000), or by reducing

compounds in the samples, e.g. metallic aluminum (Astrup et al., 2005, Bodenan et al., 2010, Abbas et al., 2001). It is also hypothesized that solid solution formation of Cr(VI) with ettringite is a possible mechanism to explain the decreased leaching in alkaline solid wastes (Cornelis et al., 2008). At temperatures above the typical sintering temperatures, vitrification occurs, and the amorphous structure that is formed upon cooling can also prevent Cr from leaching (Tuan et al., 2012). The many different mechanisms that are suggested clearly show that the available literature describing the reduced Cr leaching is sometimes incoherent.

Leaching of Mo

Leaching of Mo after thermal treatment of waste streams was less often reported than the leaching of Cr, as Mo concentrations in the leachate are not regulated in some countries and/or for some applications (i.e. it is not regulated in Flanders for use in or as construction material). Both Cr and Mo are in the same group of the periodic system of the elements (Group 6), so their chemical behavior will be similar and it can be expected that increased Mo leaching can occur together with increased Cr leaching.

Alonso-Santurde et al. (2008) observed that for contaminated marine sediments (two types of clay), the Mo leaching had increased after sintering. Gonzalez-Corrochano et al. (2012) sintered mixtures of inorganic sludge and fly ash and also observed increased leaching of Mo (and As, Sb) after sintering. Hyks et al. (2012), who treated bottom ash by heating it in a rotary kiln, observed that Mo leaching had increased 4 times after heat treatment. Quijorna et al. (2012) produced red clay bricks by mixing clay with foundry sand and Waelz slag and firing the mixture; Mo leaching after firing exceeded the limit values. Whereas attempts were made in literature to explain the

increased Cr leaching after high temperature processes, no explanation was found in literature for the increased release of Mo upon heating.

1.2.2 Adsorption of oxyanions from industrial wastewater

Occurrence of oxyanions in water

Cr in surface waters can originate from natural sources, like weathering of rock constituents. Local increases in Cr concentrations in waters can be caused by the discharge of wastewater from the metallurgical industry, electroplating and tanning industries, from dying, sanitary landfill leaching, water cooling towers and from chemical industries (Kotas and Stasicka, 2000). The main source for the occurrence of Mo in waters is discharge of wastewater from the metallurgical industry (Barceloux, 1999). As can end up in (ground) water due to its use as a wood preservative, from weathering of As containing rocks, or from its presence in mine drainage water (Bissen and Frimmel, 2003). Sources of Se in water are agricultural, mining and petrochemical industries. Major sources of Sb in water are discharge from petroleum refineries, fire retardants and electronics (US EPA).

Most industrial sources contributing to the presence of oxyanions in (waste)waters, do not just release only one single oxyanion in the water, but a range of oxyanions along with anions like chlorides, sulphates and phosphates.

Removal of oxyanions from water

Several techniques exist for the removal of oxyanions from water: oxidation/reduction reactions followed by coagulation/ (co)precipitation, adsorption, ion exchange and membrane techniques. The use of oxidation/reduction techniques might be beneficial for one

specific oxyanion forming element (e.g. the oxidation of As(III) to As(V) followed by coprecipitation with $FeCl_3$ (Holm and Wilson, 2006)), but produces toxic sludge. The use of membranes (nanofiltration, reverse osmosis and electrodialysis) and ion-exhange resins to remove oxyanions requires high capital and running costs (Mohan and Pitman, 2007). Although they are capable of removing multiple contaminants at once from a wastewater stream with high removal efficiency, membrane techniques are also prone to fouling when waters with high salt concentrations are treated, as is the case for most industrial wastewaters.

The use of adsorbents is a cheap and simple technique, capable of the simultaneous removal of different oxyanions. Examples of adsorbents that can be used for the removal of oxyanions are activated carbon, manganese oxides, aluminum and titanium based adsorbents, and iron oxides and hydroxides. Activated carbon is a relatively expensive adsorbent, which can readily adsorb organic compounds like PCBs and PAHs, pesticides, dyes and aromatic solvents. Inorganic components do not bind well to activated carbon, and to obtain good removal capacities for e.g. metals and oxyanions, the surface of activated carbon should be pretreated or coated. This can be achieved by impregnating the surface with e.g. iron oxides (Vaughan and Reed, 2005; Chen et al., 2007), or by a modification of the surface by e.g. cationic surfactants (Choi et al., 2009).

Iron oxides and hydroxides can be produced at low-cost and are widely used for the adsorption of oxyanions, as they have a high affinity for oxyanions, but their adsorption efficiency is highest only at low pH (Adegoke et al., 2012, Hua et al., 2012, Gallegos-Garcia et al., 2012). If the adsorbent cannot be regenerated, it must be disposed of as toxic solid waste.

Experiments with adsorbents have been carried out by many authors for several oxyanions. The most studied oxyanion forming element is As, as As is recognized as the number one priority pollutant by the US EPA. The poisoning of water with As is a large problem in many Asian and South American countries like India, Nepal, Bangladesh and Argentina, where many people die due to chronic intake of contaminated water.

In the most comprehensive review article to date on As adsorption (Mohan and Pitman, 2007), an overview is presented of all possible adsorbents that can be used, together with the types of water that have been treated. From the $\pm$ 160 listed experiments (Mohan and Pitman, 2007, Table 5), in only 10 % (16 papers) the authors claim that they can treat industrial wastewaters by adsorption, the others studied the adsorption of As from drinking, ground, spring or tap water or from (synthetic) aqueous solutions, which contain little or no interferences. A more thorough investigation of these 16 papers showed that, although most of these claim that industrial wastewaters can be treated, only experiments with synthetic solutions containing one or two oxyanions were performed. Only two papers (Manju et al., 1998, Navarro and Alguacil, 2002) perform tests with industrial wastewaters or synthetic solutions simulating an industrial wastewater. Navarro and Alguacil did adsorption tests with activated carbon on a copper electrorefining solution containing Cu, As, Sb and SO_4^{2-} and observed a high selectivity for As and Sb, as no Cu or SO_4^{2-} was loaded onto the carbon. Manju et al. adsorbed arsenite using coconut husk carbon from synthetic and industrial wastewaters from the fertilizer industry, containing, amongst others, 3.8 mg/l As(III), 89 mg/l PO_4^{3-}, 66 mg/l NO_3^- and 140 mg/l Cl^-.

Besides As, also other oxyanion forming elements have been studied, albeit less intensively. Results from review articles on adsorption

covering several oxyanions (Adegoke et al. 2013, Gua et al., 2012) indicate that the removal of other oxyanion forming elements is also mostly studied for synthetic aqueous solutions. Xu et al. (2013) reviewed different adsorbents for MoO_4^{2-} removal and it seems that the research had mainly been focused on adsorption from synthetic solutions. A similar review on CrO_4^{2-} removal by Owlad et al. (2009) also mainly describes results from synthetic waters.

Although many papers treat the removal of oxyanions from water by adsorption, little attention is paid to the treatment of industrial wastewaters, but there are many contaminated industrial wastewater for which appropriate treatment techniques are required. Examples of such contaminated wastewaters are leachates from residues from high temperature processes like the thermal treatment of waste (bottom ash, flue gas cleaning residue), fossil fuel combustion or metallurgy (Cornelis et al., 2008).

Adsorption of oxyanions on iron (hydr)oxides

Iron oxides and hydroxides are well-known adsorbents for oxyanions from aqueous solutions. Among the iron oxides that are used for adsorption are polymorphs of Fe_2O_3 (hematite and maghemite) and of FeOOH (goethite, akaganeite, lepidocrocite, …), green rusts ($[Fe^{II}_{(1-x)}Fe^{III}_x(OH)_2]^{x+} . [(x/n)A^{n-} \cdot mH_2O]^{x-}$ with $A^{n-} = CO_3^{2-}$, SO_4^{2-}, Cl^-, OH^-), Fe_3O_4 (magnetite) and ferrihydrite ($Fe_2O_3 . xH_2O$). Most of them are ferric (Fe(III)) oxides and hydroxides, except magnetite, which is a mixed Fe(II) - Fe(III) mineral.

These iron oxides and hydroxides can adsorb various oxyanions like chromate and chromite (CrO_4^{2-} and $Cr_2O_4^{2-}$), molybdate (MoO_4^{2-}), arsenite and arsenate (AsO_3^{3-} and AsO_4^{3-}), selenite and selenate (SeO_3^{2-} and SeO_4^{2-}), antimonite and antimonate ($Sb(OH)_4^-$ and

$Sb(OH)_6^-$), vanadate (VO_4^{3-}), tungstate (WO_4^{2-}), and anions like phosphate (PO_4^{3-}), chloride (Cl^-), sulphate (SO_4^{2-}) and carbonate (CO_3^{2-}) (Gua et al., 2012, Adegoke et al., 2012, Kolbe et al., 2011, Leuz et al., 2006, Zheng et al., 2004, Mansour et al., 2009, Gustafsson, 2003, Holm, 2002, Frau et al., 2010). Oxyanions are adsorbed on iron (hydr)oxides by the formation of surface complexes; the two main surface complexes are inner- or outer-sphere complexes.

Inner-sphere complex formation is the mechanism when ions bind directly onto specific sites on the surface of the adsorbent via a covalent or ionic bond; the water molecules on the hydrated adsorbent surface are replaced by the adsorbate molecules. Due to the strong and specific binding between adsorbate and adsorbent, an anion can bind to a mineral surface at a pH value above the point of zero charge (pH_{PZC}). The specific binding of the adsorbate onto the surface will alter the surface charge and therefore also change the pH_{PZC}. Inner-sphere complexes are monodentate complexes (adsorbate bound to the adsorbent surface at only one binding site) or polydentate complexes (the adsorbate is bound to the adsorbent surface at two or more binding sites), as shown in Figure 1.1. Inner-sphere complex formation is also called specific or chemical adsorption and due to the specific binding, which is mostly not reversible, regeneration of the adsorbent is not easy at low cost.

For outer-sphere complex formation, ions bind to the hydration shell of the adsorbent and not directly to the surface, and no water molecules are displaced from the hydrated surface. The main driving force for the adsorption is electrostatic interaction and the pH_{PZC} of the adsorbent will not be altered. Outer-sphere complex formation is also called non-specific or physical adsorption and is a reversible process.

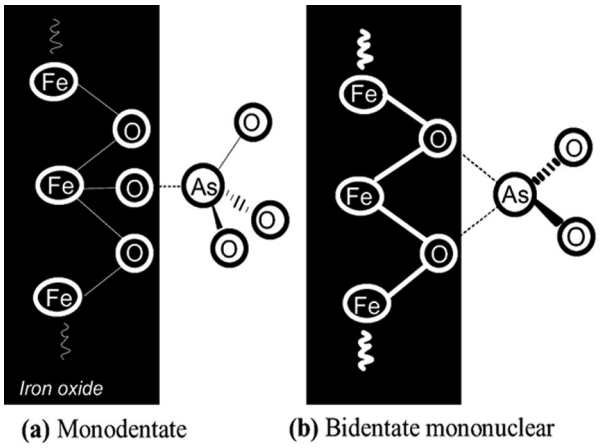

Figure 1.1. Schematic representation of monodentate and bidentate inner-sphere surface complexes (adapted from Gallegos-Garcia et al., 2012).

Use of magnetite for oxyanion adsorption

The iron oxide based adsorbent studied in this work is magnetite, an effective adsorbent for several oxyanions like arsenite and arsenate (Jönsson and Sherman, 2008, Mamindy-Pajany et al., 2011, Shipley et al., 2009, Su and Puls, 2008, Yean et al., 2005), molybdate (Rovira et al., 2006), chromate (Gallios and Vaclavikoca, 2008, Yuan et al., 2010), selenite and selenate (Martinez et al., 2006; Missana et al., 2009, Jordan et al., 2009). Magnetite is of special interest as it can easily be produced in the laboratory at very small (nanoscale particles) sizes (Yuan et al., 2010, Petrova et al., 2011), which ensures a high specific surface area and therefore also a high adsorption capacity (Petrova et al., 2011, Yean et al., 2005, Mayo et al., 2007). The influence of the particle size on the adsorption capacity was demonstrated by Mayo et al. (2007) for As adsorption on magnetite. As the particle size decreased from 300 to 12 nm the adsorption capacity per gram adsorbent for both As(III) and As(V) increased nearly 200 times. Based on the particle size only, the adsorption

capacity per gram adsorbent should be more than 600 times higher for the smaller particles than for the larger particles. The difference might be explained by the particles with a size of 300 nm partially consisting of agglomerates of somewhat smaller particles.

However, small particles inhibit the use of magnetite in continuous wastewater treatment, as nanosized material cannot be used in an adsorption column, which is the most widely used continuous adsorption setup (Petrova et al., 2011), due to a large pressure buildup in the column. For continuous column applications, nanosized material coated on a larger sized support material can be used, without significant loss of the adsorption capacity. This was demonstrated by Yuan et al. (2009 and 2010), who performed adsorption tests for the removal of Cr(VI) with montmorillonite-supported and diatomite-supported magnetite. Mostafa et al. (2011) coated hematite on perlite for the removal of AsO_4^{3-}. Vaclavikova et al. (2010) and Gallios and Vaclavikova (2008) performed experiments with zeolite-supported magnetite for the removal of AsO_4^{3-} and CrO_4^{2-}. As mentioned for the removal of As, the adsorption of oxyanions by iron oxides, or more specifically by magnetite, is mainly focused on removal from synthetic solutions and examples for real industrial wastewaters are scarce.

Adsorption modeling

To study the adsorption mechanisms of the different oxyanions, adsorption modeling was done by using the geochemical modeling program Visual Minteq (version 3.0, developed by J.P. Gustafsson, 2011). Different models can be used to model the adsorption of oxyanions onto iron oxide (i.e. magnetite) surfaces. We chose the extended Triple Layer Model (TLM) (Davis et al., 1978; Davis and Leckie, 1980; Hayes and Leckie., 1986), a multilayer surface

complexation model. Adsorption can be modelled in three different layers (Figure 1.2): ions adsorbing in the o-plane are inner-sphere complexes, adsorption of ions in the β-plane corresponds to outer-sphere complexes, and the d-plane represents the diffuse layer (Balistrieri and Chao 1990). By running separate simulations for either inner- or outer-sphere complex formation, and comparing the outcome of these simulations with experimental data, the predominant adsorption mechanism for the adsorption of each oxyanion onto magnetite can be determined. The simulation can also be run with different species of one oxyanion (e.g. fully protonated or fully deprotonated) to determine which species is the most likely to adsorb onto the magnetite surface.

In order to run a proper simulation in Visual Minteq, a number of parameters are needed to build the model. These parameters include the surface area of the adsorbent, two capacitance parameters C_1 and C_2 for the inner and outer layer (Figure 1.2), the surface site density and log K values for the protonation/deprotonation of the adsorbent surface.

The values of these parameters and how they are obtained is described in more detail in our publications[1]. The capacitance parameters C_1 and C_2 are used to relate the charge at the surface to the charge at some distance away from the surface. σ_o, σ_β and σ_d represent the charges at the o, β and d plane, respectively, while ψ_o, ψ_β and ψ_d represent the respective potentials.

[1] Verbinnen, B., Block, C., Hannes, D., Lievens, P., Vaclavikova, M., Stefusova, K., Gallios, G., Vandecasteele, C. (2012). Removal of Molybdate Anions from Water by Adsorption on Zeolite-Supported Magnetite. *Water Environment Research, 84* (9), 753-760.
Verbinnen, B., Block, C., Lievens, P., Van Brecht, A., Vandecasteele, C. (2013). Simultaneous Removal of Molybdenum, Antimony and Selenium Oxyanions from Wastewater by Adsorption on Supported Magnetite. *Waste and Biomass Valorization, 4* (3), 635-645.

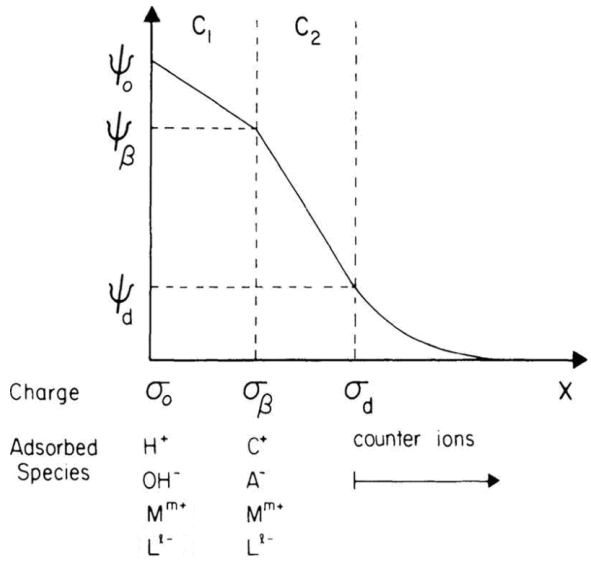

Figure 1.2. Schematic representation of ions, capacitances, charges and potentials in the TLM (adapted from Goldberg, 1992).

The regions between the o and β plane and between the β and the d plane are considered to be capacitors with capacitances C_1 and C_2, and the inner-layer capacitance C_1 relates the charge at the innermost plane of adsorption (σ_o) to the drop in potential at a distance β according to equation (4) (Sverjensky, 2001, Hayes and Leckie, 1987). The outer-layer capacitance is given by equation (5).

$$C_1 = \frac{\sigma_o}{\psi_0 - \psi_\beta} \tag{4}$$

$$C_2 = \frac{\sigma_o + \sigma_\beta}{\psi_\beta - \psi_d} \tag{5}$$

The most important parameters for adsorption modeling are the log K values for the surface complexation reactions of the different

oxyanions. These can be obtained from similar experiments described in literature, but the modeling can also be used to estimate log K values for surface complexation reactions if these are not yet or poorly described in literature. An example of the notation of the surface complexes is given in equations (6) and (7), with equation (6) representing inner-sphere complex formation and equation (7) outer-sphere complex formation. >FeOH respresents the (hydrated) iron oxide surface, and outer-sphere complexes are indicated by an underscore between the surface and the adsorbate.

$$>FeOH + SeO_3^{2-} + H^+ \leftrightarrows >FeSeO_3^- + H_2O \quad (6)$$

$$>FeOH + SeO_4^{2-} + H^+ \leftrightarrows >FeOH_2^+\_SeO_4^{2-} \quad (7)$$

1.3 Conclusions

For the leaching of oxyanions from thermally treated waste the conclusions from the literature review are:

- Literature data show that after thermal treatment of Cr and Mo containing materials, the leaching of Cr and Mo may pose problems. Possible explanations are given in literature, but no generalized explanation for the elevated leaching after heating and the influence of process conditions like heating temperature or residence time has been given.
- Some authors report a decrease in Cr and Mo leaching at temperatures above those reported for increased leaching. There is no sufficient explanation for this decrease.

For the removal of oxyanions from industrial wastewater by adsorption the conclusions from the literature review are:

- Until now, research on removal of oxyanions by adsorption mainly focused on synthetic solutions containing only one oxyanion with no or only one interfering (oxy)anion(s).
- Magnetite has a high removal capacity for oxyanions, because it can easily be produced in small sizes. However, magnetite with small particle sizes is difficult to apply in continuous water treatment systems. This could be avoided by coating nanosized magnetite on a support material. This allows using the adsorbent in a continuous column setup due to the larger size of the support material, with high adsorption capacity due to the small size of magnetite.

1.4 Research aim and objectives

The aim of this PhD thesis is to control the formation and subsequent leaching of oxyanions during high temperature processes and to study the removal of oxyanions from industrial wastewater. Thus, the possibilities to treat and recycle industrial solid residues will be increased and there will be more options to treat industrial wastewaters. To reach this goal and based on the conclusions from the literature overview, the research objectives for this thesis were defined as follows:

For the leaching of oxyanions from thermally treated waste:

- Identify the cause of elevated leaching of oxyanions from thermally treated industrial waste streams, and develop a general framework to explain this increase for both Cr and Mo.
- Identify the mechanism that is responsible for the subsequent decrease of leaching of Cr and Mo from materials heated at more elevated temperatures.
- Test the mechanisms for the initial increase and subsequent decrease at higher temperatures of Cr and Mo leaching by characterizing the leaching behavior of two industrial waste streams: the sand fraction of bottom ash from MSW incineration and contaminated sludge from soil cleaning.

For the removal of oxyanions from industrial wastewater by adsorption:

- Characterize and test an adsorbent (zeolite-supported magnetite) for simultaneous removal of Mo, Sb and Se oxyanions from synthetic solutions and industrial wastewater, with specific attention to possible interfering (oxy)anions.

- Develop a new adsorbent (perlite-supported magnetite) that can adsorb different oxyanions simultaneously, based on the good characteristics of zeolite-supported magnetite, but with improved coating of magnetite onto the support material. Test this adsorbent for the simultaneous adsorption of different oxyanions from an industrial wastewater.

1.5 Research methods

Experiments with synthetic samples are conducted to identify the mechanisms responsible for the elevated leaching of oxyanions from thermally treated industrial waste streams. The synthetic samples are prepared by mixing Cr_2O_3 with alkali and alkaline earth salts and these samples are heated at different temperatures, residence times and oxygen levels. MoS_2 was heated at different temperatures to check the possible oxidation of Mo(IV) compounds. Once a general mechanism is identified with the aid of the experimental data, it is checked by conducting thermodynamic calculations using the FactSage software (Bale et al., version 2.6). As a proof that the mechanism is also plausible for real industrial solid wastes, two types of contaminated solid wastes (the sand fraction of bottom ash from MSW incineration and sludge from soil cleaning) are subjected to the same heat treatment as the synthetic samples and their leaching behavior is compared.

The adsorption of oxyanions from wastewater is first checked by adsorption tests with zeolite-supported magnetite on synthetic solutions of Mo, Sb and Se oxyanions to determine the adsorption mechanisms and kinetics. After thorough research on the interfering compounds for adsorption, adsorption experiments for the simultaneous removal of these three elements from an industrial wastewater (the scrubber effluent of an incinerator for hazardous

waste) are performed. As the coating of zeolite by magnetite seemed to be poor, a new adsorbent, perlite-supported magnetite, is developed, incorporating the good characteristics of zeolite-supported magnetite, but improving the coating of magnetite on the support material. This adsorbent is characterized first and then tested for the removal of As, Cr, Mo, Sb and Se from the industrial wastewater.

References

Abbas, Z.; Steenari, B. M.; Lindqvist, O. (2001) A study of Cr(VI) in ashes from fluidized bed combustion of municipal solid waste: leaching, secondary reactions and the applicability of some speciation methods. *Waste Manage.*, 21, 725-739.

Adegoke, H. I.; Adekola, F. A.; Fatoki, O. S.; Ximba, B. J. (2013) Sorptive Interaction of Oxyanions with Iron Oxides: A Review. *Pol. J. Environ. Stud.*, 22, 7-24.

Alonso-Santurde, R.; Romero, M.; Rincon, J. M.; Viguri, J. R.; Andres, A. (2008) Leaching behavior of sintered contaminated marine sediments. *Fresenius Environ. Bull.*, 17, 1736-1743.

Astrup, T.; Rosenblad, C.; Trapp, S.; Christensen, T. H. (2005) Chromium release from waste incineration air-pollution-control residues. *Environ. Sci. Technol.*, 39, 3321-3329.

Bale, C.W., Chartrand, P., Degterov, S.A., Eriksson, G., Hack, K., Ben Mahfoud, R., Melançon, J., Pelton, A.D., Petersen, S. (2002) FactSage thermochemical software and databases. *Calphad*, 26, 189-228.

Balistrieri, L. S.; Chao, T. T. (1990) Adsorption of selenium by amorphous iron oxyhydroxide and manganese-dioxide. *Geochim. Cosmochim. Acta*, 54, 739-751.

Barceloux, D. G. (1999) Molybdenum. *J. Toxicol.-Clin. Toxicol.*, 37, 231-237.

Bethanis, S.; Cheeseman, C. R.; Sollars, C. J. (2004) Effect of sintering temperature on the properties and leaching of incinerator bottom ash. *Waste Manage. Res.*, 22, 255-264.

Bissen, M.; Frimmel, F. H. (2003) Arsenic - a review. - Part 1: Occurrence, toxicity, speciation, mobility. *Acta Hydrochim. Hydrobiol.*, 31, 9-18.

Bodenan, F.; Guyonnet, D.; Piantone, P.; Blanc, P. (2010) Mineralogy and pore water chemistry of a boiler ash from a MSW fluidized-bed incinerator. *Waste Manage.*, 30, 1280-1289.

Chang, F. C.; Lo, S. L.; Lee, M. Y.; Ko, C. H.; Lin, J. D.; Huang, S. C.; Wang, C. F. (2007) Leachability of metals from sludge-based artificial lightweight aggregate. *J. Hazard. Mater.*, 146, 98-105.

Cheeseman, C. R.; Makinde, A.; Bethanis, S. (2005) Properties of lightweight aggregate produced by rapid sintering of incinerator bottom ash. *Resour. Conserv. Recycl.*, 43, 147-162.

Chen, W. F.; Parette, R.; Zou, J. Y.; Cannon, F. S.; Dempsey, B. A. (2007) Arsenic removal by iron-modified activated carbon. *Water Res.*, 41, 1851-1858.

Chen, Y. L.; Chang, J. E.; Lai, Y. C.; Ko, M. S. (2012) Effects of sintering atmosphere on cement clinkers produced from chromium-bearing sludge. *J. Air Waste Manage. Assoc.*, 62, 587-593.

Choi, H. D.; Jung, W. S.; Cho, J. M.; Ryu, B. G.; Yang, J. S.; Baek, K. (2009) Adsorption of Cr(VI) onto cationic surfactant-modified activated carbon. *J. Hazard. Mater.*, 166, 642-646.

Cornelis, G.; Johnson, C. A.; Van Gerven, T.; Vandecasteele, C. (2008) Leaching mechanisms of oxyanionic metalloid and metal species in alkaline solid wastes: A review. *Appl. Geochem.*, 23, 955-976.

Davis, J. A.; James, R. O.; Leckie, J. O. (1978) Surface ionization and complexation at oxide-water interface. 1. Computation of electrical double-layer properties in simple electrolytes. *J. Colloid Interface Sci.*, 63, 480-499.

Davis, J. A.; Leckie, J. O. (1980) Surface-ionization and complexation at the oxide-water interface. 3. Adsorption of anions. *J. Colloid Interface Sci.*, 74, 32-43.

El-Hasan, T.; Szczerba, W.; Buzanich, G.; Radtke, M.; Riesemeier, H.; Kersten, M. (2011) Cr(VI)/Cr(III) and As(V)/As(III) Ratio Assessments in Jordanian Spent Oil Shale Produced by Aerobic Combustion and Anaerobic Pyrolysis. *Environ. Sci. Technol.*, 45, 9799-9805.

Frau, F.; Addari, D.; Atzei, D.; Biddau, R.; Cidu, R.; Rossi, A. (2010) Influence of Major Anions on As(V) Adsorption by Synthetic 2-line Ferrihydrite. Kinetic Investigation and XPS Study of the Competitive Effect of Bicarbonate. *Water Air Soil Pollut.*, 205, 25-41.

Gallegos-Garcia, M.; Ramirez-Muniz, K.; Song, S. X. (2012) Arsenic removal from water by adsorption using iron oxide minerals as adsorbents: a review. *Miner. Process Extr. Metall. Rev.*, 33, 301-315.

Gallios, G. P.; Vaclavikova, M. (2008) Removal of chromium (VI) from water streams: a thermodynamic study. *Environ. Chem. Lett.*, 6, 235-240.

Goldberg, S. (1992) Use of surface complexation models in soil chemical-systems. *Adv. Agron.*, 47, 233-329.

Gonzalez-Corrochano, B.; Alonso-Azcarate, J.; Rodas, M. (2012) Chemical partitioning in lightweight aggregates manufactured from washing aggregate sludge, fly ash and used motor oil. *J. Environ. Manage.*, 109, 43-53.

Gustafsson, J. P. (2003) Modelling molybdate and tungstate adsorption to ferrihydrite. *Chem. Geol.*, 200, 105-115.

Gustafsson, J. P. (2012) Visual Minteq, a free equilibrium speciation model. Version 3.0, August 10, 2011. http://www2.lwr.kth.se/English/OurSoftware/vminteq/

Hayes, K. F.; Leckie, J. O. (1986) Mechanism of lead-ion adsorption at the goethite-water interface. *Acs Symposium Series*, 323, 114-141.

Hayes, K. F.; Leckie, J. O. (1987) Modeling ionic-strength effects on cation adsorption at hydrous oxide-solution interfaces. *J. Colloid Interface Sci.*, 115, 564-572.

Holm, T. R. (2002) Effects of CO32-/bicarbonate, Si, and PO43- on arsenic sorption to HFO. *J. Am. Water Work Assoc.*, 94, 174-181.

Holm, T.R., Wilson, S.D. (2006) Chemical oxidation for arsenic removal. Illinois State Water Survey, Champaign, Illinois.

Hu, H.; Luo, G.; Liu, H.; Qiao, Y.; Xu, M.; Yao, H. (2013) Fate of chromium during thermal treatment of municipal solid waste incineration (MSWI) fly ash. *Proceedings of the Combustion Institute*, 34, 2795-2801.

Hua, M.; Zhang, S. J.; Pan, B. C.; Zhang, W. M.; Lv, L.; Zhang, Q. X. (2012) Heavy metal removal from water/wastewater by nanosized metal oxides: A review. *J. Hazard. Mater.*, 211, 317-331.

Hyks, J.; Nesterov, I.; Mogensen, E.; Jensen, P. A.; Astrup, T. (2011) Leaching from waste incineration bottom ashes treated in a rotary kiln. *Waste Manage. Res.*, 29, 995-1007.

Jönsson, J.; Sherman, D. M. (2008) Sorption of As(III) and As(V) to siderite, green rust (fougerite) and magnetite: Implications for arsenic release in anoxic groundwaters. *Chem. Geol.*, 255, 173-181.

Jordan, N.; Lomenech, C.; Marmier, N.; Giffaut, E.; Ehrhardt, J. J. (2009) Sorption of selenium(IV) onto magnetite in the presence of silicic acid. *J. Colloid Interface Sci.*, 329, 17-23.

Kirk, D. W.; Chan, C. C. Y.; Marsh, H. (2002) Chromium behavior during thermal treatment of MSW fly ash. *J. Hazard. Mater.*, 90, 39-49.

Kolbe, F.; Weiss, H.; Morgenstern, P.; Wennrich, R.; Lorenz, W.; Schurk, K.; Stanjek, H.; Daus, B. (2011) Sorption of aqueous antimony and arsenic species onto akaganeite. *J. Colloid Interface Sci.*, 357, 460-465.

Kotas, J.; Stasicka, Z. (2000) Chromium occurrence in the environment and methods of its speciation. *Environmental Pollution*, 107, 263-283.

Lehmusto, J.; Lindberg, D.; Yrjas, P.; Skrifvars, B. J.; Hupa, M. (2012) Thermogravimetric studies of high temperature reactions between potassium salts and chromium. *Corrosion Sci.*, 59, 55-62.

Leuz, A. K.; Monch, H.; Johnson, C. A. (2006) Sorption of Sb(III) and Sb(V) to goethite: Influence on Sb(III) oxidation and mobilization. *Environ. Sci. Technol.*, 40, 7277-7282.

Mamindy-Pajany, Y.; Hurel, C.; Marmier, N.; Roméo, M. (2011) Arsenic (V) adsorption from aqueous solution onto goethite, hematite, magnetite and zero-valent iron: Effects of pH, concentration and reversibility. *Desalination*, 281, 93-99.

Manju, G. N.; Raji, C.; Anirudhan, T. S. (1998) Evaluation of coconut husk carbon for the removal of arsenic from water. *Water Res.*, 32, 3062-3070.

Mansour, C.; Lefevre, G.; Pavageau, E. M.; Catalette, H.; Fedoroff, M.; Zanna, S. (2009) Sorption of sulfate ions onto magnetite. *J. Colloid Interface Sci.*, 331, 77-82.

Martinez, M.; Gimenez, J.; de Pablo, J.; Rovira, M.; Duro, L. (2006) Sorption of selenium(IV) and selenium(VI) onto magnetite. *Appl. Surf. Sci.*, 252, 3767-3773.

Mayo, J. T.; Yavuz, C.; Yean, S.; Cong, L.; Shipley, H.; Yu, W.; Falkner, J.; Kan, A.; Tomson, M.; Colvin, V. L. (2007) The effect of nanocrystalline magnetite size on arsenic removal. *Sci. Technol. Adv. Mater.*, 8, 71-75.

Missana, T.; Alonso, U.; Scheinost, A. C.; Granizo, N.; Garcia-Gutierrez, M. (2009) Selenite retention by nanocrystalline magnetite: Role of adsorption, reduction and dissolution/co-precipitation processes. *Geochim. Cosmochim. Acta*, 73, 6205-6217.

Mohan, D.; Pittman, C. U. (2007) Arsenic removal from water/wastewater using adsorbents - A critical review. *J. Hazard. Mater.*, 142, 1-53.

Mostafa, M. G.; Chen, Y.-H.; Jean, J.-S.; Liu, C.-C.; Lee, Y.-C. (2011) Kinetics and mechanism of arsenate removal by nanosized iron oxide-coated perlite. *J. Hazard. Mater.*, 187, 89-95.

Navarro, P.; Alguacil, F. J. (2002) Adsorption of antimony and arsenic from a copper electrorefining solution onto activated carbon. *Hydrometallurgy*, 66, 101-105.

Owlad, M.; Aroua, M. K.; Daud, W. A. W.; Baroutian, S. (2009) Removal of Hexavalent Chromium-Contaminated Water and Wastewater: A Review. *Water Air Soil Pollut.*, 200, 59-77.

Pandey, A. K.; Pandey, S. D.; Misra, V. (2000) Stability constants of metal-humic acid complexes and its role in environmental detoxification. *Ecotox. Environ. Safe.*, 47, 195-200.

Paoletti, F. (2002) Behavior of oxyanions forming heavy metals in municipal solid waste incineration. Ph. D. Dissertation, Institute for Technical Chemistry: Karlsruhe, Germany.

Petrova, T.M., Fachikov, L., Hristov J. (2011) The magnetite as adsorbent for some hazardous species from aqueous solutions: a review. *Int. Rev. Chem. Eng.*, 3, 134-152.

Quijorna, N.; Coz, A.; Andres, A.; Cheeseman, C. (2012) Recycling of Waelz slag and waste foundry sand in red clay bricks. *Resour. Conserv. Recycl.*, 65, 1-10.

Rovira, M.; de Pablo, J.; Ignasi Casas, L.; Gimenez, J.; Ciarens, F.; Martinez-Llado, X. (2006) Sorption of molybdenum(VI) on synthetic magnetite. Ghent, Belgium, 2006, 12-16 September; Materials Research Society, 143-150.

Selinger, A., Schmidt, V., Bergfeldt, B., Vehlow, J., Simon, F.G. (1997) Investigation of sintering processes in bottom ash to promote the reuse in civil construction - Part 1: Element balance and leaching, in: Goumans, J.J.J.M., Senden, G.J., Van der Sloot H.A. (Eds.), Waste Materials in Construction: Putting Theory in Practice, Elsevier Science, Amsterdam, pp. 41–49.

Shipley, H. J.; Yean, S.; Kan, A. T.; Tomson, M. B. (2009) Adsorption of arsenic to magnetite nanoparticles: effect of particle concentration, pH, ionic strength, and temperature. *Environ. Toxicol. Chem.*, 28, 509-515.

Sinyoung, S.; Songsiriritthigul, P.; Asavapisit, S.; Kajitvichyanukul, P. (2011) Chromium behavior during cement-production processes: A clinkerization, hydration, and leaching study. *J. Hazard. Mater.*, 191, 296-305.

Sorensen, M. A.; Koch, C. B.; Stackpoole, M. M.; Bordia, R. K.; Benjamin, M. M.; Christensen, T. H. (2000) Effects of thermal treatment on mineralogy and heavy metal behavior in iron oxide stabilized air pollution control residues. *Environ. Sci. Technol.*, 34, 4620-4627.

Stam, A. F.; Meij, R.; Winkel, H. T.; van Eijk, R. J.; Huggins, F. E.; Brem, G. (2011) Chromium Speciation in Coal and Biomass Co-Combustion Products. *Environ. Sci. Technol.*, 45, 2450-2456.

Su, C.; Puls, R. (2008) Arsenate and Arsenite Sorption on Magnetite: Relations to Groundwater Arsenic Treatment Using Zerovalent Iron and Natural Attenuation. *Water Air Soil Pollut*, 193, 65-78.

Sverjensky, D. A. (2001) Interpretation and prediction of triple-layer model capacitances and the structure of the oxide-electrolyte-water interface. *Geochim. Cosmochim. Acta*, 65, 3643-3655.

Timberlake, D. L.; Garbaciak, S. (1995) Bench-scale testing of selected remediation alternatives for contaminated sediments. *J. Air Waste Manage. Assoc.*, 45, 52-56.

Vaclavikova, M.; Stefusova, K.; Ivanicova, L.; Jakabsky, S.; Gallios, G. P. (2010) Magnetic zeolite as arsenic adsorbent, in: Vaclavikova, M.; Vitale, K.; Gallios, G. P.; Ivanicova, L. (Eds.), Water Treatment Technologies for the Removal of High-Toxicity Pollutants. Springer, Dordrecht, pp. 51-59.

Vandecasteele, C.; Cornelis, G. (2010) Oxyanions in waste: occurrence, leaching, stabilization, relation to wastewater treatment, in: Vaclavikova, M.; Vitale, K.; Gallios, G. P.; Ivanicova, L. (Eds.), Water Treatment Technologies for the Removal of High-Toxicity Pollutants. Springer, Dordrecht, pp. 149-159.

Vangelatos, I.; Angelopoulos, G. N.; Boufounos, D. (2009) Utilization of ferroalumina as raw material in the production of Ordinary Portland Cement. *J. Hazard. Mater.*, 168, 473-478.

Van Gerven, T., Chen, X., Evens, R., Hindrix, K., Vandecasteele, C. (2006) Upgrading MSWI bottom ash by extraction, heating or dense medium separation, in view of recycling, in: Ilic, M., Goumans, J.J.J.M., Miletic, S., Heynen, J.J.M., Senden, G.J. (Eds.), Waste Materials in Construction: Quality of materials and products, pp. 507-518.

Vaughan, R. L.; Reed, B. E. (2005) Modeling As(V) removal by a iron oxide impregnated activated carbon using the surface complexation approach. *Water Res.*, 39, 1005-1014.

Wang, K. S.; Sun, C. J.; Liu, C. Y. (2001) Effects of the type of sintering atmosphere on the chromium leachability of thermal-treated municipal solid waste incinerator fly ash. *Waste Manage.*, 21, 85-91.

Xu, G. R.; Zou, J. L.; Li, G. B. (2008) Stabilization of heavy metals in ceramsite made with sewage sludge. *J. Hazard. Mater.*, 152, 56-61.

Xu, N.; Braida, W.; Christodoulatos, C.; Chen, J. P. (2013) A Review of Molybdenum Adsorption in Soils/Bed Sediments: Speciation, Mechanism, and Model Applications. *Soil. Sediment. Contam.*, 22, 912-929.

Yean, S.; Cong, L.; Yavuz, C. T.; Mayo, J. T.; Yu, W. W.; Kan, A. T.; Colvin, V. L.; Tomson, M. B. (2005) Effect of magnetite particle size on adsorption and desorption of arsenite and arsenate. *J. Mater. Res.*, 20, 3255-3264.

Yeu-Juin, T.; Wang, H. P.; Juu-En, C. (2012) Tracking of Chromium in Plasma co-Melting of Fly Ashes and Sludges. *Water, Air, & Soil Pollution*, 223, 5283-5288.

Yuan, P.; Fan, M. D.; Yang, D.; He, H. P.; Liu, D.; Yuan, A. H.; Zhu, J. X.; Chen, T. H. (2009) Montmorillonite-supported magnetite nanoparticles for the removal of hexavalent chromium Cr(VI) from aqueous solutions. *J. Hazard. Mater.*, 166, 821-829.

Yuan, P.; Liu, D.; Fan, M. D.; Yang, D.; Zhu, R. L.; Ge, F.; Zhu, J. X.; He, H. P. (2010) Removal of hexavalent chromium Cr(VI) from aqueous solutions by the diatomite-supported/unsupported magnetite nanoparticles. *J. Hazard. Mater.*, 173, 614-621.

Zeng, L.; Li, X.; Liu, J. (2004) Adsorptive removal of phosphate from aqueous solutions using iron oxide tailings. *Water Res.*, 38, 1318-1326.

Zhang, H.; Xu, M.-z. (2011) Transfer behavior of PAHs and PCBs from sewage sludge in the thermal treatment process. *China Environ. Sci.*, 31, 933-937.

2. Leaching of oxyanions from thermally treated waste

In this chapter, the research on the leaching of oxyanions from thermally treated waste will be presented. The research aim for this part of the thesis was to control the formation and subsequent leaching of oxyanions during high temperature processes to increase their reuse potential. Cr and Mo oxyanions were of special interest, as high leaching concentrations of these two elements were observed during an industrial project. The following research objectives were defined:

- Identify the cause of elevated leaching of oxyanions from thermally treated industrial waste streams, and develop a general framework to explain this increase for both Cr and Mo.
- Identify the mechanism that is responsible for the subsequent decrease of leaching of Cr and Mo from materials heated at more elevated temperatures.
- Test the mechanisms for the initial increase and subsequent decrease at higher temperatures of Cr and Mo leaching by characterizing the leaching behavior of two industrial waste streams: the sand fraction of bottom ash from MSW incineration and contaminated sludge from soil cleaning.

The research will be presented by the relevant accepted or submitted papers that are included hereafter. In addition, a summary of the research is given first.

2.1 Summary

The formation mechanism of mobile Cr(VI) oxyanions in the presence of alkali and alkaline earth salts was elucidated by performing heating experiments with synthetic samples of Cr_2O_3 mixed with Na, K, Mg and Ca salts (Figure 2.1). During heating in ambient atmosphere at temperatures between 200 and 1100 °C, no formation and subsequent leaching of Cr(VI) was observed when Cr_2O_3 was heated in ambient atmosphere, or when it was mixed with MgO and heated. When Cr_2O_3 was mixed with KOH, NaOH or CaO and heated in ambient atmosphere, formation and subsequent leaching of Cr(VI) was detected. This was confirmed by thermodynamic calculations using the FactSage software (a fully integrated database computing system that can be used to calculate phase diagrams and thermodynamic equilibria, version 6.2).

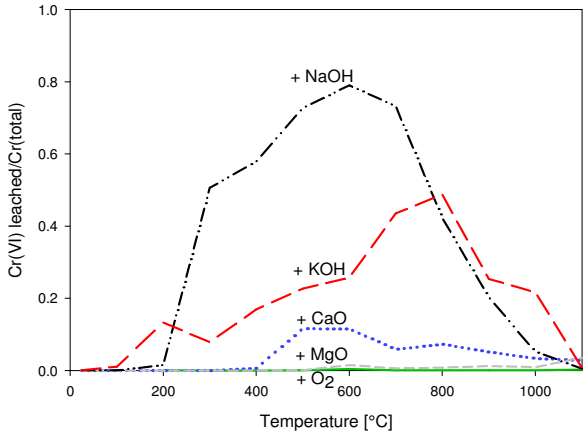

Figure 2.1: Leaching of Cr(VI) as a function of heating temperature after heating of Cr_2O_3 in the presence of O_2 and NaOH, KOH, CaO, or MgO.

The conversion of Cr(III) to Cr(VI) compounds is highest when NaOH is mixed with Cr_2O_3: after heating for 30 min at 600 °C, a maximum conversion of 79 % was detected. A kinetic evaluation

showed that the conversion proceeded faster at higher temperatures. After the maximum conversion was reached, leaching of Cr decreased again. This was attributed to the melting of the formed chromates in the presence of SiO_2 (added as bed material in the crucibles), a binary system that forms an amorphous phase upon cooling, preventing Cr from leaching.

Increased Mo leaching upon heating can be related to the presence of MoS_2 in the untreated material. MoS_2 is commonly used as a dry lubricant and is therefore probably found in soils contaminated with mineral oils. Upon heating, MoS_2 is oxidized to mobile Mo(VI) compounds and leached.

The plausibility of the two mechanisms for Cr(VI) and Mo(VI) formation and subsequent leaching after heat treatment was tested for two industrial waste streams: contaminated sludge from soil washing and the sand fraction of bottom ash from municipal solid waste incineration. The examined contaminated sludge contains high concentrations of toxic elements like Zn, Ni, Pb, Cu and Cr and the leached concentrations of the cation forming heavy metals Ni, Cu and Zn exceed the regulatory limits. The leaching of these 3 elements can be decreased below the limit values by heating the sludge, as this destroys the humic substances that form soluble organo-metallic complexes with these cation forming elements.

After destruction of the organic material, an increase in Cr and Mo leaching was observed. The leaching of Cr(VI) as a function of the heating temperature (Figure 2.2) was consistent with the findings from the tests performed for synthetic mixtures, so it is clear that the reaction of Cr(III) compounds with alkali and/or alkaline earth salts is responsible for the increased Cr leaching after heating of the contaminated sludge. A decrease in Cr leaching similar to the

synthetic mixtures is observed at higher temperatures. For contaminated sludge, several explanations can be considered for this decrease, but most likely the same explanation as for the synthetic samples (i.e. the formation of an amorphous phase upon cooling preventing Cr from leaching) holds true. However, at high temperatures (> 1000 °C), reduction (because the inner part of the sample is shielded from oxygen by the formation of a vitrified outer layer) and/or vitrification might also play a role.

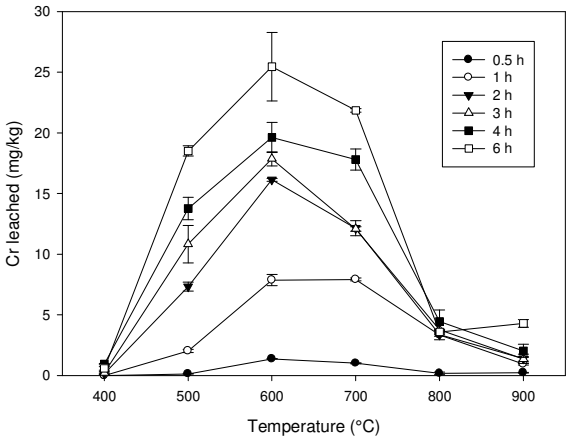

Figure 2.2: Leaching of Cr after heating from contaminated sludge as a function of heating temperature and residence time

Mo leaching from contaminated sludge increases for temperatures up to 900 °C for all residence times (Figure 2.3). Contrary to the Cr leaching behavior, Mo leaching does not decrease at temperatures above 700 °C. Above 1025 °C (shown only for a residence time of 0.5 h in Figure 2.3), the leached concentrations decrease due to vitrification of the material.

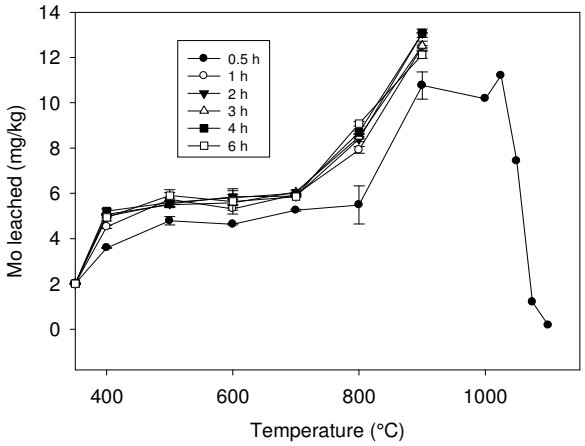

Figure 2.3: Leaching of Mo after heating from contaminated sludge as a function of heating temperature and residence time.

For the sand fraction of bottom ash (i.e. the fraction with a size 65 µm – 2 mm that is obtained after size separation and ferrous and non-ferrous separation), no increase in Mo leaching is detected anymore upon heating, as Mo is probably not present as MoS_2 in the ash, but already as Mo(VI) compounds. Contrary to the leaching behavior observed from the contaminated sludge, Mo leaching decreases after thermal treatment of the sand fraction; this is observed for residence times of 2 h and more at 600 °C and already after 30 min at 700 °C (Figure 2.4). The difference with the Mo leaching from contaminated sludge is probably that in the sludge, Mo is present as grains of MoS_2 that are oxidized to MoO_3. Because Mo is present in solid particles, it is not able to react with alkali or alkaline earth salts to form molybdates, which could in turn form a melt with SiO_2 becoming amorphous upon cooling. In the sand fraction of the bottom ash, which has already undergone thermal treatment, Mo is present as alkali or alkaline earth MoO_4^{2-} salts, and these can form a binary system with SiO_2 at temperatures above 700 °C, becoming amorphous upon cooling.

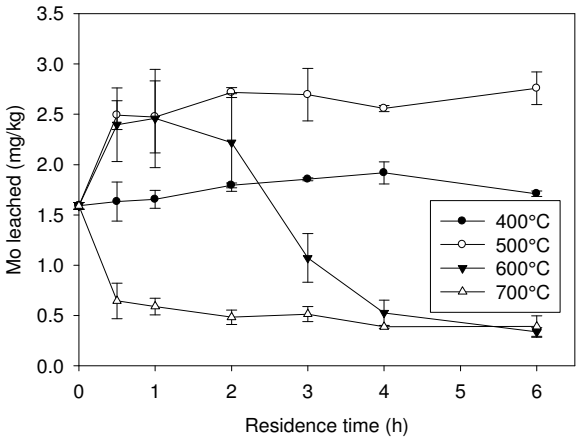

Figure 2.4: Leaching of Mo from bottom ash heated at 400 – 700 °C for 0.5 – 6 h.

The Cr leaching behavior from the thermally treated sand fraction of the bottom ash is comparable to that of thermally treated sludge. After the removal of elementary carbon and left-over humic substances responsible for increased leaching of cation forming elements, Cr(III) is oxidized and increased Cr(VI) concentrations are observed. At 600 °C, this leaching starts to decrease again at residence times of 2 h and more, and at 700 °C, the Cr leaching is low immediately (Figure 2.5).

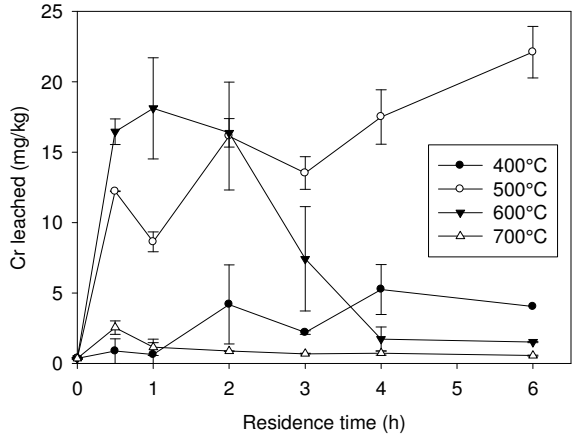

Figure 2.5: Leaching of Cr from bottom ash heated at 400 - 700 °C for 0.5 – 6 h.

2.2 Heating Temperature Dependence of Cr(III) Oxidation in the Presence of Alkali and Alkaline Earth Salts and Subsequent Cr(VI) Leaching Behavior

Verbinnen, B., Billen, P., Van Coninckxloo, M., Vandecasteele, C. (2013). Heating Temperature Dependence of Cr(III) Oxidation in the Presence of Alkali and Alkaline Earth Salts and Subsequent Cr(VI) Leaching Behavior. *Environmental Science & Technology, 47* (11), 5858-63.

Publication 1 describes the research on the formation mechanism of Cr(VI) oxyanions during thermal treatment and subsequent leaching. The cause of Cr leaching after high temperature processes is investigated by heating synthetic mixtures of Cr_2O_3 with alkali or alkaline earth salts, and by studying the influence of temperature. By varying the residence time of the mixtures at a specific temperature, the kinetics of Cr(VI) formation could be studied. Also, a decrease in Cr(VI) leaching was observed for the synthetic mixtures. Based on the observations, it has been hypothesized that this is due to the formation of an amorphous binary mixture of chromates and SiO_2, which was present as bed material in the crucibles. A first comparison was made between the Cr leaching from the synthetic mixtures and a real industrial solid waste material: contaminated sludge from soil cleaning. Based on the proposed mechanisms for Cr(VI) formation, countermeasures to prevent Cr leaching were tested for both synthetic samples and contaminated sludge.

This paper provides an explanation for the elevated Cr leaching that has often been reported in literature after high temperature processing of contaminated solid wastes, but for which up till now, no generalized explanation was found. It also formulates an hypothesis on the reason why the Cr leaching decreases again at higher temperatures.

The experiments in this paper were performed by the candidate and a master thesis student, M. Van Coninckxloo. The draft version of the manuscript was prepared by the candidate, while the other autors (P. Billen, M. Van Coninckxloo and C. Vandecasteele) acted as discussion partners and critical reviewers of the manuscript.

Environmental Science & Technology

Article

pubs.acs.org/est

Heating Temperature Dependence of Cr(III) Oxidation in the Presence of Alkali and Alkaline Earth Salts and Subsequent Cr(VI) Leaching Behavior

Bram Verbinnen,* Pieter Billen, Michiel Van Coninckxloo, and Carlo Vandecasteele

ProcESS, Process Engineering for Sustainable Systems, Department of Chemical Engineering, KU Leuven, W. De Croylaan 46, B-3001 Leuven, Belgium

ABSTRACT: In this paper, the temperature dependence of Cr(III) oxidation in high temperature processes and the subsequent Cr(VI) leaching was studied using synthetic mixtures. It was experimentally shown that in the presence of alkali and alkaline earth salts, oxidation of Cr(III) takes place, consistent with thermodynamic calculations. Heating of synthetic mixtures of Cr_2O_3 and Na, K, or Ca salts led to elevated leaching of Cr(VI); in the presence of Na, more than 80% of the initial Cr(III) amount was converted to Cr(VI) at 600−800 °C. Kinetic experiments allowed explanation of the increase in Cr(VI) leaching for increasing temperatures up to 600−800 °C. After reaching a maximum in Cr(VI) leaching at temperatures around 600−800 °C, the leaching decreased again, which could be explained by the formation of a glassy phase that prevents leaching of the formed Cr(VI). By way of illustration, Cr(VI) formation and leaching was evaluated for a case study, the fabrication of ceramic material from contaminated sludge. Based on the proposed reaction mechanisms, countermeasures to prevent Cr oxidation (addition of $NH_4H_2PO_4$, heating under inert atmosphere) were proposed and successfully tested for synthetic mixtures and for the case study.

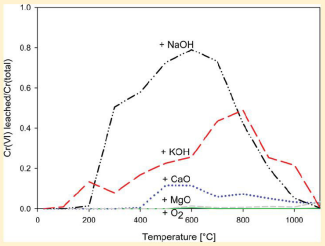

INTRODUCTION

In our recent research, we observed that (i) when expressed as a fraction of the total Cr content, Cr(VI) leaching from bottom ash of a fluidized bed waste incinerator was six times higher than from fly ash, and that (ii) when contaminated sludge was heated in order to obtain a ceramic material, leaching of the mobile and toxic Cr(VI) exceeded the regulatory limit value, at some temperatures (600−700 °C) even by 50 times. As Cr(VI) leaching from the unheated material was below the limit value, this indicates that Cr(VI) is formed during thermal treatment.

Several papers report on elevated Cr leaching or on oxidation of Cr(III) to Cr(VI) and subsequent leaching after high temperature processes but do not explain its causes. After thermal treatment of contaminated sludge in view of recycling,[1,2] combustion of waste, coal, or biomass,[3−7] and after other high temperature processes such as cement production,[8−10] elevated Cr or Cr(VI) leaching was observed. Moreover, Cr(VI) formation may be responsible for enhanced corrosion of stainless steel during high temperature processes.[11]

It is well-known that Cr(VI) is more mobile than Cr(III),[12] so increased leaching observed in the literature is probably related to oxidation of Cr(III) to Cr(VI). Moreover, Cr(VI) is highly toxic and is ranked as the second most important oxyanion (after arsenic) on the CERCLA 2011 Priority List of Hazardous Substances. Reaction 1, the oxidation of Cr(III) to Cr(VI) in the presence of ambient air does not occur at temperatures below 1500 °C,[13] as will be shown by experiments and thermodynamic calculations in this paper.

$$Cr_2O_3 + \frac{3}{2}O_2 \leftrightarrow 2CrO_3 \quad (1)$$

Therefore, Paoletti[13] hypothesized that Cr(III) (i.e., Cr_2O_3) is oxidized to Cr(VI) in the presence of oxygen and CaO according to reaction 2. This hypothesis was based on TGA observations, where a weight gain was observed starting at a temperature of around 500 °C.

$$Cr_2O_3 + 2CaO + \frac{3}{2}O_2 \leftrightarrow 2CaCrO_4 \quad (2)$$

Other researchers[5,11,14−16] pointed out that in the presence of salts of alkali and other alkaline earth metals, the oxidation of Cr(III) to Cr(VI) by oxygen is also made possible. Whereas Cr(III) oxidation and subsequent Cr(VI) leaching was thus mentioned on several occasions, a systematic description and explanation of the dependence on the oxidation temperature is still lacking. The goal of this paper is to present a framework for understanding Cr(VI) formation in the presence of salts of alkali and alkaline earth metals and its subsequent leaching. Therefore, apart from reactions 1 and 2, three other reactions, 3−5, will be considered:

Received: January 10, 2013
Revised: April 2, 2013
Accepted: May 1, 2013
Published: May 1, 2013

dx.doi.org/10.1021/es4001455 | Environ. Sci. Technol. 2013, 47, 5858−5863

$$Cr_2O_3 + 4NaOH + \frac{3}{2}O_2 \leftrightarrow 2Na_2CrO_4 + 2H_2O \quad (3)$$

$$Cr_2O_3 + 4KOH + \frac{3}{2}O_2 \leftrightarrow 2K_2CrO_4 + 2H_2O \quad (4)$$

$$Cr_2O_3 + 2MgO + \frac{3}{2}O_2 \leftrightarrow 2MgCrO_4 \quad (5)$$

Synthetic mixtures are used to study the temperature dependence of the described reactions, and the results are compared with thermodynamic calculations. The synthetic mixtures are also used to carry out kinetic experiments. By way of illustration, the formation of Cr(VI) during thermal treatment of contaminated industrial sludge is quantified and explained. It is shown that a better understanding of the reactions responsible for Cr oxidation may afford effective countermeasures against Cr(VI) formation and leaching.

MATERIALS AND METHODS

Synthetic mixtures were prepared by mixing 5 wt % of Cr(III) oxide (Cr_2O_3, Sigma-Aldrich) with 95 wt % of potassium hydroxide (KOH, Merck Eurolab), sodium hydroxide (NaOH, Fisher), magnesium oxide (MgO, Sigma-Aldrich), or calcium oxide (CaO, Chem-Lab). The finely divided mixture was homogenized by thoroughly mixing, and 1 g was placed on sand in a ceramic crucible. The crucibles were placed in a muffle furnace that was heated with a heating rate of approximately 10 °C/min until the desired temperature (100−1100 °C) was reached. They were kept at this temperature for half an hour and afterward allowed to cool in the furnace. For kinetic experiments, the mixtures were introduced in a preheated muffle furnace at the desired temperature, removed from the oven after a given time period (1 min to 12 h), and allowed to cool at room temperature.

Industrial sludges originating from the cleaning of soils (with different origin and contaminants, but all mainly inorganic), were dried at 105 °C until constant weight, ground, and then mixed in equal quantities. After homogenization, an appropriate amount (about one-third of the sludge mass) of water was added to allow good pelletization. Spherical pellets with an average diameter of 1.5 cm and an average weight of 5 g were produced and dried at 105 °C. The pellets were then introduced in the oven using the "rapid sintering"[17] technique. This method requires that the samples are placed in a preheated oven at the desired temperature and kept at this temperature for a given period, in this case at temperatures between 200 and 1100 °C for half an hour. After this period, the samples were removed from the oven and allowed to cool at room temperature.

After cooling, the samples were ground and leached with double deionized water (Millipore Milli-Q) on a shaking device (Gerhardt Laboshake, 160 rpm) for 24 h with a liquid/solid ratio of 10 (pellets) or 100 (synthetic mixtures, a higher ratio was chosen to ensure that leaching was not limited by solubility). After leaching, the samples were filtered over a 0.45 μm membrane filter (Chromafil), and the relevant metal concentrations were measured by ICP-MS (Thermo Xi series). Cr(VI) concentrations were measured spectrophotometrically (Shimadzu 1601) using the diphenylcarbazide method.

To study the effect of phase crystallinity on the leaching of Cr, pure K_2CrO_4 was heated for 30 min at temperatures ranging from 500 to 1100 °C, and after cooling, the sample was leached for 24 h with ultrapure water at an L/S ratio of 1000.

In experiments to prevent Cr(III) oxidation, an excess (twice the weight of the mixture) of $NH_4H_2PO_4$ was added to a 5% Cr_2O_3−95% NaOH mixture, which was then heated at 800 °C for 10 min. To contaminated sludge, 7% $NH_4H_2PO_4$ was added, and the sample was heated at 700 °C for 30 min. To test heating under an inert atmosphere, a sample of the contaminated sludge was heated at 700 °C for 30 min in a furnace through which a constant stream of nitrogen was flowing.

The crystal structure of the samples was determined by XRD (Philips PW1830) using monochromated Cu Kα radiation, generated at 45 kV and 30 mA. Measurements ranged from 2θ = 5° to 75°, with a step size of 0.02°.

Thermodynamic calculations were performed using data from the FactSage database and relevant literature sources[18−23] for data that were not in the FactSage database.

RESULTS AND DISCUSSION

Synthetic Samples. In Figure 1, the ratio of the Cr(VI) amount leached after heating to the initial Cr amount in the synthetic samples is plotted against the heating temperature. As all Cr(VI) salts that might be formed in these experiments are very soluble over a broad pH range, and Cr(III) salts are hardly soluble at neutral and alkaline pH values, the ratio of Cr(VI) leaching to total Cr could be considered an indication of the total Cr(III) amount that has been oxidized to leachable Cr(VI) after heating. At high temperatures however, this is not correct, as will be shown later. From the graph, it appears that Cr_2O_3 as such is not oxidized. Also, the presence of MgO leads to little oxidation: at 1100 °C, only 3.5% of the initial Cr(III) amount is leached as Cr(VI).

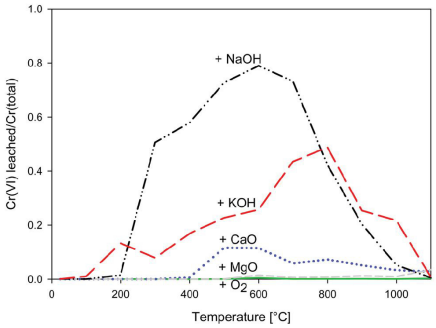

Figure 1. Leaching of Cr(VI) as a function of heating temperature in the presence of NaOH, KOH, CaO, or MgO or without other oxides/hydroxides added.

The graph corresponding to Cr(VI) leaching after heating in the presence of CaO, KOH, and NaOH shows a different behavior. Due to the addition of CaO, 12% of the initial amount of Cr(III) is leached as Cr(VI) between 500 and 600 °C. The presence of KOH leads to leaching of 49% at 800 °C, and with the addition of NaOH even 79% of Cr(III) leaches as Cr(VI) at 600 °C. The higher maximum leaching concentrations and the earlier start of increased Cr(VI) leaching for NaOH and KOH (200−300 °C vs 500 °C) in comparison to CaO can be explained by the lower melting temperature of

NaOH and KOH (318 and 406 °C, respectively) in comparison to that of CaO (2572 °C), which improves contact between (molten) hydroxides and Cr_2O_3. The three graphs show a maximum at 600–800 °C. At higher temperatures, Cr(VI) leaching decreases until it reaches values between 0.5 and 3% at 1100 °C. Thermodynamic calculations and kinetic experiments were performed to explain this behavior.

Thermodynamics. The reaction Gibbs free energies for reactions 1–5 were calculated as a function of temperature and are shown in Figure 2. The results indicate that the oxidation of

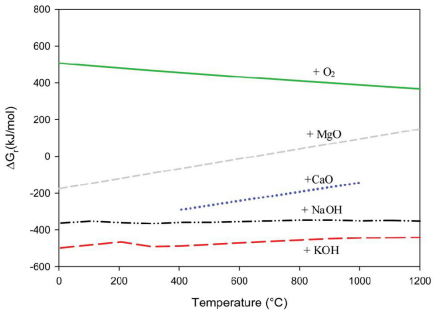

Figure 2. Reaction Gibbs free energies as a function of temperature for the formation reactions of chromates starting from Cr_2O_3, or Cr_2O_3 mixed with NaOH, KOH, CaO, or MgO.

Cr_2O_3, $Cr_2O_3 + {}^3/_2O_2 \leftrightarrow 2CrO_3$, does not take place in the temperature range studied (0–1200 °C), as the reaction Gibbs free energy is positive over the entire range. Oxidation in the presence of MgO is thermodynamically feasible for temperatures up to 650 °C, but the reaction Gibbs free energy is less negative than for the reaction in the presence of CaO, KOH, or NaOH. For the latter reactions, the reaction Gibbs free energy is negative over the whole temperature range studied. These results correspond very well with Figure 1 at the temperatures where maximum leaching was observed (600–800 °C).

The reaction Gibbs free energies for the formation of the respective chromates and chromites of calcium and sodium are shown in Figure 3. The thermodynamic data show that in the case of CaO, the formation of calcium chromate is favored over the formation of calcium chromite at temperatures up to 1000 °C. At higher temperatures, there is a lack of accurate thermodynamic data, but the trend of the Gibbs free energies suggests that the formation of calcium chromite might become dominant at temperatures higher than 1300 °C.

For sodium (shown as an example in Figure 3) and potassium (not shown), the reaction Gibbs free energies for chromite formation are much higher than for chromate formation, meaning that the formation of chromates is favored.

Kinetics. Thermodynamics alone does not suffice to describe the shape of the curves in Figure 1. Reaction Gibbs free energies as a function of temperature, as in Figure 2, do not explain the increase or the decrease of the Cr(VI) leaching as a function of temperature in Figure 1. Therefore, a kinetic study was performed using the synthetic mixture of Cr_2O_3 and NaOH, which showed the highest leaching in the earlier tests. Kinetic studies were performed in two temperature intervals:

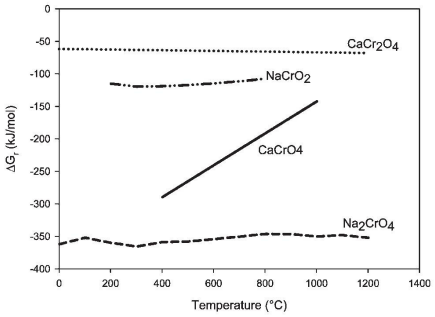

Figure 3. Reaction Gibbs free energy as a function of temperature for the formation of calcium and sodium chromates and chromites.

(1) at 300, 500, and 700 °C, where the Cr(VI) leaching from Figure 1 increases as a function of temperature, and (2) at 700, 800, and 900 °C, where the Cr(VI) leaching decreases again.

In Figure 4, the leaching of Cr(VI) as a function of heating time is shown for three different temperatures: 300, 500, and

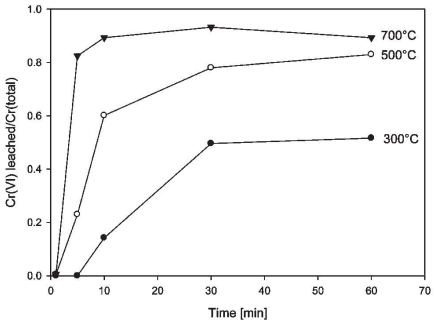

Figure 4. Cr(VI) leaching as a function of heating time for three temperatures (300–700 °C) for a 95% NaOH–5% $Cr2O_3$ mixture.

700 °C. For a given heating time (e.g., 30 min), the leaching increases from 300 to 700 °C, and maximum leaching is reached faster at higher temperatures. At 300 °C, the Cr(VI) leaching is 52% of the initial Cr content after 60 min; at 500 and 700 °C, the leaching reaches 83 and 89%, respectively. The higher leaching at 500 and 700 °C after 60 min is related to the fact that above the melting temperature of NaOH (318 °C) contact between molten NaOH and Cr_2O_3 improves, resulting in a higher leaching for the time intervals shown. The leaching ratios after 30 min from Figure 4 can be related to those from Figure 1 at the same temperatures. It can be concluded that kinetics are able to explain the oxidation behavior up to 700 °C.

At temperatures above 700 °C, the amount of leached Cr(VI) for a residence time of 30 min (Figure 1) starts to decrease again. Paoletti suggested that in the presence of CaO, a possible explanation for the reduced Cr leaching at temperatures above 850 °C could be the formation of calcium

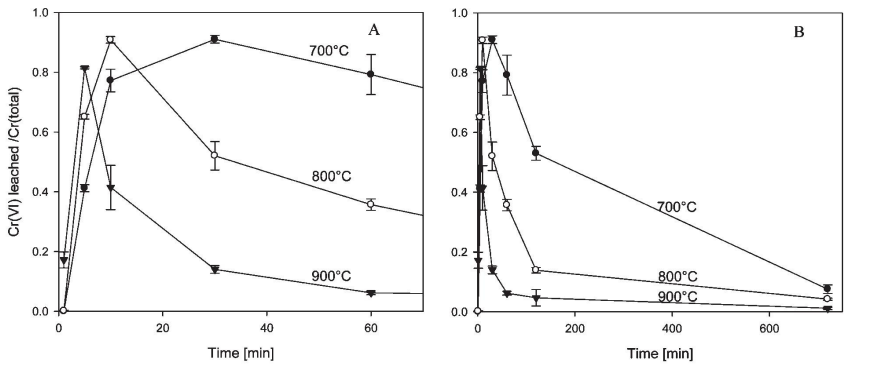

Figure 5. Cr(VI) leaching as a function of heating time (A, 0–60 min; B, 0–12 h) for three temperatures (700–900 °C) for a 95% NaOH–5% $Cr2O_3$ mixture.

chromite, competing with the formation of calcium chromate. However, the present thermodynamic calculations (Figure 3) indicate that chromite formation in the presence of alkali and alkaline earth salts is less favorable than chromate formation at temperatures up to 1200 °C, so that the decrease in Cr(VI) leaching cannot be explained by the formation of these chromites.

Figure 5A and B show the results of kinetic experiments at three different temperatures (700, 800, and 900 °C) for residence times between 1 min and 12 h. In Figure 5A, an enlargement of Figure 5B for residence times up to 60 min is shown. For all three temperatures, a maximum in leaching is observed (81–91%). Again, the maximum is reached faster at higher temperatures, in agreement with the observations from Figure 4. After the maximum has been reached, the Cr leaching decreases significantly at 800 and 900 °C. After 60 min at 900 °C, the Cr leaching is reduced to 6% and at 800 °C to 36%, but at 700 °C it is still 80% of the initial amount of Cr.

In Figure 5B, results for residence times up to 12 h are shown. From these results, it is clear that also at 700 °C, the Cr leaching decreases, but this decrease starts later and is slower than at 800 and 900 °C. After 12 h, the leached percentage of the initial Cr amount is below 8% for all three temperatures.

As previously explained, thermodynamic calculations indicate that chromates are still formed at these temperatures (700–900 °C). This is confirmed by observation of the color of the heated samples: as Cr_2O_3 is converted to CrO_4^{2-}, its color changes from green to yellow. Although leaching at elevated temperatures (e.g., for the sample heated for 60 min at 900 °C) is low, the samples are still as yellow as at lower temperatures where high Cr(VI) leaching was observed, indicating that Cr(VI) is present but does not leach. The decreased Cr(VI) leaching can be explained as follows: after heating and removal of the samples from the oven, the samples are rapidly cooled at room temperature, resulting in the formation of an amorphous, glassy chromate phase, from which leaching of Cr(VI) is prevented. It is clear from Figure 5B that the formation of the glassy phase is slower than the oxidation of Cr(III) to Cr(VI) at 700–900 °C.

The temperature at which Cr(VI) leaching starts to decrease from Figure 1 can now be linked with the melting temperature of the chromates. In the presence of NaOH, the leaching of calcium chromate starts to decrease after 600 °C; in the presence of KOH, the decrease starts after 800 °C, whereas the melting temperatures of Na_2CrO_4 and K_2CrO_4 are 792[24] and 980 °C,[11] respectively. The temperature difference between the points where the leaching starts to decrease is comparable to the temperature difference between the melting points. The presence of NaOH or KOH, which are known to be fluxing agents, explains the fact that the temperatures at which the leaching starts to decrease are lower for the synthetic mixtures than for the pure compounds.

To confirm this theory, the leaching of pure K_2CrO_4, after heating for 30 min at temperatures ranging between 500 and 1100 °C, was evaluated. The percentage of the total Cr amount that is leached is shown in Figure 6. It can be concluded that at temperatures above the melting temperature of K_2CrO_4 (980 °C), the leaching of Cr is strongly reduced.

It can be concluded from this section that the increased leaching concentrations for increasing temperatures up to 600–800 °C shown in Figure 1 could be explained by kinetics. The decrease in Cr(VI) leaching, observed after the maximum leaching was reached, was explained by the formation of a

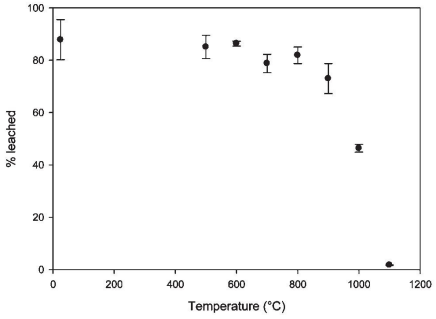

Figure 6. Percentage of Cr(VI) leached after heating K_2CrO_4 for 30 min at 500–1100 °C.

glassy chromate phase, which was formed faster at higher temperatures.

On the basis of reactions 2−5, countermeasures to prevent Cr leaching can be tested. First of all, if no oxygen is present during heating, Cr(III) will of course not be oxidized to Cr(VI). This possibility will be tested in the next section. Second, the alkali and alkaline earth salts can also be bound to other compounds (additives), to prevent them from participating in reactions 2−5. As an additive, $NH_4H_2PO_4$ was chosen because it is thermodynamically less stable than alkali and alkaline earth phosphates, which are in turn more stable than their respective chromates, so the alkali and alkaline earth metals would preferably bind with phosphate, instead of participating in reactions 2−5. The amount of $NH_4H_2PO_4$ that was added (7%) was comparable to the total amount of Ca, Mg, Na, and K in the sludge. The addition of $NH_4H_2PO_4$ reduced Cr leaching from 92% (without addition, Figure 5A) to only 1.4%. This test shows that the earth and alkaline earth salts can be bound to other compounds to prevent them participating in reactions 2−5 that give chromates and is another proof that the proposed reaction mechanisms are correct. This countermeasure will also be tested in the next section.

Thermal Treatment of Contaminated Sludge. The contaminated sludge mainly contains tectosilicates (6.0%), phyllosilicates (26.3%), quartz (31.2%), calcite (3.3%), and organic material (11.6%); the remainder is other or amorphous material. Cr(VI) leaching from the pelletized industrial sludge as a function of heating temperature is shown in Figure 7. For unheated samples and samples heated up to 500 °C, almost no Cr(VI) leaching is detected. Also, no Cr(VI) was detected in a pH-dependent leaching test of the unheated sample for the relevant pH range (7−12.5), carried out in this study. From 500 °C on, Cr(VI) leaching increases and reaches about 25 mg/kg at 600−700 °C, thus exceeding the limit value for use of waste material as a secondary raw material (0.5 mg/kg DM) in Flanders[25] significantly, almost 50 times. All of this indicates that Cr(VI) is formed during thermal treatment. Around 13% of the total amount of Cr present in the sludge (184 mg/kg) is leached as Cr(VI) after heating at 600−700 °C. After heating between 700 and 800 °C, the Cr(VI) leaching starts to decrease, but only after heating at 1100 °C is the concentration below the regulatory limit again.

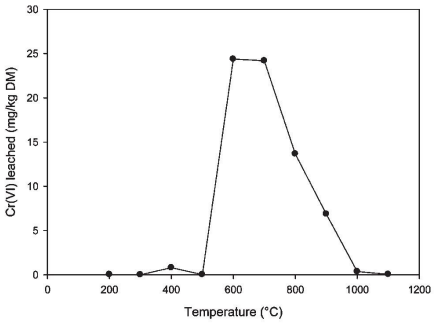

Figure 7. Leaching behavior of Cr(VI) from industrial sludge fired at temperatures between 200 and 1100 °C.

The behavior of the Cr(VI) leaching as a function of temperature is rather similar to the behavior observed for synthetic mixtures of Cr_2O_3 with Ca, Na, or K salts (Figure 1). This indicates that the elevated Cr(VI) leaching in the thermally treated industrial sludge can be attributed to reactions 2−5. Moreover, XRD measurements of the samples showed that the total amount of amorphous material is constant (about 30%) up to 1000 °C and increases to around 60% at 1100 °C. The decrease in Cr(VI) leaching between 700 and 1000 °C can thus not be explained by vitrification of the sample as a whole but should be attributed to the chromates forming a glassy phase from 700 °C on and preventing Cr from leaching, as explained before. In the synthetic samples, Cr(VI) leaching started between 200 and 500 °C, whereas for the contaminated sludge it only started at 600 °C. This can be explained by the presence of organic material in the contaminated sludge (11.5 wt %), which needs to be oxidized first, before Cr(III) can be oxidized to Cr(VI).

The shape of the Cr(VI) leaching as a function of heating temperature from Figures 1 and 7 is comparable to earlier literature findings. Prokisch et al.[26] studied the speciation of chromium during sludge incineration at temperatures between 200 and 1200 °C and observed Cr(III) oxidation to Cr(VI), with a maximum in extractable chromate concentration at 500 °C. Wang et al.[4] studied thermally treated municipal solid waste incinerator fly ash, spiked with Cr_2O_3, between 600 and 1000 °C and observed elevated Cr(VI) leaching, with a maximum in total Cr leaching at 900 °C. At 800 °C, the Cr_2O_3 peak on the XRD pattern was decreased, while the peak of K_2CrO_4 was increased. Chang et al.[1] sintered metal sludge from industrial wastewater treatment plants mixed with mining residues at temperatures between 850 and 1250 °C in order to obtain lightweight aggregates. A maximum in Cr leaching was observed at 950 °C, and the leaching was strongly reduced at 1250 °C. All of these observations, which were not or only partly explained in literature, can now be explained with the results from this paper.

The countermeasures described in the previous chapter can also be tested for this industrial sludge. Heating under an inert atmosphere at 700 °C for 30 min reduced Cr(VI) leaching, which was 24.2 mg/kg (Figure 7) after heating in ambient air, to 0.42 mg/kg.

A second method that was tested to prevent Cr oxidation is the addition of $NH_4H_2PO_4$, which was shown to be an effective method for the synthetic samples. For the industrial sludge, the measured Cr(VI) leaching was reduced from 24.2 mg/kg in an untreated sample to only 0.018 mg/kg for a sample to which $NH_4H_2PO_4$ was added and which was heated at 700 °C for 30 min.

Cr(VI) formation can thus be reduced by working under inert atmosphere or by adding an appropriate compound that binds the alkali and alkaline earth salts in the sample.

■ AUTHOR INFORMATION

Corresponding Author

*Phone: +32 16 3 22353. Fax: +32 16 3 22991. E-mail: bram.verbinnen@cit.kuleuven.be.

Notes

The authors declare no competing financial interest.

REFERENCES

(1) Chang, F. C.; Lo, S. L.; Lee, M. Y.; Ko, C. H.; Lin, J. D.; Huang, S. C.; Wang, C. F. Leachability of metals from sludge-based artificial lightweight aggregate. *J. Hazard. Mater.* **2007**, *146* (1−2), 98−105.

(2) Xu, G. R.; Zou, J. L.; Li, G. B. Stabilization of heavy metals in ceramsite made with sewage sludge. *J. Hazard. Mater.* **2008**, *152* (1), 56−61.

(3) Abbas, Z.; Steenari, B. M.; Lindqvist, O. A study of Cr(VI) in ashes from fluidized bed combustion of municipal solid waste: leaching, secondary reactions and the applicability of some speciation methods. *Waste Manage.* **2001**, *21* (8), 725−739.

(4) Wang, K. S.; Sun, C. J.; Liu, C. Y. Effects of the type of sintering atmosphere on the chromium leachability of thermal-treated municipal solid waste incinerator fly ash. *Waste Manage.* **2001**, *21* (1), 85−91.

(5) Stam, A. F.; Meij, R.; Winkel, H. T.; van Eijk, R. J.; Huggins, F. E.; Brem, G. Chromium Speciation in Coal and Biomass Co-Combustion Products. *Environ. Sci. Technol.* **2011**, *45* (6), 2450−2456.

(6) Hu, H.; Luo, G.; Liu, H.; Qiao, Y.; Xu, M.; Yao, H. Fate of chromium during thermal treatment of municipal solid waste incineration (MSWI) fly ash. *Proc. Combust. Inst.* **2013**, *34* (2), 2795−2801.

(7) Hyks, J.; Nesterov, I.; Mogensen, E.; Jensen, P. A.; Astrup, T. Leaching from waste incineration bottom ashes treated in a rotary kiln. *Waste Manage. Res.* **2011**, *29* (10), 995−1007.

(8) Vangelatos, I.; Angelopoulos, G. N.; Boufounos, D. Utilization of ferroalumina as raw material in the production of Ordinary Portland Cement. *J. Hazard. Mater.* **2009**, *168* (1), 473−478.

(9) Sinyoung, S.; Songsiriritthigul, P.; Asavapisit, S.; Kajitvichyanukul, P. Chromium behavior during cement-production processes: A clinkerization, hydration, and leaching study. *J. Hazard. Mater.* **2011**, *191* (1−3), 296−305.

(10) Chen, Y. L.; Chang, J. E.; Lai, Y. C.; Ko, M. S. Effects of sintering atmosphere on cement clinkers produced from chromium-bearing sludge. *J. Air Waste Manage. Assoc.* **2012**, *62* (5), 587−593.

(11) Lehmusto, J.; Lindberg, D.; Yrjas, P.; Skrifvars, B. J.; Hupa, M. Thermogravimetric studies of high temperature reactions between potassium salts and chromium. *Corros. Sci.* **2012**, *59*, 55−62.

(12) McLean, J. E.; Bledsoe, B. E. Behavior of metals in soils. *EPA Ground Water Issue*; Technology Innovation Office, Office of Solid Waste and Emergency Response, University of Minnesota: Minneapolis, MN, 1992.

(13) Paoletti, F. Behavior of oxyanions forming heavy metals in municipal solid waste incineration. Ph. D. Dissertation, Institute for Technical Chemistry: Karlsruhe, Germany, 2002.

(14) Xu, H. B.; Zhang, Y.; Li, Z. H.; Zheng, S. L.; Wang, Z. K.; Tao, Q.; Li, H. Q. Development of a new cleaner production process for producing chromic oxide from chromite ore. *J. Clean Prod.* **2006**, *14* (2), 211−219.

(15) El-Hasan, T.; Szczerba, W.; Buzanich, G.; Radtke, M.; Riesemeier, H.; Kersten, M. Cr(VI)/Cr(III) and As(V)/As(III) Ratio Assessments in Jordanian Spent Oil Shale Produced by Aerobic Combustion and Anaerobic Pyrolysis. *Environ. Sci. Technol.* **2011**, *45* (22), 9799−9805.

(16) Kirk, D. W.; Chan, C. C. Y.; Marsh, H. Chromium behavior during thermal treatment of MSW fly ash. *J. Hazard. Mater.* **2002**, *90* (1), 39−49.

(17) Adell, V.; Cheeseman, C. R.; Doel, A.; Beattie, A.; Boccaccini, A. R. Comparison of rapid and slow sintered pulverised fuel ash. *Fuel* **2008**, *87* (2), 187−195.

(18) Lee, Y. M.; Nassaralla, C. L. Standard free energy of formation of calcium chromate. *Mater. Sci. Eng., A* **2006**, *437* (2), 334−339.

(19) Rajendran Pillai, S.; Khatak, H. S.; Gnanamoorthy, J. B. Formation of $NaCrO_2$ in sodium systems of fast reactors and its consequence on the carbon potential. *J. Nucl. Mater.* **1995**, *224* (1), 17−2424.

(20) Qi, T. G.; Liu, N.; Li, X. B.; Peng, Z. H.; Liu, G. H.; Zhou, Q. S. Thermodynamics of chromite ore oxidative roasting process. *J. Cent. South Univ. Technol.* **2011**, *18* (1), 83−88.

(21) Jacob, K. T. Potentiometric Determination of the Gibbs Free Energy of Formation of Cadmium and Magnesium Chromites. *J. Electrochem. Soc.* **1977**, *124* (12), 1827−1831.

(22) Brittain, R. D.; Lau, K. H.; Hildenbrand, D. L. Mechanism and thermodynamics of the vaporization of K2CrO4. *J. Electrochem. Soc.* **1987**, *134* (11), 2900−2904.

(23) Chase, M. W.; Curnutt, J. L.; Prophet, H.; McDonald, R. A.; Syverud, A. N. Janaf thermochemical tables, 1975 supplement. *J. Coord. Chem.* **1975**, *4* (1), 1−175.

(24) Tathavadkar, V.; Antony, M. P.; Jha, A. Determination of the free energies of formation of $Na_2Cr_2O_4$ and Na_2CrO_4 using the sodium-beta''-Al_2O_3 soled electrolyte. In *Light Metals 2002*; Schneider, W. A., Ed.; Minerals, Metals & Materials Soc: Warrendale, PA, 2002, 31−36.

(25) Order of the Flemish Government for the establishment of the Flemish regulations relating to sustainable management of material cycles and waste. http://navigator.emis.vito.be/milnav-consult/drukwerkWettekstServlet?wettekstId=44119&actueleWetgeving=true&date=27-03-2013&appLang=en&wettekstLang=nl.

(26) Prokisch, J.; Katz, S. A.; Kovacs, B.; Gyori, Z. Speciation of chromium from industrial wastes and incinerated sludges. *J. Chromatogr., A* **1997**, *774* (1−2), 363−371.

2.3 Thermal Treatment of Solid Waste in View of Recycling: Chromate and Molybdate Formation and Leaching Behaviour

Verbinnen, B., Billen, P., Vandecasteele, C. Thermal Treatment of Solid Waste in View of Recycling: Chromate and Molybdate Formation and Leaching Behaviour. Submitted to *Waste Management and Research.*

In **publication 2** the leaching behavior of Cr and Mo after thermal treatment is studied in more detail for two industrial waste streams: the sand fraction of bottom ash from MSW incineration, and contaminated sludge from soil cleaning. Based on the results of publication 1 and on new results of experiments with MoS_2, an explanation for the leaching of Cr and Mo is formulated.

The increase and/or decrease in Cr and Mo leaching observed for synthetic samples also occurs for real industrial materials, and these observations could be explained with the knowledge gained from publications 1 and 2. These findings can help to define optimal heating conditions for high temperature processes aiming at the valorization of contaminated waste.

The experiments in this paper were performed by the candidate. The draft version of the manuscript was prepared by the candidate, while the other authors (P. Billen and C. Vandecasteele) acted as discussion partners and critical reviewers of the manuscript.

THERMAL TREATMENT OF SOLID WASTE IN VIEW OF RECYCLING: CHROMATE AND MOLYBDATE FORMATION AND LEACHING BEHAVIOUR

Bram Verbinnen[1]*, Pieter Billen[1], Carlo Vandecasteele[1]

[1*] ProcESS, Process Engineering for Sustainable Systems, Department of Chemical Engineering, KU Leuven - University of Leuven, W. De Croylaan 46, 3001 Heverlee, Belgium, e-mail: bram.verbinnen@cit.kuleuven.be

Abstract

Elevated Cr and Mo concentrations are often found in leachates of thermally treated solid waste, but there is no general explanation for this so far. Therefore, we studied the leaching behaviour after thermal treatment as a function of heating temperature and residence time for two types of solid waste: contaminated sludge and bottom ash from municipal solid waste incineration. The leaching behaviour of both waste streams was compared with experiments on synthetic samples, allowing deduction of a general mechanism for Cr and Mo leaching. Cr and Mo showed a similar leaching behaviour: after an initial increase, the leaching decreased again at higher temperatures. Oxidation of these elements from their lower oxidation states to chromate and molybdate at temperatures up to 600 °C was responsible for the increased leaching. At higher temperatures, both Mo and Cr leaching decreased again due to the formation of an amorphous phase, incorporating the newly formed chromate and molybdate salts, which prevents them from leaching.

Keywords Chromate formation; Molybdate formation; Leaching; Contaminated sludge; Bottom ash; Thermal treatment; Oxyanions; Recycling

Introduction

Leaching of heavy metals like Ni, Cu, Zn and Pb from bottom ash from municipal solid waste (MSW) incineration was already studied intensively in literature (Arickx et al., 2007; Van Gerven et al., 2007; Hyks et al., 2011). The release of these heavy metals during leaching with water can be related to the presence of organic material in the bottom ash. Fulvic and humic acids are known to form mobile organo-metallic complexes with cations of Cu, Pb, Ni and Zn (Pandey et al., 2000), so that removal or destruction of organic substances decreases the leaching of toxic cations. Additional thermal treatment is applied to oxidise the organic matter and, in some cases, also to obtain a sintered material that can be used in or as building material (Selinger et al., 1997; Bethanis et al., 2004; Van Gerven et al., 2006; Hyks et al., 2011). This treatment was

reported to be an effective way to reduce heavy metal leaching, but some authors also observed increased Cr and/or Mo leaching after such thermal treatment (Selinger et al., 1997; Van Gerven et al., 2006; Hyks et al., 2011).

Not only bottom ash from MSW incineration, but also contaminated sludges can be treated thermally. Again, the reason for treatment is twofold: obtaining a useful ceramic material in view of using it in or as construction material (Chang et al., 2007; Xu et al., 2008; Alonso-Santurde et al., 2008; Gonzalez-Corrochano et al., 2012), and reducing heavy metal leaching by destruction of the humic substances. Various cases are described in literature where these two criteria are met, but analogously to bottom ash, some authors also report increased Cr leaching after thermal treatment (Chang et al., 2007; Xu et al., 2008). The leaching of Mo after thermal treatment of sludges was less reported in literature. Alonso-Santurde et al. (2008) studied the leaching behaviour of sintered contaminated marine sediments and observed for two types of clay an increase in Mo leaching in a leaching test with a liquid to solid (L/S) ratio of 2. Gonzalez-Corrochano et al. (2012) sintered mixtures of inorganic sludge and fly ash and also observed increased leaching of Mo (and As, Sb) after sintering.

Most papers on leaching of heavy metals and/or oxyanions from thermally treated waste streams and residues from thermal processes only report leached concentrations after treatment/incineration at fixed temperatures. However, operating conditions during thermal treatment, such as temperature and residence time, are of major importance to explain the leaching behaviour of most elements, but were seldom evaluated. In a previous publication, Verbinnen et al. (2013) investigated the leaching behaviour of Cr after thermal treatment of synthetic samples containing Cr_2O_3 and alkali and alkaline earth salts. Upon heating, Cr(VI) formation and subsequent leaching in the presence of K, Na and Ca (hydr)oxides was observed. The aim of this paper is to study the leaching behaviour for two types of industrial waste: contaminated sludge and bottom ash from MSW incineration, and to link it with the behaviour observed for synthetic samples to deduce a general mechanism. Moreover, as the behaviour of Cr and Mo, two elements of the same group in the periodic table of elements, was not yet compared previously, the leaching behaviour of Mo will also be studied. The influence of the operating conditions of thermal processes on the leachability of Mo and Cr from the two waste types was studied by heating at a range of temperatures and residence times to obtain more insight into the leaching mechanisms.

Materials and methods

All reagents used were of analytical grade and all experiments were performed at least in duplicate. Thermodynamic calculations were performed using the FactSage thermochemical software.

Six industrial sludges (particle size < 63 µm) were obtained from a soil remediation company. The sludges originate from the cleaning (mainly washing and sieving) of soils with different origin; all are mainly inorganic and contaminated with several heavy metal cations and oxyanion forming

elements. The six sludges were dried at 105°C, ground, and then mixed in equal quantities to obtain a representative, homogeneous sample. About 30 w/w % of ultrapure water (Millipore MilliQ) was added to the mixture and it was pelletised to obtain spheres with a diameter of about 1.5 cm and an average weight of 5 g. The spheres were introduced in a preheated muffle furnace (Heraeus Thermicon P) and heated at temperatures ranging from 200 to 1100 °C for residence times between 0.5 and 6 h. After heating, the spheres were ground (< 4 mm). Ultrapure water was added to the material to obtain an L/S ratio of 10 (according to DIN 38414-S) and a 24 h leaching test was performed on a shaking device (Gerhardt Laboshake) rotating at 160 rpm. The supernatant was filtered over a 0.45 µm membrane filter (Chromafil) and element concentrations were measured with ICP-MS (Thermo Xi series). All concentrations were reported in mg or g per kg dry matter. Cr(VI) concentrations were also measured spectrophotometrically in some selected samples using the diphenylcarbazide method. The soil organic matter (SOM) content was determined by heating the samples at 550 °C for 4 h.

The sand fraction of bottom ash (i.e. the fraction 65 µm – 2 mm obtained after size separation and ferrous and non-ferrous separation, representing 13 % of the total amount of bottom ash) from a grate furnace incinerating MSW was dried at 105°C and was subjected to the same heat treatment as the sludge. To facilitate reading, the sand fraction of the bottom ash is always referred to as 'bottom ash'. Organic matter content and leached concentrations were determined in the same way as for the sludge. To determine the total metal concentrations for both waste types, digestion of the solid matrix was performed by the successive addition of 5 ml HNO_3, $HClO_4$ and HF to 0.1 g of the sample and boiling the mixture. After digestion, the excess acid was evaporated, the solutions were transferred to 100 ml volumetric flasks and the metal concentrations were determined with ICP-MS.

Pure K_2CrO_4 was heated at 1100 °C for 30 min with and without SiO_2 and pure $Na_2MoO_4.2H_2O$ was mixed with SiO_2 and heated at 950 °C for 30 min. After cooling, the samples were leached for 24 h with ultrapure water and an L/S ratio of 1000 (K_2CrO_4) or 20 ($Na_2MoO_4.2H_2O$). The supernatant was filtered over a 0.45 µm membrane filter and Cr or Mo concentrations were measured with ICP-MS.

Results and discussion

Total and leached concentrations of sludge and bottom ash

In Table 1, total and leached concentrations of matrix and trace elements in the sludge and bottom ash are shown. Bottom ash contains a higher total amount of cation forming heavy metals Ni, Cu, Zn and Pb than sludge, although the leached concentrations are comparable to or lower than those of sludge. This can partly be explained by the difference in pH (Table 1), but the higher organic content of the sludge might be the most important factor, as humic substances form highly soluble organo-metallic complexes with cations (Pandey et al., 2000). Elemental carbon formed during incineration is also included in the organic matter content of bottom ash (5.2 %).

Table 1: Total and leached concentrations of matrix (g kg^{-1}dry matter) and trace elements (mg kg^{-1} dry matter), pH and organic matter content for contaminated sludge and bottom ash.

	Sludge		**Bottom ash**	
	Total conc.	Leached conc.	Total conc.	Leached conc.
Na (g kg^{-1})	7.26		30.9	
Mg (g kg^{-1})	8.32		15.9	
Al (g kg^{-1})	52.4		65.9	
K (g kg^{-1})	20.0		15.9	
Ca (g kg^{-1})	29.3		106	
Fe (g kg^{-1})	54.0		89.6	
Cr (mg kg^{-1})	184	0.13	238	0.36
Ni (mg kg^{-1})	95	1.3	171	0.026
Cu (mg kg^{-1})	199	4.4	4710	4.4
Zn (mg kg^{-1})	1450	3.8	4090	0.024
As (mg kg^{-1})	10.0	0.21	< 5.0	0.017
Se (mg kg^{-1})	3.31	0.11	< 5.0	0.22
Mo (mg kg^{-1})	14.0	2.0	19.6	1.6
Cd (mg kg^{-1})	23.9	0.017	6.74	< 0.01
Sb (mg kg^{-1})	24.2	0.40	103	0.47
Pb (mg kg^{-1})	509	0.0017	1530	< 0.01
SOM (wt %)	22.0		5.2	
Leachate pH	7.58		10.80	

For bottom ash, only Cu leaching exceeds the regulatory limit for use in or as building material (0.5 mg kg^{-1}, Flemish Government Order 2008). The stability of the Cu – humic acid complex is higher than that of any of the other metal – humic acid complexes (Van Gerven et al., 2007; Pandey et al., 2000), thus explaining the elevated leaching of only Cu from the bottom ash. Bottom ash contains more Na and less K than the sludge, which may be of importance when Cr leaching as a function of heating temperature is considered in section 3.3. These alkali metals can have an influence on the Cr leaching behaviour upon heating (Verbinnen et al., 2013).

Leaching of heavy metals after heat treatment

In Figure 1A, leaching of cation forming heavy metals Ni, Cu and Zn is shown after heating of contaminated sludge for 30 min at temperatures between 200 °C and 1100 °C. In the untreated material (shown in the figure at 105 °C, the temperature at which the samples were dried), the limit values for use in or as building material for Ni (0.75 mg kg^{-1}), Cu (0.5 mg kg^{-1}) and Zn (2.8 mg kg^{-1}, Flemish Government Order 2008) are exceeded, but upon heating, leaching of these three elements decreases. Simultaneously, decrease of the SOM content is observed (Figure1B), from 22 % initially to 6.3 % at 400 °C.

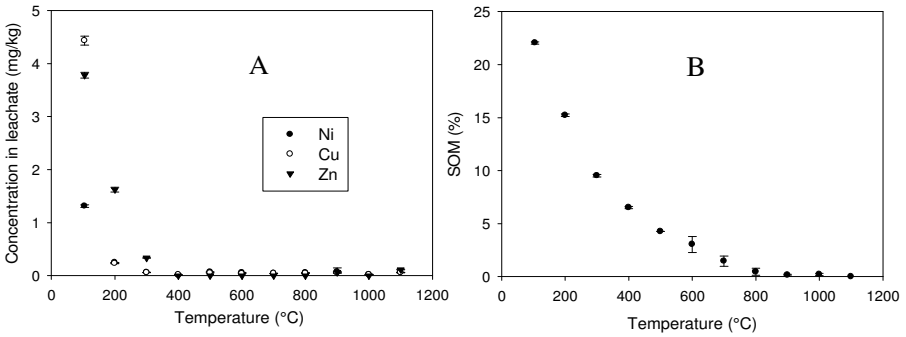

Figure 1. Leaching of Ni, Cu and Zn (A) and SOM (B) for contaminated sludge heated at 200 – 1100 °C for 30 min.

Although there is still a significant amount of organic material left at that temperature, no more leaching of heavy metals is observed. Complexation of cations by humic substances is mainly attributed to the presence of carboxylate and phenolate functional groups (Martyniuk et al. 2001).The decarboxylation of humic substances already starts at 200 °C or even at lower temperatures (Smidt and Lechner, 2005; Martyniuk et al., 2001; Kolokassidoe et al. 2007). This explains why in these experiments, a significant decrease in heavy metal leaching is observed at 200 °C, where the SOM content is only reduced from 22 to 15 %.

There was no significant change in pH - another crucial parameter when looking at heavy metal leaching - observed at temperatures up to 400 °C, so a pH change did not influence Ni, Cu or Zn leaching after treatment at these temperatures. The reduced leaching can thus be attributed to reduced formation of highly soluble organo-metallic complexes. A similar observation was made for the leaching of Cu from bottom ash (not shown): both the organic matter content and Cu leaching were reduced upon heating.

The leaching of the heavy metals Ni, Cu and Zn could thus be reduced significantly by heating the samples (Figure 1A and B). However, earlier research (Verbinnen et al., 2013) showed that heating of Cr contaminated waste can lead to elevated Cr concentrations in the leachate. Cr and Mo are chemically similar elements, appearing in the same group (Group 6) of the periodic table. Therefore, the leaching of both Cr and Mo from contaminated waste upon heating is studied together hereafter.

Leaching of Cr after heat treatment

In Figure 2, the leaching of Cr from contaminated sludge for temperatures between 400 and 900 °C and residence times between 0.5 and 6 h is shown. At 400 °C, there is a small increase in Cr leaching after a residence time of 4 h, but at 600 and 700 °C, Cr leaching increases immediately with increasing residence times. The leached concentration reaches around 25 mg kg^{-1} after 6 h at 600 °C, which is 50 times the

regulatory limit for use in or as building material (0.5 mg kg^{-1}, Flemish Government Order 2008). At higher temperatures (800-900 °C), Cr leaching is higher than for untreated samples, but the values observed at 600 and 700 °C are not reached anymore. Cr(VI) measurements in some selected samples showed that all Cr detected in ICP-MS measurements was actually Cr(VI), as can be expected due to the high mobility of Cr(VI) compounds.

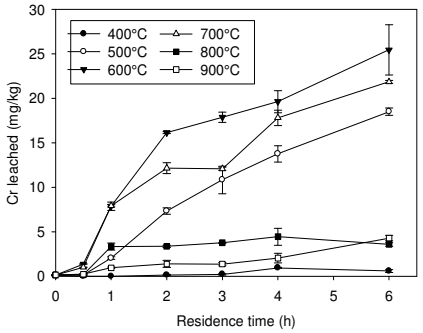

Figure 2. Leaching of Cr from contaminated sludge heated at 400 – 900 °C for 0.5 – 6 h.

Figure 3 shows Cr leaching of bottom ash for temperatures between 400 and 700 °C and residence times between 0.5 and 6 h. An increase in Cr leaching is observed at 400 °C up to values around 5 mg kg^{-1} and at 500 °C, a concentration of 22 mg kg^{-1} is reached. At 600 °C, Cr leaching increases to 18 mg kg^{-1} after 1 h, but decreases after longer residence times. At 700 °C, this decrease already starts after 30 min.

The Na/K ratio for bottom ash is 1.94, whereas for contaminated sludge this ratio is 0.63. Therefore, it is likely that more Na_2CrO_4 is formed in the bottom ash than in the sludge, where more K_2CrO_4 is formed.

For contaminated sludge (Figure 2) maximum leaching is observed after heating at 600-700 °C; for bottom ash (Figure 3), the maximum is observed at 500 °C. These maxima are consistent with observations made in a previous study by Verbinnen et al (2013): for synthetic samples, the maximum in Cr(VI) leaching in the presence of K salts was observed at higher temperatures than in the presence of Na salts.

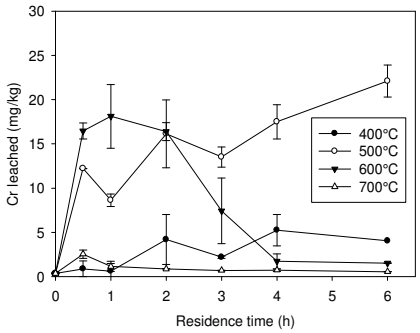

Figure 3. Leaching of Cr from bottom ash heated at 400 - 700 °C for 0.5 – 6 h.

A decrease in Cr leaching is observed at temperatures above 800 °C for sludge and above 600 °C for bottom ash. To ensure that this decrease is not due to volatilisation of Cr, the total concentration was determined for sludge heated at 1100 °C for 30 min. The average Cr concentration was 311 mg kg^{-1}, higher than in the untreated material, that can be explained by the decomposition of organic matter and certain minerals (e.g. carbonates), and shows that Cr is not volatilised.

Some authors describe a similar decrease in Cr leaching at elevated temperatures and several explanations were reported for this. Some suggest that Cr(VI) can be reduced to

Cr(III) by more reducing conditions at higher temperatures (Sorensen et al., 2000; Wei et al., 2005). However, their heating conditions differed much from the conditions in this paper as they heated their samples in covered crucibles, which promotes reduction due to lack of oxygen. Furthermore, for bottom ash heated at 600 and 700 °C in this study, Cr(VI) is formed initially, indicating oxidising conditions, and after longer residence times, the Cr leaching decreased again. Other authors claim that Cr(VI) can be reduced by reducing compounds in the samples, e.g. metallic aluminium (Astrup et al., 2005; Bodenan et al., 2010). This can occur in untreated bottom ash during leaching, but after heating at the oxidising conditions described in this study, metallic aluminium present in the samples is rather oxidised and passivated before Cr(VI) is reduced. The thermodynamic calculations confirm this: e.g. at 800 °C the change in Gibbs free energy of reaction for the oxidation of metallic aluminium is -1328 kJ mol^{-1}, whereas the change in Gibbs free energy of Cr(III) oxidation in the presence of KOH or NaOH is -456 and -346 kJ mol^{-1}, respectively. So thermodynamically, in our experiments metallic aluminium will rather be oxidised than Cr. Furthermore, tests with synthetic samples reported by Verbinnen et al. (2013) showed that Cr(VI) leaching also decreased at elevated temperatures even when no metallic aluminium was present.

Solid solution formation of Cr(VI) with ettringite is also a possible mechanism to explain the decreased leaching in alkaline solid waste (Cornelis et al., 2008), but again, a decrease in Cr(VI) leaching was also observed in synthetic samples where no ettringite was present (Verbinnen et al., 2013), so other mechanisms might dominate in this case.

The available literature seems insufficient to describe the reduced Cr leaching observed in this study adequately. It is hypothesised here that at higher temperatures the newly formed Na and K chromates can form a binary system with SiO_2, resulting in the formation of an amorphous phase after cooling and thus preventing Cr from leaching. This was confirmed by heating synthetic mixtures of K_2CrO_4: when this compound was heated to 1100 °C (well above its melting point), all Cr was leached afterwards. However, when K_2CrO_4 was mixed with SiO_2 and also heated at 1100 °C, the leaching was reduced to below 2 % of the total.

Leaching of Mo after heat treatment

In Figure 4, the leaching of Mo from contaminated sludge for temperatures 400 – 900 °C and residence times between 0.5 and 6 h is shown.

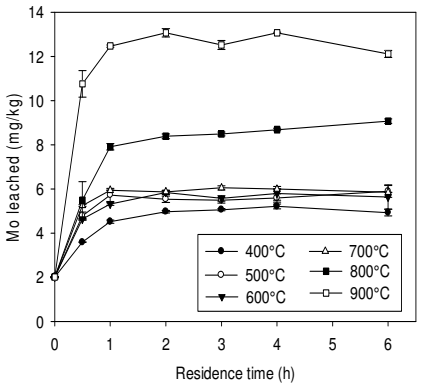

Figure 4. Leaching of Mo from contaminated sludge heated at 400 – 900 °C for 0.5 – 6 h.

At all temperatures, Mo leaching reaches a plateau after 1 h. Between 400 and 700 °C, the amount of Mo leached is 5-6 mg kg^{-1}. At 800 °C, around 8 mg kg^{-1} Mo is leached and at 900 °C almost the entire amount of Mo (around 14 mg kg^{-1}, Table 1) is leached.

The leaching of Mo can be related to the presence of mineral oils in the contaminated sludge. MoS_2 and WS_2 nano and micro particles are commonly used as dry lubricants in mineral oils (Vadiraj et al., 2010). MoS_2 can be oxidised to MoO_3 according to reaction (1); MoS_2 is only slightly soluble, whereas the solubility of MoO_3 exceeds 1g l^{-1} at 20 °C (Zelikman et al., 1966).

$$MoS_2 + 3.5\ O_2 \leftrightarrow MoO_3 + 2\ SO_2 \qquad (1)$$

(Abdel-Rehim 1999)

The change in standard free energy of reaction (1) was calculated with FactSage and is negative throughout the entire temperature range (0 – 1100 °C) relevant to this study. Abdel-Rehim (1999) studied the roasting of Egyptian molybdenite (MoS_2) as a function of temperature; the observed Mo leaching behaviour after heating was comparable to that shown in Figure 4. The lower conversion at lower temperatures was attributed to the formation of a compact thick layer of molybdenum trioxide (MoO_3) around the molybdenite particles that inhibits the diffusion of O_2 and SO_2, so that the reaction rate is low. At higher temperatures the oxide layer becomes friable and porous, and oxidation of MoS_2 can also take place inside the particles (Zelikman et al., 1966; Abdel-Rehim 1999; Marin et al., 2009).

In Figure 5, the leaching of Mo for bottom ash treated at temperatures between 400 and 700 °C and residence times between 0.5 and 6 h is shown. The leaching behaviour differs from that observed for contaminated sludge: only a small increase in Mo leaching is observed at 500 and 600 °C. In the bottom ash, most of the Mo is probably already in its hexavalent state, so that only little oxidation of Mo(IV) occurs during the heat treatment. At 400 °C, Mo leaching as a function of residence time is stable at around 1.5 – 2 mg kg^{-1}. At 500 °C, leaching increases to around 2.5 mg kg^{-1} after 0.5 h heating, probably because the part of Mo that was originally in a lower oxidation state, is oxidised. At 600 °C, Mo leaching initially increases to around 2.5 mg kg^{-1} after a residence time of 1 h, but starts to decrease for longer residence times and reaches a value of around 0.4 mg kg^{-1} after 6 h. At 700 °C, Mo leaching decreases immediately and also reaches a value of 0.4 mg kg^{-1} after 6 h.

The reduced leaching for bottom ash after a residence time of 1 h at 600 °C and the immediate decrease at 700 °C can be explained by the interaction of molybdates

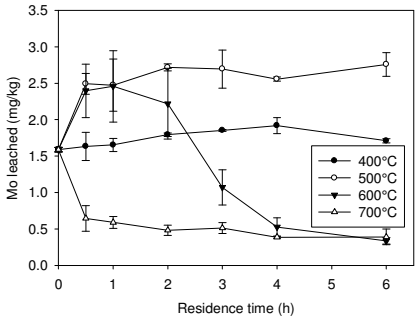

Figure 5. Leaching of Mo from bottom ash heated at 400 – 700 °C for 0.5 – 6 h.

with SiO_2 and formation of an amorphous phase preventing Mo from leaching when cooled. The reduced leaching for bottom ash after a residence time of 1 h at 600 °C and the immediate decrease at 700 °C can be explained by the interaction of molybdates with SiO_2 and formation of an amorphous phase preventing Mo from leaching when cooled. Thermodynamic calculations indicated that the formation of molybdates is thermodynamically favourable (e.g. ΔG_r = -258 kJ mol^{-1} for the formation of Na_2MoO_4 at 800 °C). Mainly Na_2MoO_4, with a melting point of 627 °C (Zelikman et al., 1966) will be formed in the bottom ash due to the high Na content, and it can form an amorphous phase together with SiO_2 from which no Mo can leach.

The hypothesis of the formation of a binary molybdate – SiO_2 system was tested by heating a synthetic mixture of $Na_2MoO_4.2H_2O$ and SiO_2. Similar to Cr, only 11 % of the total Mo content was leached after heating the mixture at 950 °C for 30 min. A similar observation of a molybdate – SiO_2 binary system was, to our knowledge, only reported by Chrenkova et al. (2001), who studied the binary system K_2MoO_4 – SiO_2 and observed a decrease in melting temperature when both components were mixed. The eutectic point was not observed, as they only investigated SiO_2 contents up to 20 %. Determination of the exact eutectic point is beyond the scope of our study, but the decreased melting temperature proves the interaction between molybdates and SiO_2.

The sludge contains more K, so it is likely that mainly K_2MoO_4, with a higher melting point (928 °C, Chrenkova et al., 2001) will be formed. However, the SiO_2 – K_2MoO_4 phase might not be melted yet, as no significant decrease in Mo leaching was observed for the sludge at 900 °C and the lowest reported melting temperature for the binary system K_2MoO_4 – SiO_2 is 913 °C (Chrenkova et al., 2001). Moreover, it might not be very likely that any molybdates are formed in the sludge. Mo is initially mainly present as MoS_2 particles in the organic fraction and will be oxidised to MoO_3, but the formed MoO_3 might not be able to react with alkali metal ions due to diffusion restrictions.

Influence of organic matter

The organic material present in the waste plays an important, yet double role. On the one hand, too much organic material (i.e. humic substances) increases leaching of heavy metals like Cu, Ni, Zn and Pb by the formation of organo-metallic complexes. On the other hand, after destruction of organic matter, Cr(III) can be oxidized to mobile and toxic chromates in the presence of oxygen and alkali or alkaline earth salts. MoS_2 can be oxidized to mobile MoO_3 or molybdates. For instance, at 400 °C, the SOM content of the sludge is reduced from 22 % to less than 7 % after 30 min, and Mo is oxidised and leached. After 3 h, the SOM content is below 2 %, and then Cr leaching also starts to increase. At 700 °C, the organic matter content is already below 2 % after 30 min, and both Cr and Mo leaching increase for higher values of residence time. To control leaching of both cation forming heavy metals and Cr and Mo after heating, an optimal heating temperature and residence time should be defined for every type of waste. For instance for the sludge optimal conditions are heating at 400 °C for 0.5 – 3

h, for which leached concentrations for both Cr and Ni, Cu and Zn are below the regulatory limits. Another option to control leaching of all regulated elements is heating at higher temperatures, where Cr leaching decreases again.

Conclusion

The leaching behaviour of Cr and Mo after thermal treatment of two solid waste types was characterised. The explanation for increased Cr leaching after thermal treatment deduced from experiments with synthetic samples is also relevant for real waste. Cr(III) is oxidised to toxic and mobile Cr(VI) in the presence of K and Na salts in both waste types and the leached concentrations reach up to 25 mg kg^{-1}, 50 times the Flemish regulatory limit for use in or as building material. Moreover, the increased leaching of Mo could also be explained by experiments with synthetic samples. Mo, mainly present as MoS_2 in the untreated material is oxidised to mobile MoO_3 in the contaminated sludge during heat treatment.

At temperatures above 600 °C, the leaching of Cr from bottom ash and sludge and of Mo from bottom ash decreased again with increasing temperatures. At these temperatures, melting of the formed chromates and molybdates in the presence of SiO_2, a binary system that forms an amorphous phase when cooled, prevents Cr and Mo from leaching. Cr and Mo seem to behave similarly during thermal treatment of bottom ash and contaminated sludge. When contaminated waste is thermally treated, the possible elevated leaching of oxyanion forming elements should be taken into consideration.

Funding

This research received no specific grant from any funding agency in the public, commercial, or not-for-profit sectors.

References

Abdel-Rehim AM (1999) Thermal analysis and X-ray diffraction of roasting of Egyptian molybdenite. *Journal of Thermal Analysis and Calorimetry* 57: 415-431.

Alonso-Santurde R, Romero M, Rincon JM, Viguri JR and Andres A (2008) Leaching behaviour of sintered contaminated marine sediments. *Fresenius Environmental Bulletin* 17: 1736-1743.

Arickx S, Van Gerven T, Knaepkens T, Hindrix K, Evens R and Vandecasteele C (2007) Influence of treatment techniques on Cu leaching and different organic fractions in MSWI bottom ash leachate. *Waste Management* 27: 1422-1427.

Astrup T, Rosenblad C, Trapp S and Christensen TH (2005) Chromium release from waste incineration air-pollution-control residues. *Environmental Science & Technology* 39: 3321-3329.

Bethanis S, Cheeseman CR and Sollars CJ (2004) Effect of sintering temperature on the properties and leaching of incinerator bottom ash. *Waste Management & Research* 22: 255-264.

Bodenan F, Guyonnet D, Piantone P and Blanc P (2010) Mineralogy and pore water chemistry of a boiler ash from a MSW fluidized-bed incinerator. *Waste Management* 30: 1280-1289.

Chang FC, Lo SL, Lee MY, Ko CH, Lin JD, Huang SC and Wang CF (2007) Leachability of

metals from sludge-based artificial lightweight aggregate. *Journal of Hazardous Materials* 146: 98-105.

Chrenkova M, Danielik V and Danek V (2001) CALPHAD: Phase diagram of the system KF-K2MoO4-SiO2. *Calphad-Computer Coupling of Phase Diagrams and Thermochemistry* 25: 435-444.

Cornelis G, Johnson CA, Van Gerven T and Vandecasteele C (2008) Leaching mechanisms of oxyanionic metalloid and metal species in alkaline solid wastes: A review. *Applied Geochemistry* 23: 955-976.

Gonzalez-Corrochano B, Alonso-Azcarate J and Rodas M (2012) Chemical partitioning in lightweight aggregates manufactured from washing aggregate sludge, fly ash and used motor oil. *Journal of Environmental Management* 109: 43-53.

Hyks J, Nesterov I, Mogensen E, Jensen PA and Astrup T (2011) Leaching from waste incineration bottom ashes treated in a rotary kiln. *Waste Management & Research* 29: 995-1007.

Kolokassidou C, Pashalidis I, Costa CN, Efstathiou AM and Buckau G (2007) Thermal stability of solid and aqueous solutions of humic acid. *Thermochimica Acta* 454: 78-83.

Marin T, Utigard T and Hernandez C (2009) Roasting kinetics of molybdenite concentrates. *Canadian Metallurgical Quarterly* 48: 73-80.

Martyniuk H, Wiekowska J and Lipman J (2001) The study of influence of metal ions on thermal decomposition of humic acids. *Journal of Thermal Analysis and Calorimetry* 65: 711-721.

Order of the Flemish Government for the establishment of the Flemish regulations relating to sustainable management of material cycles and waste 2008. 9-10.

Pandey AK, Pandey SD and Misra V (2000) Stability constants of metal-humic acid complexes and its role in environmental detoxification. *Ecotoxicology and Environmental Safety* 47: 195-200.

Selinger A, Schmidt V, Bergfeldt B, Vehlow J and Simon FG (1997) Investigation of sintering processes in bottom ash to promote the reuse in civil construction - Part 1: Element balance and leaching. In: *Proceedings of the international conference on the environmental and technical implications of construction with alternative materials* (eds Goumans JJJM, Senden GJ and Van der Sloot HA), Houthem St. Gerlach, The Netherlands, 4-6 June 1997, 41–49. Elsevier Science, Amsterdam.

Smidt E and Lechner P (2005) Study on the degradation and stabilization of organic matter in waste by means of thermal analyses. *Thermochimica Acta* 438: 22-28.

Sorensen MA, Koch CB, Stackpoole MM, Bordia RK, Benjamin MM and Christensen TH (2000) Effects of thermal treatment on mineralogy and heavy metal behaviour in iron oxide stabilized air pollution control residues. *Environmental Science & Technology* 34: 4620-4627.

Vadiraj A and Kamaraj M (2010) Comparative Wear Behaviour of MoS2 and WS2 Coating on Plasma-Nitrided SG iron. *Journal of Materials Engineering and Performance* 19: 166-170.

Van Gerven T, Chen X, Evens R, Hindrix K and Vandecasteele C (2006) Upgrading MSWI bottom ash by extraction, heating or dense medium separation, in view of recycling. In: *Proceedings of the sixth the international conference on the environmental and technical implications of construction with alternative materials* (eds Ilic M, Goumans JJJM, Miletic S, Heynen JJM and Senden GJ), Belgrade, Serbia and Montenegro, May 30 – June 2, 2006, 507-518.

Van Gerven T, Cooreman H, Imbrechts K, Hindrix K and Vandecasteele C (2007) Extraction of heavy metals from municipal solid waste incinerator (MSWI) bottom ash with organic solutions. *Journal of Hazardous Materials* 140: 376-381.

Verbinnen B, Billen P, Van Coninckxloo M and Vandecasteele C (2013) Heating Temperature Dependence of Cr(III) Oxidation in the Presence of Alkali and Alkaline Earth Salts and Subsequent Cr(VI) Leaching Behaviour. *Environmental Science & Technology* 47: 5858-5863.

.

Wei YL, Hsieh HF, Yang YW, Lee JF and Liang WS (2005) Molecular study of thermal immobilization of Chromium(VI) with clay. *Journal of the Air & Waste Management Association* 55: 411-414.

Xu GR, Zou JL and Li GB (2008) Stabilization of heavy metals in ceramsite made with sewage sludge. *Journal of Hazardous Materials* 152: 56-61.

Zelikman AN, Krein OE and Samsonov GV 1966. Metallurgy of rate metals, second ed., Israel Program for Scientific Translations, Jerusalem.

3. Adsorption of oxyanions from industrial wastewater

This chapter presents the research on the removal of oxyanions from industrial wastewater by adsorption. The research aim for this subject was to remove oxyanions from industrial wastewater to increase the options to treat industrial wastewaters. The main focus in this thesis is on the removal of Mo, Sb and Se oxyanions. These three elements are present in the scrubber effluent of an incinerator for hazardous waste, and an appropriate treatment to remove them from the effluent should be developed. The research objectives were defined as follows:

- Characterize and test an adsorbent (zeolite-supported magnetite) for simultaneous removal of Mo, Sb and Se oxyanions from synthetic solutions and industrial wastewater, with specific attention to possible interfering (oxy)anions.
- Develop a new adsorbent (perlite-supported magnetite) that can adsorb different oxyanions simultaneously, based on the good characteristics of zeolite-supported magnetite, but with improved coating of magnetite onto the support material. Test this adsorbent for the simultaneous adsorption of different oxyanions from an industrial wastewater.

The research will be presented by the relevant accepted or submitted papers that are included hereafter. In addition, a summary of the research is given first.

3.1 Summary

Zeolite-supported magnetite, as developed by the Institute of Geotechnics, Kosice, Slovakia, was first tested for the removal of molybdate from a synthetic solution. By determining the adsorption isotherm, studying the effect of ionic strength, the influence of MoO_4^{2-} on the pH_{PZC} of zeolite-supported magnetite and the influence of possible interfering (oxy)anions on the adsorption of molybdate on zeolite-supported magnetite, it could be concluded that MoO_4^{2-} is adsorbed on zeolite-supported magnetite via the formation of an inner-sphere complex. This was confirmed by modeling the adsorption capacity Q as a function of pH (Figure 3.1) with the geochemical modeling software Visual Minteq.

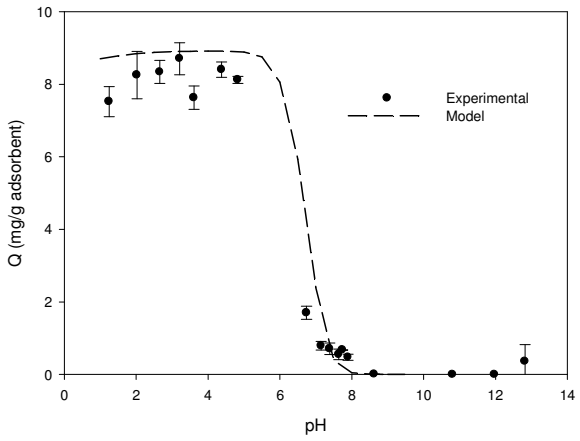

Figure 3.1: Influence of pH on the adsorption capacity of molybdenum on zeolite-supported magnetite (initial molybdenum concentration 5 mg/l, 0.5 g/l adsorbent, 25 °C, 24 h contact time), experimental data and Visual Minteq modeling using the triple layer model.

The best agreement with the experimental results was obtained by modeling the formation of an inner-sphere $FeOMoO_2(OH).2H_2O$ complex. At the ideal adsorption pH of 3, most anions commonly that

occur in wastewater, like Cl^- and SO_4^{2-} do not have a large influence on the adsorption, except PO_4^{3-}.

To test the performance of zeolite-supported magnetite for real wastewaters, the adsorption of Mo, Sb and Se from an industrial wastewater, the scrubber effluent of an incinerator for hazardous waste, was studied. The removal of the different species of Sb and Se (i.e. Sb(III), Sb(V), Se(IV) and Se(VI)) from a synthetic solution containing only one oxyanion was studied first. Similar to Mo(VI) species, Sb(III), Sb(VI) and Se(IV) oxyanions are adsorbed through the formation of an inner-sphere complex, whereas Se(VI) is adsorbed through outer-sphere complex formation. This was also confirmed by modeling the adsorption of the individual compounds with Visual Minteq. After determination of the maximum adsorption capacity and the main interfering compounds for each oxyanion, a synthetic wastewater containing the most important interfering anions occurring in the industrial wastewater was prepared. Comparing the adsorption from the synthetic wastewater with that from the industrial wastewater, this showed that the most important interferences were identified, as the adsorption from both waters was similar. For Mo and Sb, the interferences are mainly other oxyanions, and for Se also anions like Cl^- and SO_4^{2-}. Mo, Sb and Se are all three present in their highest oxidation states in the scrubber effluent, and Mo(VI) and Sb(V) form strong inner-sphere complexes, whereas Se(VI) forms weaker outer-sphere complexes so that its adsorption will also be influenced by anions like Cl^- and SO_4^{2-}. The adsorption order from the industrial wastewater was Mo > Sb > Se and removal efficiencies of 99, 97 and 77 % were obtained for Mo, Sb and Se respectively for an adsorbent concentration of 20 g/l (Figure 3.2).

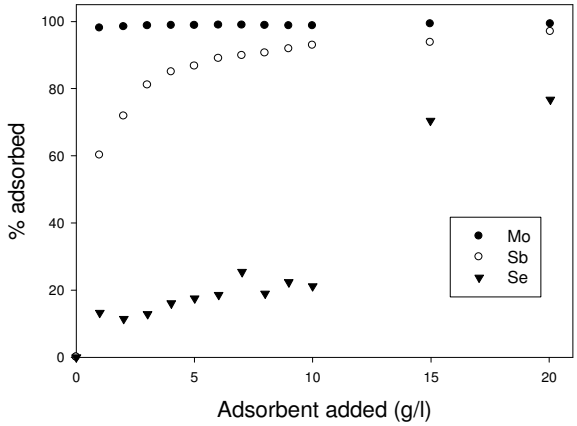

Figure 3.2: Removal percentage for Mo, Sb and Se as a function of amount of zeolite-supported magnetite added for the scrubber effluent of a solid waste incinerator, at pH 3.5

There were some indications that, although high removal efficiencies were obtained, the coating of magnetite onto the support material (i.e. zeolite) was not optimal. During column tests, magnetite detached from the zeolite surface and separate layers of magnetite and zeolite were formed in the column. In order to combine the good adsorption capacities of zeolite-supported magnetite with a better coating, magnetite was coated on some other support materials. Two other zeolite types, bentonite and perlite were tested as support materials, and perlite was chosen as the best host material for magnetite. The good coating of magnetite on the perlite surface is illustrated in Figure 3.3. When a magnet is placed above zeolite-supported magnetite, the magnetite adheres to the magnet, whereas the major part of the zeolite is unattached. Perlite-supported magnetite does not show such a separation: the whole adsorbent adheres to the magnet, indication a better coating of magnetite on perlite than on zeolite.

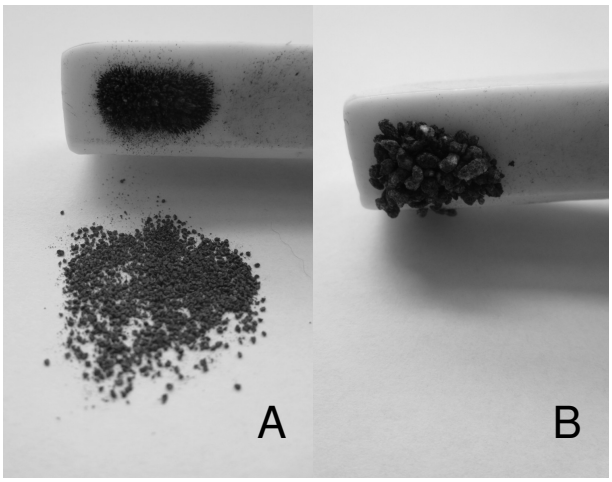

Figure 3.3: Magnetic separation of zeolite-supported magnetite (A) and perlite-supported magnetite (B).

The perlite-coated magnetite was characterized first by determining its specific surface area (55.3 m^2/g) and magnetite content (13 %) and by checking the coating by SEM analysis. It was first tested for the removal of five different oxyanion forming elements in their highest oxidation states (As(V), Cr(VI), Mo(VI), Sb(V) and Se(VI)) from a synthetic solution containing equimolar concentrations of the 5 elements. Simultaneous removal of these oxyanions was most effective at pH values between 3 and 5. Removal percentages of more than 75 % were obtained for AsO_4^{3-}, CrO_4^{2-}, $MoO_4^{2-}$and $Sb(OH)_6^-$ when only 1g/l of the adsorbent was added. The removal efficiency was less for SeO_4^{2-}, as this oxyanion is adsorbed through outer-sphere complexes that are weaker than for the other oxyanions. The adsorption order that could be derived from these tests is Mo(VI) > As(V) > Sb(V) > Cr(VI) > Se(VI).

It was demonstrated that for equal amounts of adsorbent added, perlite-supported magnetite has a higher removal efficiency for oxyanions than commercially available adsorbents and comparable

(coated iron oxides) adsorbents from literature. The removal efficiency for MoO_4^{2-} using the perlite-supported magnetite is more than 99 %, which is much higher than for commercially available adsorbents (removal efficiencies of ca. 29 – 52 %), and the maximal adsorption capacity for CrO_4^{2-} and AsO_4^{3-} removal was also superior to other coated iron oxides described in literature.

The simultaneous removal of the 5 oxyanion forming elements from an industrial wastewater, the scrubber effluent of a waste incinerator, requires higher amounts of adsorbent, as interfering (oxy)anions limit the adsorption capacity for the considered oxyanions. Good results are obtained for Mo, Sb and Se, whereas the removal percentage of As and Cr is rather low (Figure 3.4). The adsorption order also changes compared to the adsorption from synthetic wastewater due to the presence of interfering anions and because Cr is present as Cr(III) in the industrial wastewater, whereas in the synthetic wastewater it was present as Cr(VI).

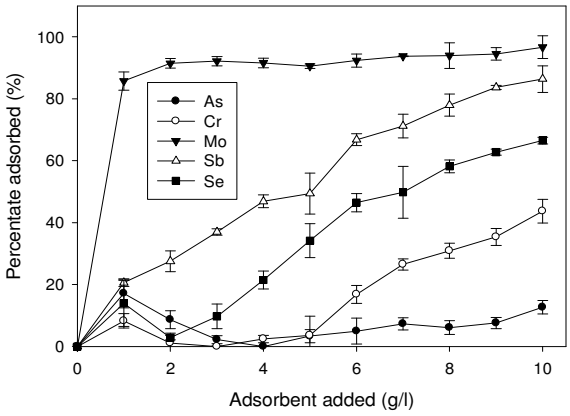

Figure 3.4: Simultaneous adsorption of Cr, As, Se, Mo and Sb from industrial wastewater for perlite-supported magnetite concentrations 1-10 g/l, pH 3.2 and 24 h contact time.

3.2 Removal of Molybdate Anions from Water by Adsorption on Zeolite-Supported Magnetite

Verbinnen, B., Block, C., Hannes, D., Lievens, P., Vaclavikova, M., Stefusova, K., Gallios, G., Vandecasteele, C. (2012). Removal of Molybdate Anions from Water by Adsorption on Zeolite-Supported Magnetite. *Water Environment Research, 84* (9), 753-760.

Publication 3 studies the potential of zeolite-supported magnetite for the removal of Mo oxyanions. The adsorption mechanism (inner- or outer sphere complex formation) is studied by varying the ionic strength of the tested synthetic solution, by performing adsorption modeling with the geochemical software Visual Minteq, by determining the main interfering (oxy)anions and by determining the adsorption isotherm. Furthermore, the ideal pH for adsorption, maximal adsorption capacity and kinetics for the adsorption are determined.

The publication shows that zeolite-supported magnetite has a high affinity for Mo oxyanions, and is only little influenced by competing (oxy)anions. Therefore, it is a promising material for the removal of Mo oxyanions from industrial wastewater.

All experiments were performed by the candidate, with some aid from his thesis student, D. Hannes. All modeling was done by the candidate. M. Vaclavikova and K. Stefusova provided the adsorbent and performed the specific surface area and pore volume measurements. G. Gallios performed the zeta potential measurements. The draft paper was prepared by the candidate, and C. Block, P. Lievens, M. Vaclavikova, G. Gallios and C. Vandecasteele acted as discussion partners and/or critical reviewers of the manuscript.

Erratum: Equation (4) should be replaced by '$\frac{t}{Q} = \frac{1}{k \cdot Q_e^2} + \frac{1}{Q_e} \cdot t$'.

Removal of Molybdate Anions from Water by Adsorption on Zeolite-Supported Magnetite

Bram Verbinnen[1*], Chantal Block[1], Dries Hannes[1], Patrick Lievens[1,2], Miroslava Vaclavikova[3], Katarina Stefusova[3], Georgios Gallios[4], Carlo Vandecasteele[1]

ABSTRACT: Industrial wastewater may contain high molybdenum concentrations, making treatment before discharge necessary. In this paper, the removal of molybdate anions from water is presented, using clinoptilolite zeolite coated with magnetite nanoparticles. In batch experiments the influence of pH, ionic strength, possible interfering (oxy)anions, temperature and contact time is investigated. Besides determination of kinetic parameters and adsorption isotherms, thermodynamic modeling is performed to get better insight into the adsorption mechanism; molybdenum is assumed to be adsorbed as a $FeOMoO_2(OH).2H_2O$ inner-sphere complex. At the optimum pH of 3, the adsorption capacity is around 18 mg molybdenum per gram adsorbent. The ionic strength of the solution has no influence on the adsorption capacity. Other anions, added to the molybdenum solution in at least a tenfold excess, only have a minor influence on the adsorption of molybdenum, with the exception of phosphate. Adsorption increases when temperature is increased. It is demonstrated that the adsorbent can be used to remove molybdenum from industrial wastewater streams, and that the limitations set by the World Health Organization (residual concentration of 70 μg/l Mo) can easily be met. *Water Environ. Res.*, **84,** 753 (2012).

KEYWORDS: molybdenum; zeolite-supported magnetite nanoparticles, adsorption, wastewater treatment, molybdate, oxyanions.

doi:10.2175/106143012X13373550427318

Introduction

Molybdenum and also arsenic, chromium, antimony, selenium, vanadium and tungsten usually occur in solution as oxyanions, containing a central metal or metalloid with several oxygen atoms around it and carrying a negative net charge. So far, (environmental) interest was mainly focused on arsenic, the number one priority pollutant according to U.S. EPA, and on chromium, but nowadays other oxyanions are also considered as "emerging pollutants" (Vandecasteele and Cornelis, 2010).

Molybdenum is mainly used in metallurgical applications as an alloying element in the production of stainless steel or cast-iron alloys (Barceloux 1999), and in the production of flame retardants, pigments and catalysts for high temperature chemical processes. The molybdate ion MoO_4^{2-}, the most common oxyanion of molybdenum, occurs in various types of wastewaters, like wastewater from a styrene monomer plant (1000 mg/l) (Swinkels et al., 2004), scrubber effluent of a municipal solid waste incinerator (0.95 mg/l) (Lievens et al., 2010) and mining water (< 0.1 to 2.2 mg/l) (Dessouki et al., 2005; Panayotova and Panayotov, 2004; Rojas and Vandecasteele, 2007). Traditional industrial wastewater treatment plants remove cations (e.g. Cu^{2+}, Zn^{2+}) by precipitation as their hydroxides. However, this process does not remove oxyanions, so that they may still be present in the effluent (Lievens et al. 2010). Near industrial sources, such as molybdenum mining areas, the molybdenum concentration in surface water may reach concentrations of 200 to 400 μg/l and in groundwater 25 mg/l (Barceloux, 1999). These high concentrations pose health problems to people living in the neighbourhood of mining areas and using well water. Subchronic and chronic oral exposure can result in gastrointestinal disturbances, growth retardation, anaemia, hypothyroidism, bone and joint deformities, sterility, liver and kidney abnormalities, and death (Namasivayam and Sangeetha, 2006). The guideline for molybdenum in drinking water established by the World Health Organization is 70 μg/l. In January 2011, a limit value of 340 μg/l molybdenum was included in the "basic quality standards for surface water" in Flanders (the northern part of Belgium). Molybdenum concentrations in effluent discharges may not exceed this value. Therefore, in order to comply with such legislation, techniques to remove molybdenum from mining water, industrial effluents, ground and surface water are needed.

Most studies on removal of oxyanions from water focus on arsenic in drinking water or in synthetic solutions. However, a number of the methods described for the removal of oxyanions, cannot be applied or are difficult to apply for most process waters and wastewaters, because the residual concentrations are too high (precipitation), because toxic compounds remain after treatment (biological methods), or because clogging and fouling occur unless elaborate pretreatment is applied (ion exchange, membrane techniques).

At high concentrations, oxyanions can be precipitated as their Ca-metalates, but this usually leaves rather high residual concentrations (Swinkels et al., 2004). Adsorption on goethite

[1] University of Leuven, Laboratory of Applied Physical Chemistry and Environmental Technology, Department of Chemical Engineering, K.U. Leuven, W. De Croylaan 46, B-3001 Leuven, Belgium.

[2] Leuven Engineering College Groep T, Department of Chemical Engineering, Vesaliusstraat 13, 3000 Leuven, Belgium.

[3] Institute of Geotechnics, Slovak Academy of Sciences, Watsonova 45, SK-043, Kosice, Slovakia.

[4] Laboratory of General and Inorganic Chemical Technology, School of Chemistry, Aristotle University of Thessaloniki, Gr-540 06, Thessaloniki, Greece.

* University of Leuven, Laboratory of Applied Physical Chemistry and Environmental Technology, Department of Chemical Engineering, K.U. Leuven, W. De Croylaan 46, B-3001 Leuven, Belgium; e-mail: bram.verbinnen@cit.kuleuven.be.

(α-FeOOH) and akageneite (β-FeOOH), is efficient for the removal of different oxyanions at low concentrations (Rovira et al., 2008, Vaclavikova et al., 2008; Watkins et al., 2006; Wainipee et al., 2010). Magnetite has also been used successfully for the adsorption of arsenate and arsenite (An et al., 2011; Jönsson and Sherman, 2008; Su and Puls, 2008;), chromate (Gallios and Vaclavikova, 2008; Yuan et al., 2010), selenite and selenate (Martinez et al., 2006; Missana et al., 2009) and molybdate (Rovira et al., 2006). Methods for the adsorption of molybdenum on other iron oxides like maghemite (Afkhami and Noroz-Asl, 2009) and goethite (Xu et al., 2006a) were also developed. Adsorbents like carbon cloth (Afkhami et al., 2009), modified chitosan resins (Elwakeel et al., 2009), γ-Al_2O_3 (Wu et al., 2000) and $ZnCl_2$ activated coir pith carbon (Namasivayam and Sangeetha, 2006) have been studied in literature. However, as most of these materials are only available as fine powders or are generated in situ as gels, they are difficult to separate in water treatment processes or cause a too large pressure build-up when used in adsorption columns.

New sorbent materials consisting of a matrix (zeolite, activated carbon, aluminum silicates, polymeric structures) hosting various types of adsorbents (e.g., hydrous ferric oxides, maghemite, polymers, HDTMA), have been developed and represent an innovative, attractive and economic approach for the removal of anions such as arsenate (Habuda-Stanic et al., 2008, Schmidt et al., 2008; Vaclavikova et al., 2010), chromate (Misaelides et al., 2008, Barquist and Larsen, 2010), sulphate and phosphate (Oliveira and Rubio, 2007, Vujakovic et al., 2000) and antimonate (Wingenfelder et al., 2006). Vaclavikova et al. (2010) tested zeolite-supported magnetite for the removal of arsenic. This material combines good sorption affinity for oxyanions (from magnetite) with high affinity for cations (from the zeolite matrix). The use of nanoparticles results in a significantly higher sorption capacity than when macroparticles are used, but the separation of nanoparticles alone, by application of a magnetic field, will become more difficult with decreasing particle size (Yavuz et al., 2006). However, because of the size of the host particles, zeolite-supported magnetite can be packed in an adsorption column giving sufficient flow.

In this work a method is investigated to remove molybdate from aqueous solutions to the µg/l level by adsorption on zeolite-supported magnetite. The goal is to study the adsorption mechanism by batch sorption experiments at different pH, adsorbent dose, ionic strength, and temperature. Thermodynamic modelling with the program Visual Minteq is also applied to study the adsorption mechanism. The adsorption isotherm for the adsorption of molybdenum and the adsorption kinetics are investigated, to determine maximal adsorption capacities and equilibration times. The interference of other oxyanions (arsenate, antimonate and antimonite) and of other anions occurring in high concentrations in different wastewaters (sulphate, chloride and phosphate) is also studied.

Materials and Methods

Reagents. All reagents were of analytical grade. Stock molybdenum solutions were prepared by dissolving Na_2-MoO4.2H_2O in ultrapure (Millipore Milli-Q) water. pH was adjusted with HNO_3 or KOH. $NaNO_3$ was used to adapt the ionic strength; H_3AsO_4, Sb_2O_3 and $KSb(OH)_6$, Na_2SO_4 and NaCl were used in the study of interferences by other (oxy)anions. The adsorption capacity of the zeolite-supported magnetite was compared to that of commercially available goethite (Fluka) and hematite (Merck Eurolab) powders.

Table 1—Characteristics of the zeolite-supported magnetite used as adsorbent.

Property	
Magnetite : zeolite ratio	1 : 2
Surface area (m^2/g)	74.2 to 113.5
Pore volume (cm^3/g)	0.118
Water content (%)	5.9

Adsorbent. The zeolite-supported magnetite consists of a zeolite matrix (clinoptilolite type, grain size 400 to 500 µm) hosting synthetic magnetite nanoparticles with an original size of 10 to 40 nm, but that can form clusters with sizes ranging from 20 to 900 nm (Vaclavikova et al., 2004). It was prepared by adding the zeolite to an equimolar solution of Fe(II) and Fe(III) salts. When the pH is increased by adding NaOH, magnetite begins to form and precipitates onto the zeolite (Vaclavicova 2010). The characteristics of this modified zeolite are summarized in Table 1. Zeta potential measurements (Zetameter, Micromeritics) were carried out to determine the point of zero charge (PZC).

Batch Experiments. Sorption experiments were carried out at different pH, adsorbent dose, ionic strength and temperature. To solutions of 5 mg/l molybdenum, 0.5 g/l of zeolite-supported magnetite was added throughout the experiments. After pH adjustment, the molybdenum solutions, together with the zeolite-supported magnetite, were put together in sealed plastic bottles and agitated on a shaking device (Gerhardt Laboshake, 160 rpm). After 24 h (unless stated otherwise), the solution was filtered over a 0.45 µm membrane filter and molybdenum and other relevant elements were determined in the filtrate with ICP-MS (Thermo Xi series). A control solution (pH adjusted, but no zeolite-supported magnetite added) was also agitated, filtered, and analysed.

To study kinetics, solutions containing 5 mg/l molybdenum were brought in contact with 0.5 and 1 g/l adsorbent and the residual molybdenum concentration in solution was determined as a function of time. Removal efficiency was determined by adding varying concentrations of adsorbent (0.025 to 0.175 g/l adsorbent) to a known concentration of molybdenum (0.1 and 1 mg/l).

To determine the adsorption isotherm, 0.5 g/l of the zeolite-supported magnetite was added to solutions with varying concentrations of molybdenum (ranging from 1.5 to 37.5 mg/l); pH and contact time were selected based on preliminary experiments.

To study the effect of competitive anions, different solutions at pH 3, containing 1 mg/l molybdenum and 0.1 g/l zeolite-supported magnetite were spiked with possible interfering oxyanions Sb(III), Sb(V) and As(V), and with chloride, phosphate, and sulphate. The concentrations of these competitive anions were selected according to a realistic case: the effluent of a scrubber of a municipal solid waste (MSW) incinerator (Lievens 2010).

Results and Discussion

Sorption Studies. *Effect of pH.* Experimental data for MoO_4^{2-} adsorption onto zeolite-supported magnetite for equilibrium pH

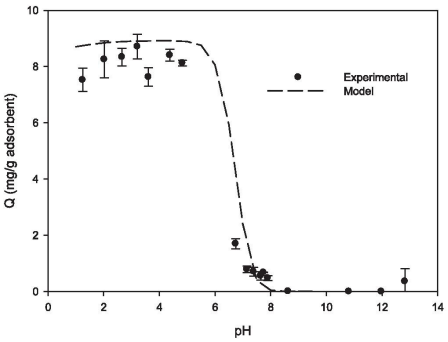

Figure 1—Influence of pH on the adsorption of molybdenum on zeolite-supported magnetite (initial molybdenum concentration 5 mg/l, 0.5 g/l adsorbent, 25 °C, 24 h contact time), experimental data and Visual Minteq modelling using the triple layer model.

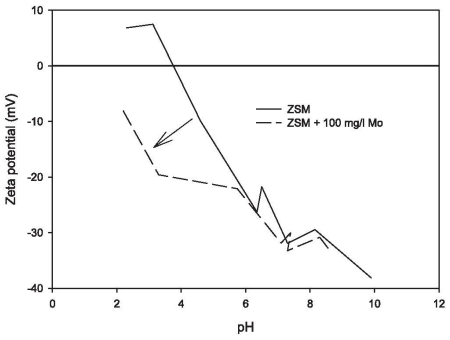

Figure 2—Zeta potential measurements as a function of pH for zeolite-supported magnetite (ZSM) and for mixtures of zeolite-supported magnetite with 100 mg/l molybdenum.

ranging from 1.2 to 12.8 are shown in Figure 1. Measurements of the control solutions (with pH adjusted, but no zeolite-supported magnetite added), showed no molybdenum precipitation within 24 h for this pH range; the molybdenum removal is thus clearly because of adsorption onto the zeolite-supported magnetite. The optimal pH for removal of molybdenum lies between 2 and 5. At a pH lower than 2, the magnetite fraction of the adsorbent goes into solution, resulting in a lower adsorption capacity. This was confirmed by measuring iron (not shown) in the solution after 24 h; the iron concentration increased significantly at a pH lower than 2. At a pH higher than 5, the adsorption of molybdate onto the modified zeolite decreases because the surface becomes more and more negatively charged. Therefore, for most subsequent experiments the pH was adjusted to 3, where maximal adsorption of molybdate, and minimal magnetite or zeolite dissolution (iron concentrations < 0.34 mg/l and aluminium concentrations < 0.012 mg/l) was observed.

It is clear that the synthetic magnetite is responsible for the removal of molybdenum oxyanions from solution as it is well known that zeolites are not effective in removing oxyanions. The effect of pH on the zeta potential of synthetic magnetite in the absence and presence of molybdenum is given in Figure 2. The pH at which the zeta potential is zero is called the point of zero charge (pH_{pzc}) and lies, in the absence of molybdenum, around pH 4.0, in fair agreement with an earlier paper that reported a pH_{pzc} of 4.86 for the same adsorbent (Vaclavikova 2010). Below pH 4, the adsorbent is positively charged. Above pH 4, the negative charge on the magnetite surface increases sharply and the zeta potential reaches about −35 mV at pH 10.0.

In the presence of molybdenum, the zeta potential curve of synthetic magnetite changes drastically and a point of zero charge is no longer observed; the surface charge is negative over the whole pH range studied (2 to 10). This indicates chemical adsorption of molybdate onto the zeolite-supported magnetite, whereby specifically adsorbed anions cause the pH_{pzc} to shift to a lower value (Cornell and Schwertmann, 2003; Stumm and Morgan, 1996).

The graph of the zeta potential as a function of pH shows that the zeta potential in the presence of molybdenum is lower than in the absence of molybdenum until a pH of around 6.5, from where both curves coincide. Before the pH_{pzc}, the surface is positively charged in the absence of molybdenum; in the presence of molybdenum, the soluble negatively charged molybdenum species $HMoO_4^-$ and MoO_4^{2-} are attracted to the surface of magnetite by electrostatic forces and bind chemically to the Fe(III) on the surface of magnetite, giving it a negative charge and lowering the zeta potential, compared to the solution without molybdenum. Even in the region between pH 4 and 6.5, where the overall surface charge is negative because of the decreased H^+ concentration, the attractive specific sorption forces still overcome the repulsive electrostatic forces; molybdenum species coming close to the surface form a chemical bond with Fe(III) on the surface of magnetite, explaining why the zeta potential is still lower than without molybdenum. When specific adsorption is involved, an overall positive surface charge is not required (only $FeOH_2^+$ groups), which explains why adsorption can still occur at pH's above the pH_{pzc} (Cornell and Schwertmann, 2003).

As the pH increases further, the negative charge on the surface increases (mainly FeO^- groups) and the repulsive forces predominate over the attractive forces and do not allow the species (now mainly the strongly negative MoO_4^{2-}) to come close to the surface. So, from pH 6.5 on, the presence of molybdenum has no effect anymore on the surface charge of magnetite, and the zeta potential coincides with that without molybdenum present.

Adsorption Modeling. The effect of the pH on the adsorption of molybdate onto magnetite was modelled with the geochemical modelling software program Visual Minteq. The model is built according to the triple layer model (Davis et al., 1978; Davis and Leckie, 1980; Hayes and Leckie, 1986) for adsorption of molybdate onto magnetite. The triple layer model is a multilayer surface complexation model and adsorption can be modelled in three different layers: ions that adsorb in the o-plane are considered to be inner-sphere complexes, while the adsorption of ions in the β-plane represents the formation of outer-sphere

Table 2—Parameters used for the triple layer model.

Parameter	Value	Reference
Inner layer capacitance C_1 (F m^{-2})	1.13	Sverjensky (2001)
Outer layer capacitance C_2 (F m^{-2})	0.2	Sverjensky (2001)
Surface site density (sites nm^{-2})	2.31	Martinez et al. (2006)
Surface area (m^2 g^{-1})	74.5	This work
Reaction	**Log K**	**Reference**
$FeOH_2^+ \leftrightarrow FeOH + H^+$	- 5.1	Missana et al. (2006)
$FeOH \leftrightarrow FeO^- + H^+$	- 9.1	Missana et al. (2006)
$FeOH + MoO_4^{2-} + 2H^+ + H_2O \leftrightarrow FeOMoO_2(OH).2H_2O$	18.28	Gustafsson (2003)
$2FeOH + MoO_4^{2-} + 2H^+ \leftrightarrow Fe_2MoO_4^{2-} + 2H_2O$	21.6	Balistrieri and Chao (1990)
$FeOH + MoO_4^{2-} + H^+ \leftrightarrow FeOMoO_3^- + H_2O$	11.17	Gustafsson (2003)
$FeOH + MoO_4^{2-} \leftrightarrow FeOHMoO_4^{2-}$	3.14	Gustafsson (2003)

complexes, and the d-plane represents the diffuse layer (Balistrieri and Chao, 1990). The triple layer model uses two capacitance parameters, C1 and C2, that express the charge at the surface relative to the drop in electrical potential at some distance away from the surface (Sverjensky, 2001). These capacitance parameters, and the surface site density for magnetite were obtained from the literature and are summarized in Table 2. Log K values for protonation/deprotonation reactions and possible adsorption reactions are also given in Table 2. Four different inner-sphere complexes were modelled and the best fit was obtained by modelling the formation of a $FeOMoO_2(OH).2H_2O$ complex. The formation of $FeOMoO_2(OH).2H_2O$ is also known to be the main adsorption mechanism for molybdenum onto other iron oxides, like goethite (Xu et al., 2006b) and ferrihydrite (Gustafsson, 2003). In these two papers the complex is noted as $FeOMo(OH)_5$, but here another notation is chosen, to make clear that the adsorbed species is dihydrated molybdic acid. This is in accordance with the predominant molybdenum species at low total concentrations and at low pH in aqueous solution, dihydrated molybdic acid (Gustafson, 2003). For an initial molybdenum concentration of 5 mg/l the modelling results are also shown in Figure 1. The model fits the experimental data very well: the residual molybdenum concentrations predicted are comparable with the experimental results. The conclusion is that the formation of a $FeOMoO_2(OH).2H_2O$ complex is responsible for the adsorption of molybdate onto magnetite.

Effect of Contact Time. In Figure 3 the molybdenum adsorption capacity is shown as a function of the contact time for 2 different adsorbent concentrations, 0.5 and 1 g/l, for an initial molybdenum concentration of 5 mg/l and at pH 3. The results indicate that the equilibrium is achieved within 12 h for an adsorbent concentration of 0.5 g/l and within 3 h for an adsorbent concentration of 1 g/l. Furthermore, it is clear that the uptake of molybdenum is fast at the beginning: 50% of the initial molybdenum quantity is adsorbed after 0.04 h for an adsorbent concentration of 1 g/l. At equilibrium, about the same percentage of molybdenum is removed (72% and 69% for adsorbent concentrations of 0.5 and 1 g/l, respectively) for the two adsorbent concentrations.

Adsorbent Concentration Variation. Two solutions containing molybdenum with starting concentrations of 1 mg/l and 0.1 mg/l at pH 3 were brought in contact with varying concentrations of adsorbent (0.025 to 0.175 g/l). For an adsorbent concentration of 0.1 g/l and an initial molybdenum concentration of 1 mg/l and 0.1 mg/l, a removal efficiency of 72% and 93% was obtained, respectively. For the highest adsorbent concentration of 0.175 g/l removal efficiencies of 99.1% and 98.0%, respectively, were obtained for initial solution concentrations of 1 mg/l and 0.1 mg/

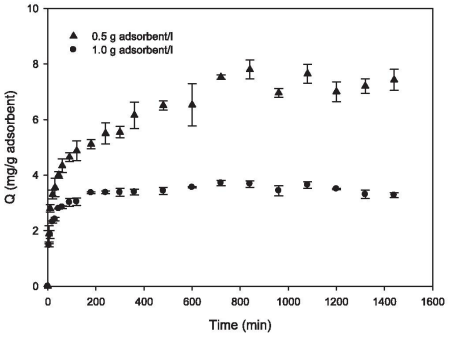

Figure 3—Influence of contact time with zeolite-supported magnetite for removal of molybdenum (initial molybdenum concentration 5 mg/l, pH 3, 25 °C).

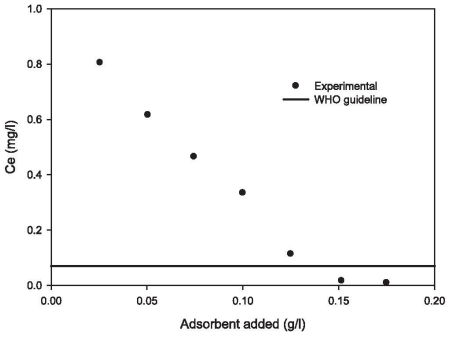

Figure 4—Residual molybdenum concentration as a function of adsorbent concentration (initial molybdenum concentration 1 mg/l, pH 3, contact time 24 h, 25 °C).

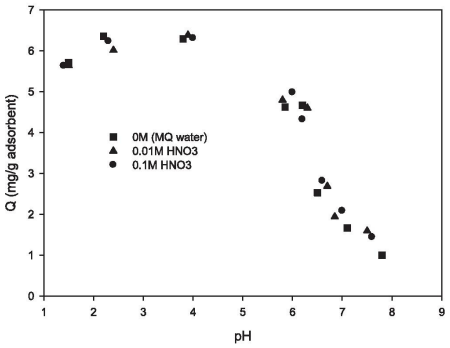

Figure 5—Effect of ionic strength on the adsorption of molybdenum (initial molybdenum concentration 6.4 mg/l, contact time 24 h, 1g/l adsorbent, 25 °C).

l, corresponding to residual concentrations in solution of 9 µg/l and 2 µg/l. These residual concentrations are far below the drinking water limit of the WHO (70 µg/l) (Figure 4).

Effect of Ionic Strength. The ionic strength of a solution can affect the adsorption process: it determines the thickness of the electrostatic double layer around the sorbent particles and can thus influence the electrostatic forces between the sorbent and the species to be adsorbed.

Figure 5 shows the adsorption load for solutions containing 6.4 mg/l molybdenum and 1 g/l adsorbent at varying ionic strength (concentrations of 0, 0.01 and 0.1 M $NaNO_3$) for a range of pH's. It is obvious that molybdenum adsorption is not significantly influenced by ionic strength. This correlates well with zeta potential data and indicates that the interaction between molybdate and magnetite is chemical (chemisorption) rather than electrostatic (physisorption). Chemisorption is not influenced by the extent of the double layer, as there is a specific bond between the charged species and the sorbent surface.

Cation Adsorption and Regeneration. Adsorption of the cations copper and zinc was investigated at pH 3.5, an adsorbent concentration of 0.5 g/l, a contact time of 24 h and at 25 °C; maximum adsorption capacities of 11.15 and 4.20 mg/g respectively, were observed. This shows that the zeolite part of the adsorbent is capable of removing cations, even in an acidic solution, where the adsorbent is positively charged. The adsorption of cations could be a strong advantage for the adsorbent, but in practice, the adsorptions places for the cations (on the zeolite) would be filled much faster than the adsorption places for the oxyanions (on magnetite), because of the high cation concentrations in industrial wastewater. In industrial applications with high cation concentrations, cations are mostly removed by precipitation as their hydroxides.

Regeneration of the adsorbent was investigated with NaOH solutions at pH 8, 10 and 12, with a 0.1M NaCl solution and a 0.1M EDTA solution. None of these solutions gave good results: the desorption of molybdate was too low after 24 h reaction time (between 1.29% and 2.77% molybdenum recovery for NaOH and NaCl solutions respectively), or the magnetite itself was dissolved (for the EDTA solution). The reason for the low desorption is probably because of the strong chemical binding of molybdate with magnetite. The difficult regeneration justifies the choice of zeolite as the supporting material, as this is an inexpensive, readily available material.

Adsorption Isotherms. Experimental data for MoO_4^{2-} adsorption onto the zeolite-supported magnetite at pH 3.0 were fitted using both the Freundlich and Langmuir adsorption model. The Freundlich model belongs to the class of poly-layer models (physisorption); the Langmuir isotherm model to the mono-layer models (chemisorption) (Guo et al., 2010).

The Freundlich adsorption-isotherm is given by eq 1.

$$Q_e = kC_e^{1/n} \quad (1)$$

where Q_e [mg/g adsorbent] is the adsorbed amount per gram adsorbent at equilibrium, C_e [mg/l] is the residual concentration in solution at equilibrium, and k and n are constants.

The Langmuir model is described by eq 2:

$$Q_e = \frac{Q_{max} b C_e}{1 + bC_e} \quad (2)$$

where Q (mg Mo/g adsorbent) is the adsorbed amount at equilibrium, Q_{max} (mg/g) the maximum adsorption capacity, b (l/mg) a constant and C_e the residual molybdenum concentration in solution at equilibrium.

Fitting the experimental data (Figure 6) by the linearized forms (Watkins 2006) of eqs 1 and 2 gave r^2 values of 0.99 (Langmuir model) and 0.75 (Freundlich model). It is clear from the r^2 values and from Figure 6 that the data are significantly better fitted by a Langmuir isotherm. The maximum adsorption capacity Q_{max} for molybdenum as MoO_4^{2-} onto the zeolite-supported magnetite as determined by this model is 17.92 mg Mo/g adsorbent. Maximum adsorption capacities were also determined for commercially available goethite and hematite and were found to be only 1.76 mg/g and 1.43 mg/g, respectively. Xu et al. (2006a) found a maximum adsorption capacity of 15.5 mg/g for the adsorption of molybdate onto goethite (no size reported, surface area 43.96 m^2/g). Afkhami and Noroz-Asl (2009) reported a maximal adsorption capacity of

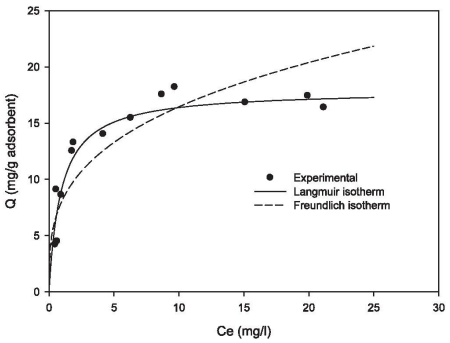

Figure 6—Experimental data fitted with Langmuir and Freundlich isotherms (contact time 24h, 0.5 g/l adsorbent, 25 °C, pH 3).

33.4 mg/g for the adsorption onto maghemite nanoparticles. Both studies were performed with adsorbents consisting of 100% iron oxides, whereas the material in this study consists for only one third of magnetite. Moreover, nanosized materials are not suitable for application in a column because of a large pressure build-up.

Langmuir adsorption indicates chemical bonding between adsorbent and adsorbate, assuming a 1:1 stoichiometry between adsorbate molecule and adsorption site (Stumm and Morgan, 1996), so that finally a monolayer of molybdate molecules is formed on the magnetite surface.

Sorption Kinetics. From Figure 3, giving the adsorption of molybdenum as a function of contact time, it followed that equilibrium is reached after about 3 h for an adsorption concentration of 1 g/l and after about 12 h for an adsorbent concentration of 0.5 g/l. To investigate the kinetics of the molybdenum adsorption onto zeolite-supported magnetite, data from Figure 3 were fitted by the 'pseudo second order' rate equation (Ho 1999).

The 'pseudo second order' (PSO) rate equation is given by eq 3:

$$\frac{dQ}{dt} = k \times (Q_e - Q_t)^2 \tag{3}$$

with k [g/mg·h] is the rate constant, Q_e is the absorbed amount [mg/g adsorbent] at equilibrium and Q the adsorbent amount [mg/g adsorbent] at contact time t. The pseudo second order rate equation, first introduced by Ho and McKay (1999), has been widely applied to describe the kinetics of trace element sorption on different sorbents. The model is based on the assumption that the rate-limiting step is chemisorption of sorbate onto the sorbent. Linearization of eq 3 gives:

$$\frac{t}{Q} = \frac{1}{k \times Q_e^2} + \frac{1}{Q_e} \tag{4}$$

From the correlation coefficients summarized in Table 3, it appears that the 'pseudo second order' rate equation adequately describes the kinetics of the adsorption of molybdenum onto the zeolite-supported magnetite. As the model assumes that chemisorption is the rate-limiting step, the good data fit indicates that molybdate is chemisorbed onto the zeolite-supported magnetite. On using the PSO model, it should be kept in mind that it does not correspond to any specific physical models; it simply approximates well the adsorption data predicted by many different theoretical approaches (El-Khaiary et al., 2010).

The practical parameters $t_{1/2}$, the reaction half life (time needed to adsorb half the amount of molybdenum adsorbed at equilibrium) and h, the initial adsorption rate, were derived from the parameters k and Q_e for adsorbent concentrations of 0.5 and 1 mg/l, using eqs 5 and 6 and are given in Table 3.

$$t_{1/2} = \frac{1}{k \times Q_e} \tag{5}$$

$$h = k \times Q_e^2 \tag{6}$$

Increasing the amount of modified zeolite from 0.5 g/l to 1.0 g/l, leads to a decrease in reaction half life and to an increase of the initial adsorption rate. For the sorbent concentration of 1.0 g/l, 50% sorption is reached after only 0.04 hours ($t_{1/2}$). The adsorption rate constant (k) is much higher for the adsorbent concentration of 1.0 g/l in comparison to 0.5 g/l (respectively 0.17 and 6.76 g/(mg h)). The higher adsorption rate constant indicates that the adsorption goes much faster for an adsorption concentration of 1.0 g/l and the equilibrium is reached faster (Plazinski et al., 2009).

Table 3—Kinetic parameters for the adsorption of molybdenum with zeolite-supported magnetite for a "pseudo second order" rate reaction (initial molybdenum concentration 5 mg/l, pH 3, 25 °C).

	0.5 g adsorbent/l	1 g adsorbent/l
Correlation coefficient (R^2)	0.994	0.996
$t_{1/2}$ (h)	0.84	0.04
h (mg/(g h))	8.56	80
k (g/(mg h))	0.17	6.76

Study of Interferences. Real wastewaters contain many other species that can significantly affect the efficiency of the adsorbent to remove molybdenum. The interference of sulphate, phosphate and chloride and of the oxyanions of Sb(III), Sb(V) and As(V) was investigated. The anions sulphate, phosphate and chloride were added in concentrations of 5 g/l (sulphate, phosphate) or 36 g/l (chloride) to a solution containing 1 mg/l molybdenum and 0.1 g/l adsorbent at pH 3. For sulphate and chloride, these are concentrations as appearing in the effluent of a scrubber of a municipal solid waste (MSW) incinerator (Lievens et al., 2010). Table 4 gives the residual molybdenum concentrations in solutions spiked with the interfering anions, for an adsorption time of 24 h. Without addition of any interfering anion 83% of molybdenum is removed. Sulphate and chloride, even at high concentrations, do not seriously inhibit the removal of molybdenum, as respectively 62% and 56% of the original molybdenum is still removed. The most important interference is PO_4^{3-}. In the presence of 5000 mg/l PO_4^{3-}, 12% of the initial molybdenum amount is adsorbed.

Sb(III), Sb(V), and As(V) were added in a 10/1 ratio to separate solutions containing 1 mg/l molybdenum and 0.1 g/l adsorbent at pH 3: this ratio is much higher than the ratio in the scrubber effluent of the considered municipal solid waste incinerator, where they range from 1.5/1 (Sb/Mo) to 0.08/1 (As/Mo). The residual molybdenum concentrations after 24 h adsorption in the presence of these oxyanions are also given in Table 4. The influence of Sb(III) is the smallest: the residual molybdenum concentration increases from 0.17 mg/l in a solution without interferences to 0.49 mg/l in the presence of an excess of Sb(III), this means that 51% is still removed. In the

Table 4—Interferences study of competitive (oxy)anions for molybdenum adsorption onto modified zeolite (pH 3, 25 °C, 0.1 g/l adsorbent, contact time 24 h).

Interference	Residual concentration (mg/l)
1 mg/l Mo	0.17
1 mg/l Mo + 5000 mg/l SO_4^{2-}	0.38
1 mg/l Mo + 36000 mg/l Cl^-	0.44
1 mg/l Mo + 5000 mg/l PO_4^{3-}	0.88
1 mg/l Mo + 10 mg/l Sb(III)	0.49
1 mg/l Mo + 10 mg/l As (V)	0.59
1 mg/l Mo + 10 mg/l Sb(V)	0.65

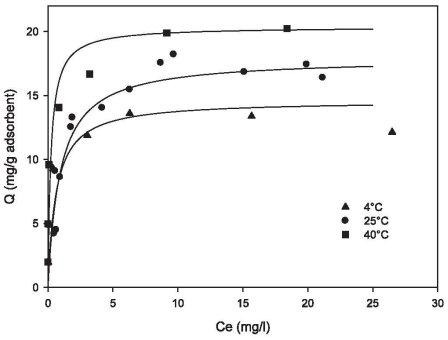

Figure 7—Adsorption isotherms of molybdenum onto modified zeolite as a function of temperature (pH 3, contact time 24 h), with fitted Langmuir isotherms.

presence of a tenfold higher concentration of As(V) or Sb(V), the residual molybdenum concentration increases to 0.59 and 0.65 mg/l, respectively.

All the above findings match well with the theory of Frau et al. (2010) that oxyanions form stronger bonds with iron oxides than with other anions (except phosphate). Chlorides and sulphates (in low concentrations) only form weak outer-sphere complexes that do not compete with (or only have a moderate influence on) the adsorption of oxyanions that form inner-sphere complexes. Phosphates form strong inner-sphere complexes, which can have a major impact on the adsorption of oxyanions. Phosphate is known to form strong inner-sphere complexes with iron oxides (Frau et al., 2010), but even at a 5000 times higher concentration of phosphate, some molybdenum is still adsorbed.

Although the adsorption of molybdenum is influenced by a number of interferences, chemical attraction between adsorbent surface and molybdenum oxyanions is still strong enough to adsorb a significant amount of molybdenum, even when these interferences are present in high concentrations.

Thermodynamics. The adsorption of molybdenum was investigated at three different temperatures: 4, 25 and 40 °C as shown in Figure 7. The maximum adsorption capacity increases from 13.6 mg/g at 4 °C to 20.2 mg/g at 40 °C. This indicates that adsorption of molybdenum is endothermic. As physisorption can only be exothermic, and chemisorption can be both exo- and endothermic (Gupta et al. 2005); this observation points again to chemisorption as adsorption mechanism for molybdenum.

Conclusions

It was demonstrated that zeolite-supported magnetite is capable of removing hexavalent molybdenum from water, and that the optimal pH is around 3. The adsorption capacity for molybdenum at this pH and 25 °C is 17.9 mg per gram of adsorbent. The residual concentration after adsorption at pH 3 for an initial concentration of 1 mg/l molybdenum and 0.175 g/l adsorbent, is 9 µg/l, far below the WHO limit for drinking water (70 µg/l). The adsorption of molybdenum increases when temperature increases from 4 to 40 °C, indicating endothermic adsorption. The kinetics of the adsorption process can be described by a 'pseudo second order' rate equation.

In general, the interference of oxyanions As(V), Sb(V), or Sb(III) on the molybdenum adsorption is larger than that of anions PO_4^{3-}, SO_4^{2-} or Cl^- (except for phosphate). In a solution containing 1 mg/l molybdenum and 0.1 g/l adsorbent without interfering anion, 83% of the initial molybdenum is removed after 24 h at pH 3. With addition of a tenfold higher concentration of the oxyanions, a significant amount of molybdenum (35% to 51%) is still adsorbed. From the interfering anions studied, PO_4^{3-} is the most important, but even at a high concentration of 5000 mg/l PO_4^{3-}, 12% of the initial molybdenum amount is still adsorbed.

In order to understand the adsorption mechanism, thermodynamic modelling was performed using the software Visual Minteq. The formation of an inner-sphere $FeOMoO_2(OH).2H_2O$ complex is responsible for the adsorption of molybdate onto the zeolite-supported magnetite. The predicted mechanism of chemisorption was confirmed by experimental data (effect of ionic strength and temperature, adsorption isotherm).

Acknowledgment

The support of the Slovak Research and Development Agency under the contract No. APVV-0252-10 is greatly acknowledged.

Submitted for publication September 9, 2011; accepted for publication May 8, 2012.

References

Afkhami, A.; Madrakian, T.; Amini, A. (2009) Mo(VI) and W(VI) Removal from Water Samples by Acid-Treated High Area Carbon Cloth. *Desalination*, **243,** 258–264.

Afkhami, A.; Norooz-Asl, R. (2009) Removal, Preconcentration and Determination of Mo(VI) from Water and Wastewater Samples Using Maghemite Nanoparticles. *Colloid Surf. A-Physicochem. Eng. Asp.*, **346,** 52–57.

An, B.; Liang, Q. Q.; Zhao, D. Y. (2011) Removal of Arsenic(V) from Spent Ion Exchange Brine Using a New Class of Starch-Bridged Magnetite Nanoparticles. *Water Res.*, **45,** 1961–1972.

Balistrieri, L. S.; Chao, T. T. (1990) Adsorption of Selenium by Amorphous Iron Oxyhydroxide and Manganese-Dioxide. *Geochim. Cosmochim. Acta*, **54,** 739–751.

Barceloux, D. G. (1999) Molybdenum. *J. Toxicol.-Clin. Toxicol.*, **37,** 231–237.

Barquist, K.; Larsen, S. C. (2010) Chromate Adsorption on Bifunctional, Magnetic Zeolite Composites. *Microporous Mesoporous Mater.*, **130,** 197–202.

Cornell, R. M.; Schwertmann, U. (2003) *The Iron Oxides: Structure, Properties, Reactions, Occurrences and Uses*. Wiley-VCH: Verlag, Weinheim.

Davis, J. A.; James, R. O.; Leckie, J. O. (1978) Surface Ionization and Complexation at Oxide–Water Interface .1. Computation of Electrical Double-Layer Properties in Simple Electrolytes. *J. Colloid Interface Sci.*, **63,** 480–499.

Davis, J. A.; Leckie, J. O. (1980) Surface-Ionization and Complexation at the Oxide–Water Interface .3. Adsorption of Anions. *J. Colloid Interface Sci.*, **74,** 32–43.

Dessouki, T. C. E.; Hudson, J. J.; Neal, B. R.; Bogard, M. J. (2005) The Effects of Phosphorus Additions on the Sedimentation of Contaminants in a Uranium Mine Pit-Lake. *Water Res.*, **39,** 3055–3061.

El-Khaiary, M. I.; Malash, G. F.; Ho, Y. S. (2010) On the Use of Linearized Pseudo-Second-Order Kinetic Equations for Modeling Adsorption Systems. *Desalination*, **257,** 93–101.

Elwakeel, K. Z.; Atia, A. A.; Donia, A. M. (2009) Removal of Mo(VI) as Oxoanions from Aqueous Solutions Using Chemically Modified Magnetic Chitosan Resins. *Hydrometallurgy*, **97,** 21–28.

Frau, F.; Addari, D.; Atzei, D.; Biddau, R.; Cidu, R.; Rossi, A. (2010) Influence of Major Anions on As(V) Adsorption by Synthetic 2-Line Ferrihydrite. Kinetic Investigation and XPS Study of the Competitive Effect of Bicarbonate. *Water Air Soil Pollut.*, **205,** 25–41.

Gallios, G. P.; Vaclavikova, M. (2008) Removal of Chromium (VI) from Water Streams: A Thermodynamic Study. *Environ. Chem. Lett.*, **6,** 235–240.

Guo, H. M.; Li, Y.; Zhao, K. (2010) Arsenate Removal from Aqueous Solution Using Synthetic Siderite. *J. Hazard. Mater.*, **176,** 174–180.

Gupta, V. K.; Ali, I.; Saini, V. K.; Van Gerven, T.; Van der Bruggen, B.; Vandecasteele, C. (2005) Removal of Dyes from Wastewater Using Bottom Ash. *Ind. Eng. Chem. Res.*, **44,** 3655–3664.

Gustafsson, J. P. (2003) Modelling Molybdate and Tungstate Adsorption To Ferrihydrite. *Chem. Geol.*, **200,** 105–115.

Habuda-Stanic, M.; Kalajdzic, B.; Kules, M.; Velic, N. (2008) Arsenite and Arsenate Sorption by Hydrous Ferric Oxide/polymeric Material. *Desalination*, **229,** 1–9.

Hayes, K. F.; Leckie, J. O. (1986) Mechanism of Lead-ion Adsorption at the Goethite-water Interface. *Acs Symposium Series*, **323**, 114–141.

Ho, Y. S.; McKay, G. (1999) Pseudo-second Order Model for Sorption Processes. *Process Biochem.*, **34,** 451–465.

Ho, Y. S.; McKay, G. (2000) The Kinetics of Sorption of Divalent Metal Ions onto Sphagnum Moss Flat. *Water Res.*, **34,** 735–742.

Jonsson, J.; Sherman, D. M. (2008) Sorption of As(III) and As(V) to Siderite, Green Rust (Fougerite) and Magnetite: Implications for Arsenic Release in Anoxic Groundwaters. *Chem. Geol.*, **255,** 173–181.

Lievens, P.; Block, C.; Cornelis, G.; Vandecasteele, C.; De Voogd, J. C.; Van Brecht, A. (2010) Mo, Sb and Se Removal from Scrubber Effluent of a Waste Incinerator. In: *Water Treatment Technologies for the Removal of High-Toxicity Pollutants*; Vaclavikova, M.; Vitale, K.; Gallios, G. P.; Ivanicova, L., Eds.; Springer, Dordrecht.

Martinez, M.; Gimenez, J.; de Pablo, J.; Rovira, M.; Duro, L. (2006) Sorption of Selenium(IV) and Selenium(VI) onto Magnetite. *Appl. Surf. Sci.*, **252,** 3767–3773.

Misaelides, P.; Zamboulis, D.; Sarridis, P.; Warchol, J.; Godelitsas, A. (2008) Chromium (VI) Uptake by Polyhexamethylene-guanidine-modified Natural Zeolitic Materials. *Microporous Mesoporous Mat.*, **108,** 162–167.

Missana, T.; Alonso, U.; Scheinost, A. C.; Granizo, N.; Garcia-Gutierrez, M. (2009) Selenite Retention by Nanocrystalline Magnetite: Role of Adsorption, Reduction and Dissolution/co-precipitation Processes. *Geochim. Cosmochim. Acta*, **73,** 6205–6217.

Namasivayam, C.; Sangeetha, D. (2006) Removal of Molybdate from Water by Adsorption onto $ZnCl_2$ Activated Coir Pith Carbon. *Bioresour. Technol.*, **97,** 1194–1200.

Oliveira, C. R.; Rubio, J. (2007) New Basis for Adsorption of Ionic Pollutants onto Modified Zeolites. *Miner. Eng.*, **20,** 552–558.

Panayotova, M.; Panayotov, V. (2004) An Electrochemical Method for Decreasing the Concentration of Sulfate and Molybdenum Ions in Industrial Wastewater. *J. Environ. Sci. Health Part A-Toxic/Hazard. Subst. Environ. Eng.*, **39,** 173–183.

Plazinski, W.; Rudzinski, W.; Plazinska, A. (2009) Theoretical Models of Sorption Kinetics Including a Surface Reaction Mechanism: A Review. *Adv. Colloid Interface Sci.*, **152,** 2–13.

Rojas, J. C.; Vandecasteele, C. (2007) Influence of Mining Activities in the North of Potosi, Bolivia on the Water Quality of the Chayanta River, and its Consequences. *Environ. Monit. Assess.*, **132,** 321–330.

Rovira, M.; de Pablo, J.; Ignasi Casas, L.; Gimenez, J.; Ciarens, E.; Martinez-Llado, X. (2006) Sorption of Molybdenum(VI) on Synthetic Magnetite. *Materials Research Society*; 12–16 September; Ghent, Belgium.

Rovira, M.; Gimenez, J.; Martinez, M.; Martinez-Llado, X.; de Pablo, J.; Marti, V.; Duro, L. (2008) Sorption of Selenium(IV) and Selenium (VI) onto Natural Iron Oxides: Goethite and hematite. *J. Hazard. Mater.*, **150,** 279–284.

Schmidt, G. T.; Vlasova, N.; Zuzaan, D.; Kersten, M.; Daus, B. (2008) Adsorption Mechanism of Arsenate by Zirconyl-functionalized Activated Carbon. *J. Colloid Interface Sci.*, **317,** 228–234.

Stumm, W.; Morgan, J. J. (1996) *Aquatic Chemistry*. John Wiley & Sons, New York, N.Y.

Su, C. M.; Puls, R. W. (2008) Arsenate and Arsenite Sorption on Magnetite: Relations to Groundwater Arsenic Treatment using Zerovalent Iron and Natural Attenuation. *Water Air Soil Pollut.*, **193,** 65–78.

Sverjensky, D. A. (2001) Interpretation and Prediction of Triple-layer Model Capacitances and the Structure of the Oxide-electrolyte-water Interface. *Geochim. Cosmochim. Acta*, **65,** 3643–3655.

Swinkels, P. L. J.; van der Weijden, R. D.; Ajah, A. N.; Arifin, Y.; Loe, H. L.; Manik, M. H.; Siriski, I.; Reuter, M. A. (2004) Conceptual Process Design as a Prerequisite for Solving Environmental Problems: A Case Study of Molybdenum Removal and Recovery from Wastewater. *Miner. Eng.*, **17,** 205–215.

Vandecasteele, C.; Cornelis, G. (2010) Oxyanions in Waste Occurrence, Leaching, Stabilisation, Relation to Wastewater Treatment. In *Water Treatment Technologies for the Removal of High-Toxicity Pollutants*; Vaclavikova, M.; Vitale, K.; Gallios, G. P.; Ivanicova, L., Eds.; Springer, Dordrecht.

Vaclavikova, M.; Jakabsky, S.; Hredzak, S. (2004) Magnetic Nanoscale Particles as Sorbents for Removal of Heavy Metal Ions. *Nano-engineered Nanofibrous Materials*. **169,** 481–486.

Vaclavikova, M.; Gallios, G. P.; Hredzak, S.; Jakabsky, S. (2008) Removal of Arsenic from Water Streams: An Overview of Available Techniques. *Clean Technol. Environ. Policy*, **10,** 89–95.

Vaclavikova, M.; Stefusova, K.; Ivanicova, L.; Jakabsky, S.; Gallios, G. P. (2010) Magnetic Zeolite as Arsenic Adsorbent. In *Water Treatment Technologies for the Removal of High-Toxicity Pollutants.*Vaclavikova, M.; Vitale, K.; Gallios, G. P.; Ivanicova, L., Eds.; Springer, Dordrecht.

Vujakovic, A. D.; Tomasevic-Canovic, M. R.; Dakovic, A. S.; Dondur, V. T. (2000) The Adsorption of Sulphate, Hydrogenchromate and Dihydrogenphosphate Anions on Surfactant-modified Clinoptilolite. *Appl. Clay Sci.*, **17,** 265–277.

Wainipee, W.; Weiss, D. J.; Sephton, M. A.; Coles, B. J.; Unsworth, C.; Court, R. (2010) The Effect of Crude Oil on Arsenate Adsorption on Goethite. *Water Res.*, **44,** 5673–5683.

Watkins, R.; Weiss, D.; Dubbin, W.; Peel, K.; Coles, B.; Arnold, T. (2006) Investigations into the Kinetics and Thermodynamics of Sb(III) Adsorption on Goethite (Alpha-FeOOH). *J. Colloid Interface Sci.*, **303,** 639–646.

Wingenfelder, U.; Furrer, G.; Schulin, R. (2006) Sorption of Antimonate by HDTMA-modified Zeolite. *Microporous Mesoporous Mat.*, **95,** 265–271.

Wu, C. H.; Lo, S. L.; Lin, C. F. (2000) Competitive adsorption of molybdate, chromate, ulphate, selenate, and selenite on gamma-Al2O3. *Colloid Surf. A-Physicochem. Eng. Asp.*, **166,** 251–259.

Xu, N.; Christodoulatos, C.; Braida, W. (2006) Adsorption of Molybdate and Tetrathiomolybdate onto Pyrite and Goethite: Effect of pH and Competitive Anions. *Chemosphere*, **62,** 1726–1735.

Xu, N.; Christodoulatos, C.; Braida, W. (2006) Modeling the Competitive Effect of Phosphate, Sulfate, Silicate, and Tungstate Anions on the Adsorption of Molybdate onto Goethite. *Chemosphere*, **64,** 1325–1333.

Yavuz, C. T.; Mayo, J. T.; Yu, W. W.; Prakash, A.; Falkner, J. C.; Yean, S.; Cong, L. L.; Shipley, H. J.; Kan, A.; Tomson, M.; Natelson, D.; Colvin, V. L. (2006) Low-field Magnetic Separation of Monodisperse Fe3O4 Nanocrystals. *Science*, **314,** 964–967.

Yuan, P.; Liu, D.; Fan, M. D.; Yang, D.; Zhu, R. L.; Ge, F.; Zhu, J. X.; He, H. P. (2010) Removal of Hexavalent Chromium Cr(VI) from Aqueous Solutions by the Diatomite-supported/unsupported Magnetite Nanoparticles. *J. Hazard. Mater.*, **173,** 614–621.

3.3 Simultaneous Removal of Molybdenum, Antimony and Selenium Oxyanions from Wastewater by Adsorption on Supported Magnetite

Verbinnen, B., Block, C., Lievens, P., Van Brecht, A., Vandecasteele, C. (2013). Simultaneous Removal of Molybdenum, Antimony and Selenium Oxyanions from Wastewater by Adsorption on Supported Magnetite. *Waste and Biomass Valorization, 4* (3), 635-645.

In publication 3 it was shown that zeolite-supported magnetite is a promising material for the removal of oxyanions from wastewater. The actual removal of Mo, Sb and Se oxyanions from a real industrial wastewater is described in **publication 4**. First, the adsorption mechanisms are shown for the oxyanions of Sb(III), Sb(V), Se(IV) and Se(VI) separately. Then, the main interfering (oxy)anions are determined for each oxyanion. A synthetic wastewater, mimicking the concentration in the real wastewater was prepared and the adsorption behavior from this wastewater is explained with the earlier gained knowledge on interferences. Finally, the adsorption of Mo, Sb and Se from an industrial wastewater, the scrubber effluent of an incinerator for hazardous waste is studied.

Unlike previous publications from other authors, this paper does not only provide adsorption data for the removal of one single oxyanion from synthetic water, but also studies the removal from a synthetic water containing multiple oxyanions and/or interfering anions, and from a real industrial wastewater. It seems that for some oxyanions good adsorption capacities can still be obtained for industrial wastewater, while other oxyanions suffer more from interferences.

All experiments were performed by the candidate, with some aid of thesis students S. Van Ostaeyen and S. Van Gompel. All modeling was done by the candidate. A. Van Brecht provided the industrial wastewater. The candidate prepared the draft paper; and C. Block, P. Lievens, A. Van Brecht and C. Vandecasteele acted as discussion partners or critical reviewers of the manuscript.

Waste Biomass Valor (2013) 4:635–645
DOI 10.1007/s12649-013-9200-8

ORIGINAL PAPER

Simultaneous Removal of Molybdenum, Antimony and Selenium Oxyanions from Wastewater by Adsorption on Supported Magnetite

Bram Verbinnen · Chantal Block · Patrick Lievens · Andres Van Brecht · Carlo Vandecasteele

Received: 31 August 2012 / Accepted: 22 January 2013 / Published online: 6 February 2013

Abstract Mo, Sb and Se form oxyanions in solution, and are therefore difficult to remove by traditional wastewater treatment methods (e.g. alkaline precipitation). In this paper, a method for the simultaneous removal of these three elements from wastewater by adsorption, zeolite-supported magnetite is developed. The adsorbent consists of finely divided magnetite particles on a zeolite substrate as carrier material. Basic adsorption parameters such as ideal pH, maximum adsorption capacity and equilibration time, are determined for the oxyanions separately. Much attention is paid to the study of interferences that can limit adsorption. Anions like sulphate and chloride, which often occur in large amounts in wastewaters, do not really compete for adsorption places on magnetite, but oxyanions largely interfere with each other. The reason for this competition is a similar adsorption mechanism (inner-sphere complex formation) for all studied oxyanions, except for selenate, that forms outer-sphere complexes, as was confirmed by geochemical modeling. The adsorption of Mo, Sb and Se oxyanions from an aqueous solution containing the most important detected interferences and from a real wastewater containing also cations is compared, showing that the most important interferences are identified. The order of adsorption is Mo(VI) > Sb(V) > Se(VI). As a case study, Mo, Sb and Se oxyanions are removed by adsorption from an industrial wastewater, the flue gas cleaning effluent of a waste incinerator. For an adsorbent concentration of 20 g/l, removal efficiencies of 99, 97 and 77 % are obtained for Mo, Sb and Se.

Keywords Oxyanion adsorption · Selenate · Antimonate · Molybdate · Magnetite · Wastewater

B. Verbinnen (✉) · C. Block · P. Lievens · C. Vandecasteele
Laboratory of Applied Physical Chemistry and Environmental Technology, Department of Chemical Engineering, University of Leuven, KU Leuven, W. De Croylaan 46, 3001 Leuven, Belgium
e-mail: bram.verbinnen@cit.kuleuven.be

P. Lievens
Department of Chemical Engineering, Leuven Engineering College Groep T, Vesaliusstraat 13, 3000 Leuven, Belgium

A. Van Brecht
INDAVER nv, Dijle 17 a, 2800 Mechelen, Belgium

Introduction

Mo, Sb and Se mainly occur as oxyanions in (waste)water. The predominant form of Mo in dilute solutions is the molybdate anion, MoO_4^{2-} [1]. Se is usually present in amounts ranging from 0.1 to 20 mg/l in aqueous effluents. Selenite (Se(IV)) and selenate (Se(VI)) are the predominant chemical forms of Se; most of their salts are soluble and mobile [2–4]. In water, Sb occurs mainly as antimonite (Sb(III)) under anoxic conditions and as antimonate (Sb(V)) in the presence of oxygen [5].

During waste combustion, Se, Sb and Mo can pass into the flue gas stream due to the high volatility of some of their compounds. Jung et al. [6] performed a literature survey and did experiments on the distribution of heavy metals in incineration residues. Although literature data for Se and Sb were limited, they indicated that the major part of these two elements was transferred into fly ash rather than into bottom ash, indicating high volatility. This was confirmed by their experimental work. Thermodynamic calculations performed by Paoletti et al. [7] indicated that during waste incineration, Sb oxides are likely to be formed, together with Sb chlorides in the case of a local excess of chlorine in the incinerator. Sb(III) oxide and Sb(III) and (V) chlorides are all highly

volatile, due to their high vapour pressure at temperatures comparable to incineration temperatures in a rotary kiln. Not much is known about the behaviour of Mo during waste incineration. Although elemental Mo, with a melting point of 2,610 °C, is highly involatile, thermodynamic calculations [8] showed that during incineration the volatile MoO_3 (sublimation starts at 750 °C) is very likely to be formed. Moreover, Mo chlorides are also volatile. During a lab-scale incineration experiment, 10 % of the total Mo input was found in the fly ash [8].

Recently (January 2011), new or lower limit values were included in the "basic quality standards for surface water" (Vlarem II.2.3) in Flanders (Belgium), as an implementation of the European Water Framework Directive (2000/60/EC). For Se, the limit value was lowered from 10 to 3 μg/l (i.e. the limit value for drinking water set by the WHO). For Mo and Sb, there were no previous limit values, but they were now set at 350 and 100 μg/l, respectively. When concentrations in effluents exceed these values, companies have to ask for appropriate discharge limits. The more stringent limit values indicate that new techniques to remove Mo, Sb and Se from wastewater are needed in order to comply with legislation.

Here, a method is presented for the simultaneous removal of oxyanions of Mo, Sb and Se from wastewater by adsorption on zeolite-supported magnetite [9]. The finely divided magnetite is, like other iron oxides, known to have a high adsorption capacity for negatively charged ions [10]. Adsorption capacity is related to specific surface area, so the smaller the adsorbent particles, the higher the adsorption capacity. This was demonstrated for magnetite by Mayo et al. [11]. Application of nanosized magnetite as such in a column is no option: the small particles cause a too large pressure drop in the column. To overcome these problems, the nanosized magnetite particles are deposited onto a carrier material, in this case zeolite (clinoptilolite). Research on this same adsorbent was done by Gallios and Vaclavikova [12] for Cr(VI) removal and for arsenic by Vaclavikova et al. [9].

In this paper, some basic parameters for the different oxyanions (optimal pH, maximum adsorption capacity, equilibration time, …), are determined, together with the adsorption mechanism, which is determined via geochemical modeling. A large part of this paper deals with interferences. The adsorption order for the different oxyanions is determined and the major interferences are identified. Finally, the adsorbent is tested on an industrial wastewater, the scrubber effluent from solid waste incineration in a rotary kiln.

Occurrence of Species

Simulation of the speciation as a function of pH using the geochemical modeling program Visual Minteq showed that Sb(V), Mo(VI) and Se(IV) occur as their fully protonated neutral acid at a pH up to 2–4. From this pH on, they form oxyanionic species up till pH 14. Se(VI) forms oxyanions in the whole pH range, and Sb(III) forms neutral $Sb(OH)_3$ between pH 1.5 and 11.5. This may be of importance when looking at adsorption as a function of pH later on.

Redox reactions are often neglected in papers dealing with the adsorption of oxyanions on iron oxides. It is important to verify if the species studied can be reduced in the presence of magnetite, to ensure that no precipitation of reduced species (e.g. zerovalent Se or Sb) can occur. Reduction or oxidation of a species can also alter the adsorption behaviour. The reduction of Se in the presence of magnetite has already been discussed extensively in literature. Loyo et al. [13] observed no reduction of selenite during adsorption experiments with magnetite at pH values between 4.8 and 8.0. Rapid reduction of selenite in the presence of magnetite was reported by Scheinost and Charlet [14] by XAS measurements, but these findings were countered in another paper that stated that the observed selenite reduction was a misinterpretation of the XAS results [3]. In this later paper was shown that reduced Se species, if present at all, constitute to less than 5 % of the total amount in the presence of magnetite particles with sizes between 50 and 200 nm and a contact time of at least 1 day.

Based on their redox potentials, selenate and molybdate reduction by magnetite is feasible, but no literature data on the kinetics of these reactions are available.

Oxidation of Sb(III) to Sb(V) by magnetite is not possible according to redox potential calculation, but oxygen is able to oxidize trivalent Sb. Leuz and Johnson [15] showed experimentally that at high pH, oxidation by dissolved oxygen can be important: at pH 10.9 half of Sb(III) was oxidized in 229 days, at pH 11.9 this reaction half-life was reduced to 35 days, and at pH 12.9 it took only 3 days to oxidize half of the Sb(III). The oxide of Sb(V), Sb_2O_5, is more soluble than the oxide of Sb(III), Sb_2O_3, so precipitation of Sb_2O_5 is no issue in this case, but the formation of Sb(V) can have an influence on the adsorption characteristics at high pH.

Reduction of Sb(V) to Sb(III), and further reduction to Sb(0) by magnetite is possible. Kirsch et al. [16] showed that the reduction of Sb(V) under anoxic conditions is pH-dependent: at pH 5.0 and 6.0, hardly any ($\leq$5 %) Sb(V) is reduced in a 22 h experiment, but at pH 8.0, around 40 % is reduced. Sb(V) is first reduced to Sb(III) and then adsorbed to the magnetite surface: the same surface complex was observed when Sb(III) was added directly to a solution containing magnetite, as when Sb(V) was reduced at the magnetite surface at high pH. Further reduction of Sb(III) has not been discussed in literature.

Materials and Methods

Reagents

All reagents were of analytical grade. Stock Mo(VI), Sb(V), Sb(III), Se(IV) and Se(VI) solutions were prepared by dissolving $Na_2MoO_4{\cdot}2H_2O$ (Merck Eurolab), $KSb(OH)_6$ (Fluka), Sb_2O_3 (Merck Eurolab, from a 1,000 mg/l analytical standard), Na_2SeO_3 (Fluka) and Na_2SeO_4 (Fluka), respectively, in ultrapure (Millipore Milli-Q) water. pH was adjusted with HNO_3 (Sigma-Aldrich) or KOH (Merck Eurolab). H_3AsO_4 (Merck Eurolab, prepared from a 1000 mg/l analytical standard), Na_2SO_4 (Acros), Na_2SO_3 (Merck Eurolab), NaCl (Fisher Scientific) and Na_3PO_4 (Sigma-Aldrich) were used in interference studies. For redox speciation, sodium benzene sulfonate (Sigma-Aldrich) and ammonium pyrrolidine dithiocarbamate (APDC, Sigma-Aldrich) were used.

Redox Speciation

Redox speciation of Sb and Se in the industrial wastewater that was used in the case study, was performed using the selective solid phase extraction method developed by Mulugeta et al. [17]. As solid phase extraction columns, Supelco Supelclean C18 columns were used, which were pretreated with 2 ml methanol, followed by 2 ml ultrapure water. A sample of the industrial wastewater was passed through a 0.45 μm membrane filter, diluted 10 times and the pH was brought to 7. The water was pretreated by adding 0.5 % (w/v) sodium benzene sulfonate and passed through the column to remove interfering metal ions, at a flow rate of 2 ml/min. The effluent was collected and treated with 0.08 % (w/v) ADPC, that forms complexes with Sb(III) and Se(IV), but not with the species of higher oxidation states. 10 ml of the solution was then passed through a new, but identical column, which captures the formed complexes, at a flow rate of 2 ml/min. The species of the highest oxidation states, Sb(V) and Se(VI), pass through the column, while Sb(III) and Se(IV) species can be eluted in a next step using 10 ml of a 3 M HNO_3 solution at a flow rate of 0.2 ml/min. The effluent and eluent were measured separately with ICP-MS. As the method was developed for As, Sb and Se only, no Mo results are given here.

Adsorbent

For this study, finely divided magnetite deposited on a natural zeolite as supporting material, further called 'zeolite-supported magnetite' was used. The zeolite-supported magnetite used in this study was provided by the Institute of Geotechnics, Slovakia. The zeolite type is clinoptilolite (grain size 400–500 μm), obtained from Nizny Hrabovec, Slovakia) [9].

The clinoptilolite acts as a host for magnetite nanoparticles, that have a size ranging from 10 to 40 nm, but that can form clusters with sizes between 20 and 900 nm [18]. The zeolite-supported magnetite is prepared by adding clinoptilolite to a reaction vessel containing an equimolar solution of Fe(II) and Fe(III) salts. Adjustment of pH with NaOH leads to precipitation of magnetite onto the zeolite [9]. The ratio zeolite/magnetite was 2/1. The zeolite-supported magnetite was characterized by its surface area (74–126 m^2/g).

Batch Experiments

Sorption experiments were carried out for the different oxyanions separately at pH values ranging from 0.5 to 13.5. To solutions containing 5 mg/l of the studied oxyanion, 0.5 g/l of zeolite-supported magnetite was added throughout the experiments. After pH adjustment, the separate solutions were transferred to sealed PE bottles, together with the zeolite-supported magnetite and agitated on a shaking device (Gerhardt Laboshake, 160 rpm). After 24 h, the solution was filtered over a 0.45 μm membrane filter (Chromafil) and the oxyanions or other relevant elements were determined in the filtrate with ICP-MS (Thermo Xi series). Chloride, sulphate and phosphate were measured using ion chromatography (Dionex ICS 2000). A control solution (pH adjusted, but no zeolite-supported magnetite added) was also agitated, filtered and analysed, to avoid false conclusions due to the possible effect of pH on the oxyanion solubility or adsorption to the PE bottle.

To determine equilibration time, separate solutions containing 5 mg/l of the different oxyanions were brought in contact with 0.5 g/l adsorbent and the residual oxyanion concentration in solution was determined as a function of time.

The adsorption isotherms, together with the maximum adsorption capacities, were determined for the different oxyanions separately. To solutions with oxyanion concentrations ranging from 1 to 100 mg/l, 0.5 g/l of zeolite-supported magnetite was added. pH and contact time were selected based on preliminary experiments.

To study the influence of other oxyanions and anions commonly occurring in wastewater on the adsorption of Mo(VI), Sb(V) and Se(VI) oxyanions, solutions containing 1 mg/l adsorbent at pH 3.5 and increasing concentrations (1–50 mg/l) of one oxyanion were prepared, to which one possible interfering (oxy)anion (molybdate, selenate, arsenate, chloride, sulphate, sulfite or phosphate) was added. The concentrations in which interfering (oxy)anions were added are given in Table 1. The oxyanions were added in their highest oxidation state, as these are the ones that are expected to occur in the scrubber effluent.

The adsorption order (i.e. determination for which oxyanion magnetite has the highest affinity) of the different oxyanions was determined by adding increasing amounts of adsorbent (from 0.05 to 1.4 g/l) to a solution containing equal molar concentrations (2×10^{-5} mol/l, equal to 1–2 mg/l) of antimonate, molydate and selenate. After agitation, the residual concentrations were measured.

The adsorption behavior for Mo, Sb and Se oxyanions was also studied for a synthetic wastewater containing oxyanions and the most important interferences in concentrations matching these of the effluent of a flue gas scrubber of a waste incinerator. These concentrations are comparable to those given in Table 1: 4 g/l sulfate, 36.3 g/l chloride, 1.7 g/l antimonate, 950 μg/l molybdate, 175 μg/l selenate and 75 μg/l arsenate. Increasing amounts of adsorbent were added (from 0 to 5 g/l) and the solutions were equilibrated with the adsorbent at pH 3.5 for 24 h.

Finally, increasing amounts of adsorbent (1–20 g/l) were added to a real wastewater at the predetermined ideal pH, residual concentrations were measured after 24 h contact time to determine the removal efficiency for the different oxyanions.

Results and Discussion

Effect of pH

Experimental data of selenate and selenite, antimonate and antimonite adsorption onto zeolite-supported magnetite for equilibrium pH values ranging from 0.5 to 13.5 are summarized in Figs. 1 and 2. The measurements of the control solutions (with pH adjusted, but no zeolite-supported magnetite added), showed that no Sb or Se species precipitate within 24 h for this pH range.

From Fig. 1a, b can be concluded that for both Se species, adsorption decreases at higher pH values. Selenite adsorbs in a broader pH range (pH 2–10) in comparison to selenate (pH 2–7). Figure 2b shows that for Sb(V) maximal adsorption occurs at an equilibrium pH between 2 and 4. Sb(III) adsorption (Fig. 2a) is almost independent of pH and only shows a decrease in adsorption at very high and very low pH-values. In previous work [19], an optimal pH of 3–3.5 was determined for the adsorption of Mo(VI); it was also observed that at a pH above 2, magnetite dissolution is minimal. For all subsequent experiments, the pH was adjusted to 3–3.5. As mentioned earlier, it is unlikely that any of the oxyanion species are reduced by magnetite at this pH.

Table 1 Concentrations of the interfering (oxy)anions

	Concentration (mg/l)
SO_4^{2-}	4,000
SO_3^{2-}	4,000
PO_4^{3-}	5,000
Cl^-	36,000
MoO_4^{2-}	50
SeO_4^{2-}	50
AsO_4^{3-}	50

Adsorption Modeling

The adsorption of selenate, selenite, antimonate and antimonite as a function of pH was modeled with the geochemical modeling program Visual Minteq, which was also used to model the adsorption of molybdate onto zeolite-supported magnetite in a previous article [19]. The adsorption model used is the Triple Layer Model [20–22], which takes into account the formation of both outer- and inner-sphere complexes. A number of parameters are needed to build the model. The first parameters are the surface area, taken from Vaclavikova et al. [9] for the same adsorbent, and the capacitance parameters C1 (inner layer) and C2 (outer layer), that express the charge at the surface relative to the drop in electrical potential at some distance away from the surface [23]. For the surface site density, literature values range from 1.8 to 6.7 sites/nm^2 [3, 24–28]. As this parameter only slightly influences the modeling, an intermediate value of 4.2 was used, which provided a good fit. Finally, log k values for protonation/deprotonation of the magnetite surface, and for the surface complexation reactions of the different oxyanions are needed. All parameters used, and the respective literature references, are summarised in Table 2. Acid dissociation constants for the different species are taken from the Minteq database.

The adsorption of selenite, selenate, antimonite, antimonite and molybdate on magnetite as a function of pH, as modeled with the Triple Layer Model, are superposed on the experimental data in Figs. 1 and 2. The modeled graphs are in good agreement with the experimental data. For selenate, the best fit was obtained by modeling an outer-sphere $>FeOH_2^+\_SeO_4^{2-}$ complex. This is in accordance with literature, as most of the papers on this topic state that, based on surface complexation modeling, selenate is physically adsorbed onto iron oxides, rather than chemically [26, 29–32]. In literature, the adsorption of selenite onto magnetite or other iron oxides is sometimes modeled using two inner-sphere complexes: $>FeSeO_3^-$ and $>FeHSeO_3$ [25, 31]. In this paper, selenite adsorption was best fitted by the formation of an $>FeSeO_3^-$ complex alone, in agreement with previous work of Kim et al. [27] and Jordan et al. [25]. The log K value for the formation of this complex as determined by Jordan et al. [25] provided the best fit for the experimental results.

For Sb, the surface complexation reactions as suggested by Guo et al. [33] provide the best fit for the experimental

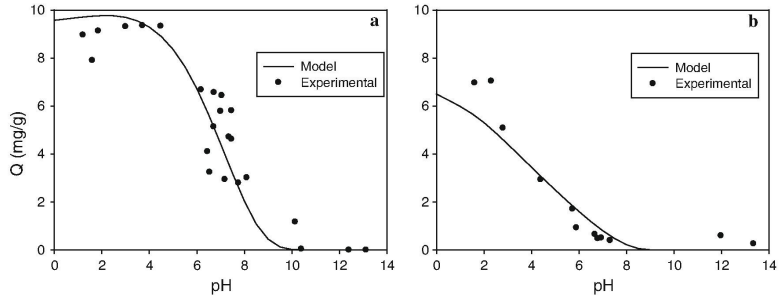

Fig. 1 Adsorption capacity (Q) of selenite (**a**) and selenate (**b**) as a function of pH; 5 mg/l starting solution, 0.5 g/l adsorbent, 24 h contact time at 25 °C

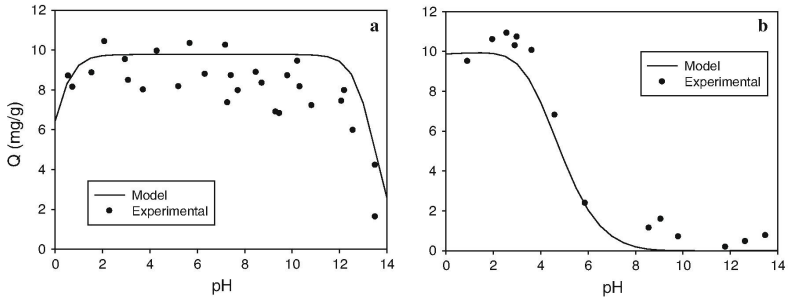

Fig. 2 Adsorption capacity (Q) of antimonite (**a**) and antimonate (**b**) as a function of pH; 5.1 mg/l starting solution, 0.5 g/l adsorbent, 24 h contact time at 25 °C

Table 2 Surface complexation modeling parameters used in the triple layer model

Parameter	Value	References
Inner layer capacitance C_1 (F/m^2)	1.13	[23]
Outer layer capacitance C_2 (F/m^2)	0.2	[23]
Surface site density (sites/nm^2)	4.2	This work
Surface area (m^2/g)	125.7	[9]
Reaction	**Log K**	**References**
$>FeOH_2^+ \leftrightarrow >FeOH + H^+$	−5.1	[3]
$>FeOH \leftrightarrow >FeO^- + H^+$	−9.1	[3]
$>FeOH + SeO_4^{2-} + H^+ \leftrightarrow >FeOH_2^+\_SeO_4^{2-}$	11.7	[32]
$>FeOH + SeO_3^{2-} + H^+ \leftrightarrow >FeSeO_3^- + H_2O$	6.06	[25]
$>FeOH + Sb(OH)_3 \leftrightarrow >FeOSb(OH)_2 + H_2O$	5.7	[33]
$>FeOH + Sb(OH)_6^- \leftrightarrow >FeOSb(OH)_5^- + H_2O$	3.1	[33]
$>FeOH + MoO_4^{2-} + 2H^+ + H_2O \leftrightarrow >FeOMoO_2(OH).2H_2O$	18.28	[34]

results and the surface complexation reactions are similar for both Sb species: Sb(III) is adsorbed as an inner-sphere >FeOSb(OH)$_2$ complex, Sb(V) as an inner-sphere >FeOSb(OH)$_5^-$ complex. Mo adsorption on magnetite was modeled in an earlier paper [19] as inner-sphere complex formation, the parameters used are also given in Table 2.

The adsorption curves from Figs. 1 and 2 show large similarities with the speciation as a function of pH for the respective oxyanions. The pH for which the adsorption capacity for Se(IV), Se(VI) and Sb(III) starts to decrease coincides with the pH for which the concentration of the respective species $HSeO_3^-$, $HSeO_4^{2-}$ and $Sb(OH)_3$ starts to decrease. These species are also the ones that provided the best fit in the adsorption modeling, except for Sb(V). Sb(V) is modelled best by the adsorption of $Sb(OH)_6^-$, whereas $Sb(OH)_5$ is the predominant species in the pH range where the highest adsorption capacities were observed, but no log K values for the adsorption of $Sb(OH)_5$ on magnetite were found in literature. Furthermore, the surface complexation models for the different oxyanions all incorporate the hydrated, non-ionic, surface species >FeOH. Visual Minteq modeling showed that despite the fact that the overall surface charge is positive at low pH values and negative at high pH values, >FeOH is the predominant surface species over the whole pH range at concentrations similar to the ones in this study, as can be seen in Fig. 3. Both observations indicate that the surface complexation reactions that were used in the modeling, are good approximations for the real reactions occurring at the surface.

From the modeling can be concluded that the species antimonate, antimonite, selenite and molybdate form inner-sphere complexes when adsorbed on magnetite. Selenate forms an outer-sphere complex. Species that form similar complexes on the magnetite surface can compete with each other for adsorption places, as will be discussed later.

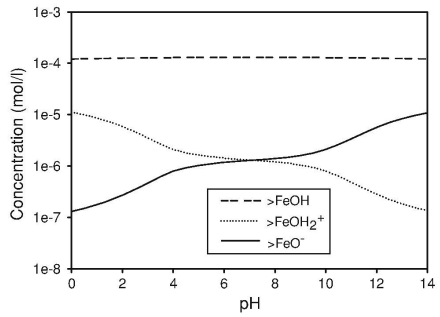

Fig. 3 Concentration of >FeOH, >$FeOH_2^+$ and >FeO^- species as a function of pH for a total FeOH concentration of 0.16 g/l

Adsorption Kinetics

Residual selenate, selenite and antimonate concentrations after adsorption are measured as a function of contact time for an adsorbent concentration of 0.5 g/l, an initial oxyanion concentration of 5 mg/l and pH 3. The results are fitted with the 'pseudo-second order' model [35] and equilibration times are determined. The pseudo second order rate equation is given by Eq. (1):

$$\frac{dQ}{dt} = k \cdot (Q_e - Q)^2 \tag{1}$$

where k (g/mg h) is the rate constant, Q_e is the absorbed amount (mg/g adsorbent) at equilibrium and Q the adsorbed amount (mg/g adsorbent) at contact time t.

The pseudo second order reaction has been widely applied to describe the kinetics of trace element sorption on different sorbents. It does not correspond to any specific physical model, it simply approximates well the adsorption data predicted by many different theoretical approaches [36]. From the correlation coefficients summarized in Table 3, it appears that the pseudo second order model is adequate to describe the kinetics of the adsorption of the different oxyanions onto the zeolite-supported magnetite. The time needed to reach equilibrium is also given in Table 3 for the different oxyanions. Selenate has the shortest equilibration time followed by molybdate and antimonate; selenite has the longest equilibration time. Kinetic properties for Mo were determined in previous research [19].

Adsorption Isotherms

Maximum adsorption capacities at pH 3 for Sb(V), Se(IV) and Se(VI) onto zeolite-supported magnetite were determined from the respective adsorption isotherms. Experimental data were fitted using both Freundlich and Langmuir adsorption models. Langmuir adsorption assumes adsorbate molecules to bind only at a series of distinct sites on the surface of the solid [37], and the adsorption isotherm is represented by the equation:

$$Q_e = \frac{Q_{\max} b C_e}{1 + b C_e} \tag{2}$$

Table 3 Correlation coefficient for the pseudo-second order model and equilibration time (h) for Mo, Sb and Se oxyanions

Oxyanion	Correlation coefficient	Equilibration time (h)
Mo(VI)	0.994	12
Sb(V)	0.998	13
Se(VI)	0.998	10
Se(IV)	0.998	22

Q (mg oxyanion/g adsorbent) is the adsorbed amount at equilibrium, Q_{max} (mg/g) the maximum adsorption capacity, b (l/mg) a constant and C_e (mg/l) the residual oxyanion concentration in solution at equilibrium. The Langmuir model belongs to the class of monolayer models, indicating chemisorption or inner-sphere adsorption.

The Freundlich adsorption isotherm is the most important multisite isotherm, and is given by the equation [37]:

$$Q_e = kC_e^{1/n} \quad (3)$$

where Q_e (mg/g adsorbent) is the adsorbed amount per gram adsorbent at equilibrium, C_e (mg/l) is the residual concentration in solution at equilibrium, and k and n are constants. The Freundlich model belongs to the class of poly-layer models, indicating physisorption or outer-sphere complexation.

Experimental data were fitted by Eqs. (1) and (2) for the different oxyanions. R^2 values for the Langmuir and Freundlich model and the maximum adsorption capacities are given in Table 4. The Langmuir isotherm for Sb(V) is shown in Fig. 4.

It is clear from the R^2 values that for molybdate, selenite and antimonate the data are significantly better fitted by a Langmuir isotherm. This is in agreement with the adsorption modeling that showed that these oxyanions form inner-sphere complexes with magnetite. For selenate both Freundlich and Langmuir models fit the data well. The surface complexation modeling in this paper showed that the best fit for selenate adsorption onto magnetite is provided by an outer-sphere complex, corresponding to a Freundlich adsorption isotherm. As mentioned earlier, there is also more evidence in literature for the formation of a selenate outer-sphere complex. Therefore, preference is given to the Freundlich model in this paper also. The maximum adsorption capacities for the different oxyanions onto the zeolite-supported magnetite as determined by the Langmuir model are given in Table 4. For antimonite and selenate no maximum adsorption capacity is determined: for antimonite because Sb_2O_3 starts to precipitate at Sb(III) concentrations above 7.7 mg/l [38], for selenate because it follows a Freundlich adsorption isotherm.

Table 4 Correlation coefficients for Mo, Sb and Se oxyanions for Langmuir and Freundlich isotherm, and maximum adsorption capacities

Oxyanion	Langmuir R^2	Freundlich R^2	Maximum adsorption capacity Q_{max} (mg/g)
Mo(VI)	0.99	0.75	18
Sb(V)	0.99	0.93	19
Se(VI)	0.95	0.93	–
Se(IV)	0.99	0.83	23

Study of Interferences

Figure 4a, b show the Langmuir isotherm for antimonate without interference added and with the addition of molybdate, selenate, arsenate, sulfate or chloride. These figures illustrate that selenate and sulphate have no influence on the adsorption of Sb(V), in line with the earlier conclusions that selenate forms outer-sphere complexes on the magnetite surface, whereas antimonate forms inner-sphere complexes. Sulphate, with an atomic structure similar to selenate, is also known to form outer-sphere complexes [24, 39]. Molybdate, arsenate and chloride interfere with antimonate adsorption. Arsenate and molybdate also form inner-sphere complexes with magnetite [8, 19]. The influence of chloride on antimonate adsorption is remarkable, as generally chloride is known to form relatively weak outer-sphere complexes with iron oxides [39]. The lower adsorption for antimonate in the presence of chloride might be explained by the formation of Sb hexachloride complexes.

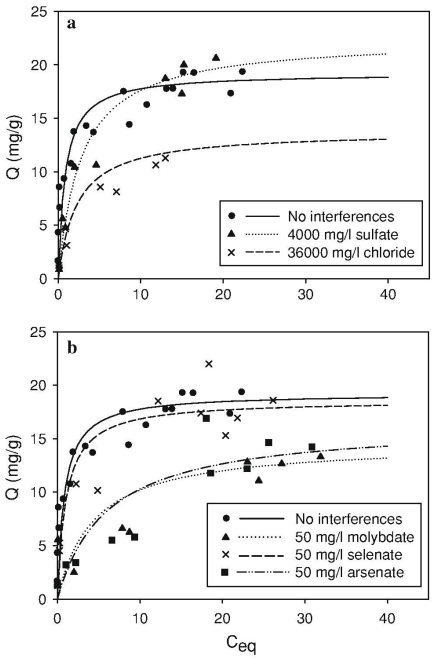

Fig. 4 Influence of anions sulphate and chloride (**a**) and oxyanions molybdate, selenate and arsenate (**b**) on Sb(V) adsorption (points represent experimental data, lines represent the fitted Langmuir isotherms)

Similar experiments indicated that the adsorption of selenite is mainly influenced by the anions sulfite and phosphate and by the oxyanions molybdate and arsenate. Like molybdate and arsenate, phosphate is known to form inner-sphere complexes with iron oxides [39]. Sulfite can hinder selenite adsorption because of its similar molar structure. Selenate is largely influenced by sulphate due to their similar molar structure. A previous article on Mo adsorption on the same adsorbent [19] identified phosphate to be the most interfering anion.

The adsorption order of molybdate, antimonate and selenate for zeolite-supported magnetite can be derived from Fig. 5, showing the adsorption for an equimolair mixture of oxyanions as a function of increasing amounts of adsorbent. The adsorption order is: Mo(VI) > Sb(V) > Se(VI). Magnetite has thus the largest affinity for molybdate, followed by antimonate, and finally selenate. This can be attributed to the fact that molybdate and antimonate adsorb via an inner-sphere complex, and molecules that form inner-sphere complexes are known to have a high affinity for the surface due to the formation of covalent bonds at specific surface sites. The lower affinity of magnetite for selenate is another indication of outer-sphere complexation.

Figure 6 compares residual Sb concentrations as a function of the added adsorbent concentration for three different solutions: an aqueous solution containing only Sb, a synthetic wastewater containing oxyanions and interfering anions in concentrations similar to those in the industrial wastewater, and the industrial wastewater itself, containing also cations. It is clear that for both the synthetic and the real wastewater, the adsorption of Sb in influenced by the occurrence of interfering (oxy)anions, as much more adsorbent is needed to reach low residual Sb concentrations compared to the aqueous solution. From Fig. 6 can also be concluded that, since the curves for the synthetic and the real wastewater coincide, the most important interferences (for Sb mostly other oxyanions) were identified, and that the cations present in the industrial wastewater do not interfere with the adsorption of the oxyanions.

Case Study: Industrial Wastewater

As a case study, the method described in this paper for the adsorption of Mo, Sb and Se, was applied to a real wastewater obtained from Indaver, a waste treatment company in Belgium. The wastewater is the effluent of wet treatment of flue gases from a rotary kiln for industrial waste combustion. Polluting elements in the flue gas stream are captured by scrubbers. Up to now the treatment consists of the following steps. The pH of the highly acidic scrubber effluent is increased from 1 to 10, and cations are removed by coagulation and flocculation. Mercury is removed by precipitation with *trimercaptotriazine* (TMT). Table 5 gives the elemental composition of the scrubber effluent sampled in 2008, before and after the coagulation/flocculation treatment [40]. The treatment of coagulation/flocculation ensures good removal of several cations like iron, calcium and magnesium, complying with local legislation, but the effluent still contains oxyanion forming elements like Mo and Sb. Anions like chloride and sulphate are hardly affected by the treatment.

For this study, a new sample of the acidic scrubber effluent was analysed for the most important elements. Their concentrations are given in Table 6. The pH of the sampled wastewater (pH = 1) was adjusted to the optimal adsorption pH of 3.5 and the wastewater was analysed again. No significant changes in the oxyanion concentrations due to the pH change were observed.

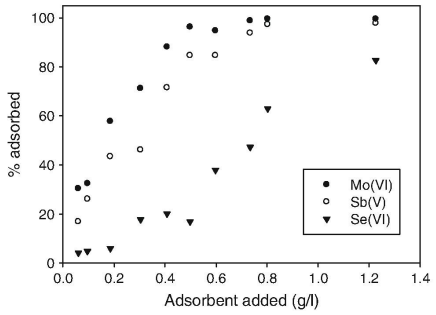

Fig. 5 Adsorption order of Mo, Sb and Se for zeolite supported magnetite; 24 h contact time at 25 °C, oxyanion concentrations 2×10^{-5} mol/l

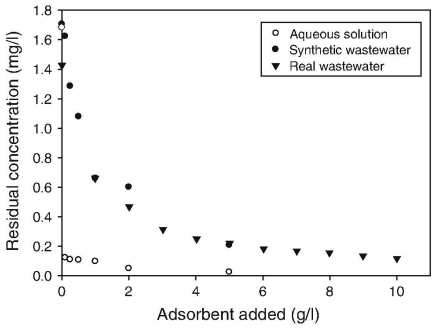

Fig. 6 Adsorption of Sb as a function of initial adsorbent concentration for an aqueous solution containing only Sb, a synthetic wastewater and a real wastewater

Table 5 Elemental composition of the scrubber effluent of a solid waste incinerator before and after coagulation/flocculation treatment [40]

	Before coagulation/ flocculation	After coagulation/ flocculation
pH	1.1	10.3
As (μg/l)	75	<10
Cr (μg/l)	111	<10
Mo (μg/l)	950	460
Sb (μg/l)	1,420	81
Se (μg/l)	175	<10
Fe (mg/l)	19	Not detected
Ca (mg/l)	11,600	Not detected
Mg (mg/l)	160	Not detected
Cl^- (mg/l)	36,300	13,000
$SO4^{2-}$ (mg/l)	4,000	1,500

Table 6 Concentrations of oxyanion forming elements and anions in the studied scrubber effluent

Element/ compound	Concentrations before adsorption	Concentrations after adsorption (20 g/l)
Mo (μg/l)	872	7
Sb (μg/l)	1,661	49
Se (μg/l)	208	49
Cr (μg/l)	108	Not detected
As (μg/l)	812	Not measured
Cl^- (g/l)	24.7	Not measured
SO_4^{2-} (g/l)	17.1	Not measured
PO_4^{3-} (g/l)	Not detected	Not measured

Due to the highly oxidizing conditions of the combustion process, oxyanions are expected to occur in their highest oxidation state in the considered wastewater. This was confirmed by the study of the redox species in the wastewater. Of the total Sb amount, 99 % was recovered after application of the speciation procedure, of which 97 % was Sb(V). 76 % of the initial Se amount was recovered, of which 96 % was in the hexavalent form. This is important information, as Se(VI) is shown to form outer-sphere complexes, whereas the other oxyanions form inner-sphere complexes.

The removal percentages for Mo, Sb and Se from the considered wastewater as a function of increasing adsorbent concentrations (0–20 g/l) are presented in Fig. 7. The adsorption order is similar to the one that was observed in synthetic wastewater containing these three oxyanions (Fig. 5) Mo is adsorbed first, followed by Sb, shown to be present as antimonate. Se, mainly present as selenate and therefore adsorbed via an outer-sphere complex, is largely influenced by the presence of high concentrations of other

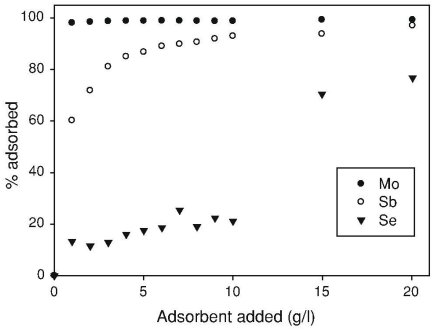

Fig. 7 Removal percentage for Mo, Sb and Se as a function of amount of adsorbent added for the scrubber effluent of a solid waste incinerator, at pH 3.5

anions in the industrial wastewater, like chlorides and sulphates, which are also adsorbed via an outer-sphere complex. Relatively high adsorbent concentrations are needed to adsorb significant amounts of Se. For a concentration of 1 g/l adsorbent, 98 % of Mo and 60 % of Sb originally present in the wastewater is removed. For Se, the removal percentage is lower (13 %) due to the competition of interfering anions. For a concentration of 20 g/l adsorbent, the removal percentages for Mo, Sb and Se increase to 99, 97 and 77 %, respectively; the residual concentrations after adsorption are respectively 7, 49 and 49 μg/l. This shows that zeolite-supported magnetite is a promising material for adsorption of oxyanions Mo, Sb and Se from industrial wastewater; large percentages of these three elements are removed and the residual concentrations are low.

Conclusion

Zeolite-supported magnetite is suitable as an adsorbent for the simultaneous adsorption of oxyanions from wastewater. In this paper it was shown that at the ideal pH (3–3.5), the adsorption capacities for Mo, Sb and Se oxyanions are high (18–23 mg/g). From geochemical modeling, the determination of the adsorption isotherms and the adsorption order, it followed that the adsorption mechanism for the oxyanions of Mo(VI), Sb(III), Sb(V) and Se(IV) is inner-sphere complexation, and for selenate outer-sphere complexation. It was shown that the oxyanions appear in their highest oxidation states in the real wastewater that was studied. The adsorption order on zeolite-supported magnetite is Mo(VI) > Sb(V) > Se(VI), both in a synthetic wastewater containing oxyanions and interfering anions in concentrations similar to those in the industrial wastewater, and in

the industrial wastewater itself. As Mo(VI) and Sb(V) compounds both form inner-sphere complexes, they compete with each other for adsorption places on magnetite. Anions that are commonly present in industrial wastewaters, like sulphates and chlorides, do not interfere with the adsorption of Mo and Sb oxyanions on zeolite-supported magnetite, but they do with selenate as the adsorption mechanism is similar.

By addition of 20 g/l adsorbent to the effluent of wet treatment of flue gases from a rotary kiln for industrial waste combustion, removal efficiencies of 99, 97 and 77 % and residual concentrations of 7, 49 and 49 μg/l were obtained for Mo, Sb and Se respectively.

Acknowledgments Miroslava Vaclavikova (Institute of Geotechnics, Slovakia) and Georgios Gallios (Aristotle University of Thessaloniki, Greece) are acknowledged for provision of the adsorbent. Sander Van Gompel and Stijn Van Ostaeyen are greatly acknowledged for their preparatory work.

References

1. Barceloux, D.G.: Clin. Toxicol. **37**(2), 231–237 (1999)
2. Sheha, R.R., El-Shazly, E.A.: Kinetics and equilibrium modeling of Se(IV) removal from aqueous solutions using metal oxides. Chem. Eng. J. **160**(1), 63–71 (2010)
3. Missana, T., Alonso, U., Scheinost, A.C., Granizo, N., Garcia-Gutierrez, M.: Selenite retention by nanocrystalline magnetite: role of adsorption, reduction and dissolution/co-precipitation processes. Geochim. Cosmochim. Acta **73**(20), 6205–6217 (2009)
4. Nogueira, C.W., Rocha, J.B.T.: Toxicology and pharmacology of selenium: emphasis on synthetic organoSe compounds. Arch. Toxicol. **85**(11), 1313–1359 (2011)
5. Kolbe, F., Weiss, H., Morgenstern, P., Wennrich, R., Lorenz, W., Schurk, K., Stanjek, H., Daus, B.: Sorption of aqueous antimony and arsenic species onto akaganeite. J. Colloid Interface Sci. **357**(2), 460–465 (2011)
6. Jung, C.H., Matsuto, T., Tanaka, N., Okada, T.: Metal distribution in incineration residues of municipal solid waste (MSW) in Japan. Waste Manag. **24**(4), 381–391 (2004)
7. Paoletti, F., Sirini, P., Seifert, H., Vehlow, J.: Fate of antimony in municipal solid waste incineration. Chemosphere **42**(5–7), 533–543 (2001)
8. Paoletti, F.: Behaviour of oxyanions forming heavy metals in municipal solid waste incineration. Ph.D. Thesis, Univ. Stuttgart (2002)
9. Vaclavikova, M., Stefusova, K., Ivanicova, L., Jakabsky, S., Gallios, G.P.: Magnetic zeolite as arsenic sorbent. In: Vaclavikova, M., Vitale, K., Gallios, G.P., Ivanicova, L. (eds.) Water Treatment Technologies for the Removal of High-Toxicity Pollutants. NATO Science for Peace and Security Series C-Environmental Security, pp. 51–59. Springer, Dordrecht (2010)
10. Petrova, T.M., Fachikov, L., Hristov, J.: The magnetite as adsorbent for some hazardous species from aqueous solutions: a review. Int. Rev. Chem. Eng. **3**(2), 134–152 (2011)
11. Mayo, J.T., Yavuz, C., Yean, S., Cong, L., Shipley, H., Yu, W., Falkner, J., Kan, A., Tomson, M., Colvin, V.L.: The effect of nanocrystalline magnetite size on arsenic removal. Sci. Technol. Adv. Mater. **8**(1–2), 71–75 (2007)
12. Gallios, G.P., Vaclavikova, M.: Removal of chromium (VI) from water streams: a thermodynamic study. Environ. Chem. Lett. **6**(4), 235–240 (2008)
13. Loyo, R.L.D., Nikitenko, S.I., Scheinost, A.C., Simonoff, M.: Immobilization of selenite on Fe_3O_4 and Fe/Fe_3C ultrasmall particles. Environ. Sci. Technol. **42**(7), 2451–2456 (2008)
14. Scheinost, A.C., Charlet, L.: Selenite reduction by mackinawite, magnetite and siderite: XAS characterization of nanosized redox products. Environ. Sci. Technol. **42**(6), 1984–1989 (2008)
15. Leuz, A.K., Johnson, C.A.R.: Oxidation of Sb(III) to Sb(V) by O-2 and H_2O_2 in aqueous solutions. Geochim. Cosmochim. Acta **69**(5), 1165–1172 (2005)
16. Kirsch, R., Scheinost, A.C., Rossberg, A., Banerjee, D., Charlet, L.: Reduction of antimony by nano-particulate magnetite and mackinawite. Mineral. Mag. **72**(1), 185–189 (2008)
17. Mulugeta, M., Wibetoe, G., Engelsen, C.J., Lund, W.: Speciation analysis of As, Sb and Se in leachates of cementitious construction materials using selective solid phase extraction and ICP-MS. J. Anal. At. Spectrom. **25**(2), 169–177 (2010)
18. Vaclavikova, M., Jakabsky, S., Hredzak, S.: Magnetic Nanoscale Particles as Sorbents for Removal of Heavy Metal Ions, Vol. 169. Nanoengineered Nanofibrous Materials. Springer, Dordrecht (2004)
19. Verbinnen, B., Block, C., Hannes, D., Lievens, P., Vaclavikova, M., Stefusova, K., Gallios, G., Vandecasteele, C.: Removal of molybdate anions from water by adsorption on zeolite-supported magnetite. Water Environ. Res. **84**(9), 753–760 (2012)
20. Davis, J.A., James, R.O., Leckie, J.O.: Surface ionization and complexation at oxide-water interface.1. Computation of electrical double-layer properties in simple electrolytes. J. Colloid Interface Sci. **63**(3), 480–499 (1978)
21. Davis, J.A., Leckie, J.O.: Surface-ionization adnd complexation at the oxide-water interface.3. Adsorption of anions. J. Colloid Interface Sci. **74**(1), 32–43 (1980)
22. Hayes, K.F., Leckie, J.O.: Mechanism of lead-ion adsorption at the goethite-water interface. ACS Symp. Ser. **323**, 114–141 (1986)
23. Sverjensky, D.A.: Interpretation and prediction of triple-layer model capacitances and the structure of the oxide-electrolyte-water interface. Geochim. Cosmochim. Acta **65**(21), 3643–3655 (2001)
24. Mansour, C., Lefevre, G., Pavageau, E.M., Catalette, H., Fedoroff, M., Zanna, S.: Sorption of sulphate ions onto magnetite. J. Colloid Interface Sci. **331**(1), 77–82 (2009)
25. Jordan, N., Lomenech, C., Marmier, N., Giffaut, E., Ehrhardt, J.J.: Sorption of selenium(IV) onto magnetite in the presence of silicic acid. J. Colloid Interface Sci. **329**(1), 17–23 (2009)
26. Martinez, M., Gimenez, J., de Pablo, J., Rovira, M., Duro, L.: Sorption of selenium(IV) and selenium(VI) onto magnetite. Appl. Surf. Sci. **252**(10), 3767–3773 (2006)
27. Kim, S.S., Min, J.H., Lee, J.K., Baik, M.H., Choi, J.W., Shin, H.S.: Effects of pH and anions on the sorption of selenium ions onto magnetite. J. Environ. Radioact. **104**, 1–6 (2012)
28. Philippini, V., Naveau, A., Catalette, H., Leclercq, S.: Sorption of silicon on magnetite and other corrosion products of iron. J. Nucl. Mater. **348**(1–2), 60–69 (2006)
29. Balistrieri, L.S., Chao, T.T.: Adsorption of selenium by amorphous iron oxyhydroxyde and manganese-dioxide. Geochim. Cosmochim. Acta **54**(3), 739–751 (1990)
30. Hayes, K.F., Leckie, J.O.: Modeling ionic-strength effects on cation adsorption at hydrous oxide-solution interfaces. J. Colloid Interface Sci. **115**(2), 564–572 (1987)
31. Zhang, P.C., Sparks, D.L.: Kinetics of selenate and selenite adsorption desorption at the goethite water interface. Environ. Sci. Technol. **24**(12), 1848–1856 (1990)

32. Rovira, M., Gimenez, J., Martinez, M., Martinez-Llado, X., de Pablo, J., Marti, V., Duro, L.: Sorption of selenium(IV) and selenium(VI) onto natural iron oxides: goethite and hematite. J. Hazard. Mater. **150**(2), 279–284 (2008)
33. Guo, X.J., Wu, Z.J., He, M.C.: Removal of antimony(V) and antimony(III) from drinking water by coagulation-flocculation-sedimentation (CFS). Water Res. **43**(17), 4327–4335 (2009)
34. Gustafsson, J.P.: Modelling molybdate and tungstate adsorption to ferrihydrite. Chem. Geol. **200**(1–2), 105–115 (2003)
35. Ho, Y.S., McKay, G.: Pseudo-second order model for sorption processes. Process Biochem. **34**(5), 451–465 (1999)
36. El-Khaiary, M.I., Malash, G.F., Ho, Y.S.: On the use of linearized pseudo-second-order kinetic equations for modeling adsorption systems. Desalination **257**(1–3), 93–101 (2010)
37. Masel, R.I.: Principles of Adsorption and Reaction on Solid Surfaces. Wiley-Interscience, New York (1996)
38. Leuz, A.K., Monch, H., Johnson, C.A.: Sorption of Sb(III) and Sb(V) to goethite: influence on Sb(III) oxidation and mobilization. Environ. Sci. Technol. **40**(23), 7277–7282 (2006)
39. Frau, F., Addari, D., Atzei, D., Biddau, R., Cidu, R., Rossi, A.: Influence of major anions on As(V) adsorption by synthetic 2-line ferrihydrite. Kinetic investigation and XPS study of the competitive effect of bicarbonate. Water Air Soil Pollut. **205**(1–4), 25–41 (2010)
40. Lievens, P., Block, C., Cornelis, G., Vandecasteele, C., De Voogd, J.C., Van Brecht, A.: Mo, Sb and Se removal from scrubber effluent of a waste incinerator. In: Vaclavikova, M., Vitale, K., Gallios, G.P., Ivanicova, L. (eds.) Water Treatment Technologies for the Removal of High-Toxicity Pollutants. NATO Science for Peace and Security Series C-Environmental Security, pp. 193–202. Springer, Dordrecht (2010)

3.4 Adsorption of Oxyanions from Industrial Wastewater using Perlite-Supported Magnetite

Verbinnen, B., Block, C., Vandecasteele, C. Adsorption of Oxyanions from Industrial Wastewater using Perlite-Supported Magnetite. Submitted to *Water Environment Research*.

P**ublication 5** describes a new adsorbent, developed on the basis of the good characteristics of zeolite-supported magnetite, but with improved coating of magnetite on the support material, perlite. Perlite-supported magnetite is characterized first, and then tested for the simultaneous removal of As, Cr, Mo, Sb and Se oxyanions. The adsorption order, a measure for the strength of adsorption, can be deduced from this test. Perlite-supported magnetite is compared with other commercially available iron oxide adsorbents, and with other comparable (coated iron oxides) adsorbents from literature. Finally, the adsorption of As, Cr, Mo, Sb and Se from the scrubber effluent of an incinerator for hazardous waste is tested.

In this publication an adsorbent is developed that can be used in industrial, continuous applications. The fineness of the magnetite particles ensures a good adsorption capacity, while the good coating ensures the use in adsorption columns. The adsorption capacities are superior to other comparable (coated iron oxides) adsorbents from literature or commercially available adsorbents.

All adsorption experiments were performed by the candidate, and the candidate also prepared the draft paper. C. Block and C. Vandecasteele acted as discussion partners or critical reviewers of the manuscript.

Adsorption of oxyanions from industrial wastewater using perlite-supported magnetite

Bram Verbinnen[1]*, Chantal Block[1], Carlo Vandecasteele[1]

[1]*ProcESS, Process Engineering for Sustainable Systems, Department of Chemical Engineering, University of Leuven, W. De Croylaan 46, 3001 Heverlee, Belgium; e-mail: bram.verbinnen@cit.kuleuven.be.

Abstract

Most studies on oxyanion adsorption focus on their removal from synthetic solutions. It is often claimed that the considered adsorbents can be used to treat real (industrial) wastewaters, but this is seldom tested. Perlite-supported magnetite was characterized first by determining its specific surface area, magnetite content and by examining the coating. Tests on a synthetic solution showed that at the ideal pH values (pH 3-5), the order of adsorption is Mo(VI) > As(V) > Sb(V) > Cr(VI) > Se(VI). Most oxyanions can be removed for more than 75 % removal with an adsorbent dosage of 1 g/l. Furthermore, perlite-supported magnetite has a higher removal efficiency for oxyanions than commercially available adsorbents and comparable adsorbents described in literature. Perlite-supported magnetite is suitable for treating real wastewaters: it can remove several oxyanions simultaneously from the considered industrial wastewater, but the adsorption order changes due to the presence of interfering anions.

Keywords Oxyanions; Adsorption; Industrial wastewater; Perlite-supported magnetite

Introduction

Cations of heavy metals like Pb, Zn, Ni and Cu can easily be removed from wastewater by adsorption, ion exchange or precipitation as their hydroxides at alkaline pH, the latter being the most used method (Blais et al., 1999). Oxyanions like AsO_4^{3-}, CrO_4^{2-}, MoO_4^{2-}, $Sb(OH)_6^-$ and SeO_4^{2-} cannot be precipitated by increasing the pH alone (Cornelis et al., 2008) and therefore, other techniques should be used. Adsorption on iron oxides is an appropriate method and is widely described in literature (Adegoke et al., 2013), but most described methods focus only on the removal of oxyanions from synthetic solutions. These methods might not be applicable as such for the removal of oxyanions from industrial wastewaters, as these also contain anions and other oxyanions that can compete for adsorption with the considered oxyanions.

Competition for adsorption sites usually occurs between adsorbates that are adsorbed

via a similar adsorption mechanism. The two main adsorption mechanisms are inner-sphere complex formation (ionic binding on specific adsorbent sites) and outer-sphere complex formation (electrostatics interactions, adsorbate molecules do not bind directly to the surface, but are placed in the hydration shell). MoO_4^{2-} and $Sb(OH)_6^-$ adsorb via inner-sphere complex formation on iron oxides and SeO_4^{2-} via outer-sphere complex formation (Verbinnen et al., 2013). The adsorption of AsO_4^{3-} is usually considered to happen via inner-sphere complex formation (Mohan and Pittman, 2007), but for the adsorption of CrO_4^{2-} on iron oxides, both inner-and outer-sphere complexes are described (Fendorf et al., 1997; Khaodhiar et al., 2000; Gallios and Vaclavikova, 2008; Adegoke et al., 2013).

The interfering anions for adsorption of individual oxyanions on iron oxides are already described adequately in literature. AsO_4^{3-} and MoO_4^{2-} adsorption on iron oxides is interfered by PO_4^{3-}(Xu et al., 2006; Frau et al., 2010; Verbinnen et al., 2012; Kanematsu et al., 2013). CrO_4^{2-} is interfered by PO_4^{3-} and SO_4^{2-} (Chowdury and Yanful, 2010; Haitao et al., 2011). SO_4^{2-} is competing with SeO_4^{2-} adsorption on iron oxides due to the chemical similarity of both compounds (Fukushi and Sverjensky, 2007; Verbinnen et al., 2013). Not much is known about the competition of anions with $Sb(OH)_6^-$ for adsorption on iron oxides, but Wang et al. (2012) stated that PO_4^{3-}, CO_3^{2-}, SO_4^{2-} or SiO_3^{2-} do not have an influence on the Sb(V) adsorption onto manganite. Besides anions, the main compounds that compete for adsorption are other oxyanions having a similar adsorption mechanism.

Magnetite (Fe_3O_4) is known to be an effective adsorbent for several oxyanions like arsenite and arsenate (Yean et al., 2005; Shipley et al., 2009; Mamindy-Pajany et al., 2011) molybdate (Rovira et al., 2006; Verbinnen et al., 2012), chromate (Gallios and Vaclavikova, 2008; Yuan et al., 2010), selenite and selenate (Martinez et al., 2006; Missana et al., 2009), antimonate and antimonite (Verbinnen et al., 2012). Magnetite is easily synthesized on nanoscale (Yuan et al., 2010; Petrova et al., 2011), which is useful as adsorption capacity increases with decreasing particle size (Yean et al., 2005; Mayo et al., 2007; Petrova et al., 2011). However, small particles inhibit the use of magnetite in continuous wastewater treatment, as nanosized materials cannot be used in an adsorption column, the most widely used continuous adsorption setup (Petrova et al., 2011), due to a large pressure buildup in the column. For column applications, nanosized materials have to be coated on a larger sized carrier material, which allows the use in adsorption columns. Even when the volume of the support material is taken into account and the adsorption capacity is expressed per total bed volume, high adsorption capacities can thus be obtained. Due to the strong specific bonds of most oxyanions with magnetite, desorption of the oxyanions and regeneration of magnetite based adsorbents is not easy at a low cost and the adsorbent should be disposed after use. Therefore, a cheap carrier material is preferred.

In a previous study (Verbinnen et al., 2013) the removal efficiency for MoO_4^{2-}, $Sb(OH)_6^-$, $Sb(OH)_3$, SeO_4^{2-} and SeO_3^{2-} from industrial wastewater by adsorption on zeolite-supported magnetite was

investigated. High adsorption capacities were obtained, but the coating of magnetite onto the zeolite was not optimal, as most of the magnetite was not fixed onto the zeolite, but appeared as chunks next to it. Just like zeolite, perlite is a cheap and readily available material, but nevertheless, perlite is seldom used as coating material for adsorbents.

This paper focuses on the simultaneous adsorption of multiple oxyanions from industrial wastewater by adsorption on perlite-supported magnetite. As the main mechanisms and interferences for adsorption of oxyanions on magnetite are already described in literature, the aim of this paper is 1) to develop a new adsorbent based on the good adsorption characteristics of zeolite-supported magnetite described by Verbinnen et al. (2012, 2013), but with improved coating of magnetite on the carrier material, i.e. perlite, 2) to characterize the adsorbent and investigate the coating and distribution of magnetite on the perlite surface, and to determine optimal pH and adsorption order for the five oxyanions, 3) to compare the performance of perlite-coated magnetite with this of commercially available adsorbents and other similar (coated iron oxides) adsorbents from literature, and 4) to test the simultaneous adsorption of 5 oxyanion forming elements from an industrial wastewater, the scrubber effluent of a waste incinerator.

Methodology

All reagents used were of analytical grade. All experiments were performed at least in duplicate and the averages and standard deviations are reported in the figures.

Magnetite is prepared by mixing equimolar quantities of $Fe^{II}SO_4$ (Acros) and $Fe^{III}Cl_3$ (Merck Eurolab) in a glass beaker while the solution is continuously purged with nitrogen gas to prevent oxidation of reagents or products. A 1M NH_4OH (Fluka) solution is added dropwise to the stirred mixture and nanosized magnetite (size 10 – 40 nm) is formed in the solution and precipitates as clusters with a size ranging between 20 and 900 nm (Vaclavikova et al., 2004). Magnetite is removed from the solution by centrifugation and mixed with perlite (size between 0.4 and 2.4 mm), allowing the magnetite to be fixed onto the perlite. The product is then dried in a vacuum oven at 40 °C. The amount of magnetite that was retained on the perlite was determined by adding concentrated HNO_3 to the adsorbent and boiling it for two h to dissolve the magnetite; the Fe concentration was measured with ICP-MS (Thermo Xi series).

BET analysis was performed on a Micromeritics Tristar 3000 to determine the specific surface area of perlite-supported magnetite. XRD analysis was performed on a Philips PW1830 using monochromated Cu Kα radiation, generated at 45 kV and 30 mA, to determine the quality of the product (percentage of magnetite compared to other possible formed iron oxides). Measurements ranged from $2\theta = 5°$ to 75°, with a step size of 0.02°. SEM analysis (Philips XL 30 ESEM FEG) was performed to check the fixation of magnetite on perlite. The fixation was also checked visually and with the aid of a magnet.

Synthetic solutions of oxyanions were prepared by dissolving $Na_2HAsO_4.7H_2O$ (Sigma-Aldrich), $K_2Cr_2O_7$ (Chem-lab),

$Na_2MoO_4.2H_2O$ (Merck Eurolab), $KSb(OH)_6$ (Fluka) and Na_2SeO_4 (Fluka) to obtain an equimolar mixture (0.02 mmol/l) of As(V), Cr(VI), Mo(VI), Sb(V) and Se(VI). Batch adsorption tests were performed in plastic containers by adding the adsorbent to synthetic or industrial water. The closed containers were placed on a shaking device (Gerhardt Laboshake) and shaken at 160 rpm for 24 h at 25 °C, as contact times up to 22 h (e.g. for Se(IV), Verbinnen et al., 2013) are needed to reach adsorption equilibrium. The pH was varied by adding HNO_3 or NaOH to the water. As, Cr, Mo, Sb and Se concentrations before and after adsorption were determined using ICP-MS after filtration of the water through a 0.45 µm membrane filter (Chromafil).

To compare the adsorbent with other adsorbents for oxyanions that are described in literature, the Langmuir isotherms and the corresponding maximum adsorption capacities for AsO_4^{3-}, CrO_4^{2-} and MoO_4^{2-} were determined. Therefore, 0.5 g/l of the adsorbent was added to solutions with concentrations ranging from 0.5 to 25 mg/l of As(V), Cr(VI) or Mo(VI) at pH 3 and shaken at 160 rpm for 24 h at 25 °C. After measuring the residual concentrations, the Langmuir isotherm was determined for each oxyanion. The removal efficiency of commercially available adsorbents and perlite-supported magnetite was compared for the adsorption of Mo (as an example). To different solutions, each containing 5 mg/l of Mo (as MoO_4^{2-}) at pH 3.1, 1 g/l of the commercially available adsorbents (goethite (Fluka), Fe_2O_3 (Vel) or magnetite (< 5 µm, Sigma-Aldrich), all powders)) was added. The same test was also performed with 1 g/l zeolite-supported magnetite, perlite-supported magnetite and with perlite and lab-synthesized nanoscale magnetite separately. After 24h shaking at 160 rpm on a shaking device, the samples were filtered through a 0.45 µm filter and the residual concentrations were measured with ICP-MS.

An industrial wastewater was obtained from Indaver NV, the largest waste incinerating company in Flanders, Belgium. The wastewater is the acidic effluent (pH 1.1) of wet treatment of flue gases from a rotary kiln for industrial waste incineration. It contains heavy metal cations (of e.g. Cu, Ni, Pb, Zn), and oxyanion forming elements like As, Cr, Mo, Sb and Se. The speciation of As, Sb and Se in the industrial wastewater was done by applying the selective solid phase extraction (SPE) method developed by Mulugeta et al. (2010). Cr speciation was performed by measuring Cr(VI) concentrations spectrophotometrically (Shimadzu 1601) using the diphenylcarbazide method.

Results and discussion

Characterization of the adsorbent

A SEM picture of perlite-supported magnetite is shown in Figure 1A and can be compared with the surface of the zeolite-supported magnetite (Figure 1B) from a previous study (Verbinnen et al., 2013). The normally smooth perlite surface (Mostafa et al., 2011; Sari et al., 2012) is now covered with chunks of magnetite and the covered surface area is much larger than that of zeolite-supported magnetite. The picture of the perlite-supported magnetite is comparable to the picture of Mostafa et al. (2011), who coated perlite with hematite, but their perlite surface seemed less covered.

The magnetite percentage of the perlite-supported magnetite was 13 % and zeolite-supported magnetite consists for 27 % of magnetite. Although zeolite-supported magnetite has a higher magnetite content than perlite-supported magnetite, the SEM pictures showed that the surface of the former is less covered than that of the latter. This is because the coating of magnetite on the zeolite surface is worse than on the perlite surface, and magnetite occurs as chunks next to zeolite, instead of covering the surface. This was confirmed visually, and with the help of a magnet: when the magnet was placed above both adsorbents, chunks of magnetite, but almost no zeolite-supported magnetite adhered to the magnet. For perlite-supported magnetite, the whole adsorbent adhered to the magnet, indicating a good coating of the magnetite to the perlite surface. BET analysis showed that the perlite-supported magnetite has a specific surface area of 55.3 $\pm$ 0.2 m^2/g, compared to 0.02 m^2/g for virgin perlite and 87.3 $\pm$ 0.2 m^2/g for the nanosized magnetite that was used to coat perlite. The perlite-supported adsorbent developed by Mostafa et al. (2011) had a specific surface area of only 9.26 m^2/g, another indication that their perlite surface was less covered.The XRD analysis showed that lab-synthesized magnetite, which was used to coat perlite, consists for 100 % of magnetite. No oxidized species (e.g. hematite) were detected in the analysis.

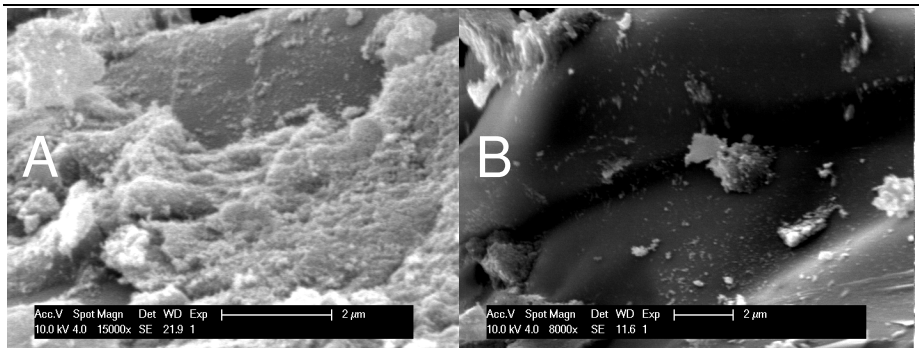

Figure 1 SEM picture of perlite-supported magnetite (A) and zeolite-supported magnetite (B)

Characterization of the industrial wastewater

The concentrations of the oxyanion forming elements Mo, Sb, Se, Cr and As in the scrubber effluent are shown in Table 1, together with their speciation and the concentrations of the possible interfering anions Cl^-, SO_4^{2-} and PO_4^{3-}. PO_4^{3-} is not detected in the wastewater, as most phosphates are not volatile and therefore do not end up in the flue gas. Chlorides and sulphates are detected in relatively high concentrations, as HCl and SO_x are emitted by the incinerator. The speciation shows that the oxyanions occur mainly in their highest oxidation states (as was expected due to the oxidizing conditions in the incinerator), except for Cr, which was present for 90 % as Cr(III) in the wastewater.

Table 1 Concentrations and speciation of (oxy)anions in the untreated industrial wastewater

Element/ Compound	Concentrations before adsorption	Speciation
Mo (µg/l)	872 ± 12	
Sb (µg/l)	1661 ± 33	5 % Sb(III) 95 % Sb(V)
Se (µg/l)	208	18 % Se(IV) 82 % Se(VI)
Cr (µg/l)	108	90 % Cr(III) 10 % Cr(VI)
As (µg/l)	812	7 % As(III) 93 % As(V)
Cl^- (g/l)	24.7	
SO_4^{2-} (g/l)	17.1	
PO_4^{3-} (g/l)	Not detected	

Optimal pH and removal efficiencies

Figure 2 shows the adsorption of As(V), Cr(VI), Mo(VI), Sb(V) and Se(VI) from a synthetic solution containing 0.02 mmol/l of each of the elements as a function of end pH (1-9) for an adsorbent concentration of 0.5 g/l. The oxyanion forming elements were added in their highest oxidation states, as these are the oxidation states that could be expected in the water due to the oxidizing conditions in the incinerator. Table 1 showed that this is true for all elements, except for Cr. In the acidic pH region (pH values between 2 and 5), the adsorption percentages are highest, and the adsorption order is Mo(VI) > As(V) > Sb(V) > Cr(VI) > Se(VI). Previous experiments (Verbinnen et al., 2012) showed that magnetite starts to dissolve in 24 h adsorption experiments at pH values lower than 2. In general, the optimal pH for oxyanion removal is between 3 and 5 and at a pH higher than 5 the adsorption decreases for all elements. As(V) is adsorbed over a broader pH range than the other elements, whereas adsorption of Cr(VI) from the synthetic solution shows a maximum in only a narrow pH range, around pH 5. At pH values higher than 5, the percentage adsorbed decreases for all oxyanions, but this is due to a different cause for oxyanions that adsorb via inner- or outer-sphere complex formation. For oxyanions that adsorb via outer-sphere complex formation (e.g. Se(VI)), the decrease is related to the pH_{pzc} of magnetite, which lies around 6.4-7.2 (Yean et al., 2005; Shipley et al., 2009; Mamindy-Pajany et al., 2011). Oxyanions can adsorb via electrostatic interactions at pH values below this pH_{pzc}. Above this value there is less adsorption because the opposite charges of the adsorbent surface and the adsorbate will repel each other.

For oxyanions that adsorb via inner-sphere complex formation, adsorption can occur at pH values above the pH_{pzc}, and the decrease in adsorption is related to the speciation of the adsorbate. For instance, Mo(VI) is

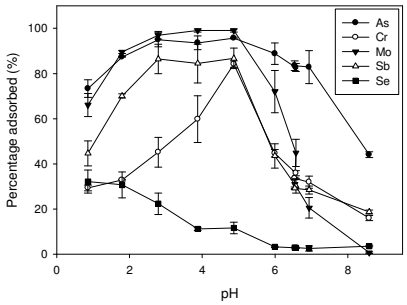

Figure 2 Percentage of Cr(VI), As(V), Se(VI), Mo(VI) and Sb(V) adsorbed from a synthetic solution containing 0.02 mmol/l of each of the five elements as a function of end pH, 24h contact time, amount of adsorbent = 0.5 g/l

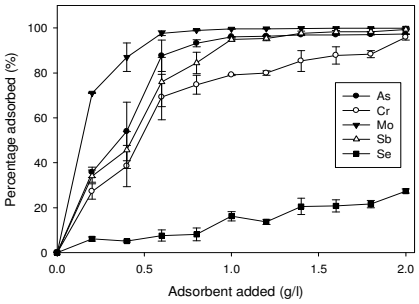

Figure 3 Percentage of As(V), Cr(VI), Mo(VI), Sb(V) and Se(VI) adsorbed from a synthetic solution containing 0.02 mmol/l of each of the five elements, end pH=3.1, 24h contact time

adsorbed on magnetite as $H_2MoO_4.2H_2O$ and Sb(V) as $Sb(OH)_5$ (Verbinnen et al., 2012, 2013).The relative concentrations of these species decrease with increasing pH in favor of more negatively charged species, so that the adsorption of Mo(VI) and Sb(V) decreases.

Figure 3 shows the percentage of As(V), Cr(VI), Mo(VI), Sb(V) and Se(VI) oxyanions adsorbed from the synthetic solution containing equimolar concentrations (0.02 mmol/l) of the 5 elements, as a function of the amount of adsorbent added. All oxyanion forming elements except Se(VI) can be removed for more than 75 % with an adsorbent dosage of only 1 g/l.

At an adsorbent dosage of 0.5 g/l, the adsorption order is of course similar to that shown in Figure 2 at pH 3: magnetite has the highest affinity for Mo(VI), followed by As(V), Sb(V), Cr(VI) and Se(VI).The adsorption order does not change with increasing adsorbent concentrations.

The adsorption order derived from Figures 2 and 3 is in accordance with earlier research on zeolite-supported magnetite (Verbinnen et al., 2013), for which the adsorption order was Mo(VI) > Sb(V) > Se(VI). The low adsorption percentages for Se(VI) can be explained by the formation of weak outer-sphere complexes of Se(VI) with iron (hydr)oxides (Verbinnen et al., 2013). Cr(VI) is after Se(VI) the second worst adsorbed species, but based on Figure 3, it looks plausible that CrO_4^{2-} forms inner-sphere complexes in this case.

Comparison with other adsorbents

To evaluate the performance of perlite-supported magnetite, a comparative test between commercially available adsorbents (goethite, Fe_2O_3 and magnetite, < 5 µm), lab-synthesized adsorbents (zeolite-supported magnetite, perlite-supported magnetite and nanoscale magnetite) and the support material (perlite) was done for the removal of Mo from a synthetic solution.

Table 2 Residual Mo concentrations and removal percentages for commercially available adsorbents, perlite-supported magnetite, zeolite-supported magnetite, perlite and magnetite for the adsorption of Mo from a 5000 µg/l Mo solution at pH 3.1, a contact time of 24h and an adsorbent concentration of 1 g/l

Commercially available adsorbents	Residual concentration (µg/l)	Mo adsorbed (%)
Commercial magnetite	2425	51.5
Commercial goethite	3250	35.1
Commercial Fe(III) oxide	3580	28.6
Perlite	5000	0.0
Lab-synthesized adsorbents		
Nanosized magnetite	3.1	99.94
Perlite-supported magnetite	5.3	99.89
Zeolite-supported magnetite	8.1	99.84

The removal percentages (Table 2) clearly indicate that the lab-synthesized adsorbents perform better than the commercially available adsorbents; the latter adsorb 29 to 52 % of the initial amount of Mo, whereas the former have removal percentages of at least 99.8 % and low residual concentrations. This can probably be attributed to the larger particle size of the commercial magnetite in comparison to the lab-synthesized magnetite. Adsorption by perlite alone is minimal, thus magnetite is mainly responsible for the removal of oxyanions from the water.

Perlite-supported magnetite was also compared with other adsorbents from literature by determining its maximum adsorption capacity at the ideal pH via the Langmuir isotherm. For MoO_4^{2-}, the maximal adsorption capacity for perlite-supported magnetite is 11.9 mg/g, compared to 17.9 mg/g for zeolite-supported magnetite (Verbinnen et al., 2012). Expressed per unit mass of magnetite, the maximum adsorption capacity is 91.5 mg/g for perlite-supported magnetite and 66.3 mg/g for zeolite-supported magnetite, knowing that the former contains 13 % magnetite, and the latter 27 %. For AsO_4^{3-} a maximal adsorption capacity of 7.1 mg/g perlite-supported magnetite was determined. This is higher than the maximal adsorption capacity found by Mostafa et al. (2011), who coated hematite on perlite and obtained a maximal adsorption capacity of 0.39 mg/g for AsO_4^{3-}. The maximal adsorption capacity for CrO_4^{2-} (i.e. predominantly $Cr_2O_7^{2-}$ at pH 3) is 4.2 mg/g perlite-supported magnetite, or 32.3 mg/g expressed per unit mass magnetite, compared to 15.3 mg/g and 11.4 mg/g per unit mass magnetite for montmorillonite- and diatomite-supported magnetite found by Yuan et al. (2009, 2010). Perlite-supported magnetite performs better than commercially available adsorbents or other comparable (coated iron oxides) adsorbents from literature.

Adsorption from industrial wastewater

In Figure 4 the adsorption of As, Cr, Mo, Sb and Se from the industrial wastewater is shown for increasing adsorbent

concentrations. Removal efficiencies for an adsorbent concentration of 10 g/l were 13 % for As, 44 % for Cr, 97 % for Mo, 86 % for Sb and 67 % for Se.

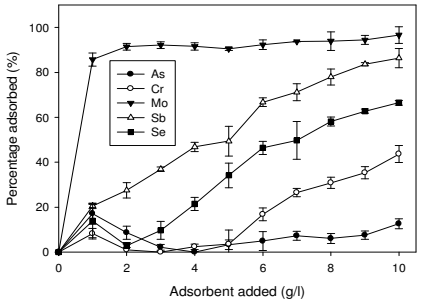

Figure 4 Adsorption of Cr, As, Se, Mo and Sb from industrial wastewater for adsorbent concentrations 1-10 g/l, end pH 3.2 and 24 h contact time

There are some differences in adsorption and adsorption order between synthetic and real wastewater. As is adsorbed as second best from the synthetic water, whereas it is hardly adsorbed from the industrial wastewater, even for an adsorbent concentration of 10 g/l. No satisfactory explanation could be found for this. The removal of Cr from the industrial wastewater is also low compared to the synthetic water. This is because in the synthetic water, Cr is present as Cr(VI), but the speciation of the industrial wastewater showed that Cr is mainly present as Cr(III) in that water. Cr(III) forms weak outer-sphere complexes with magnetite (Shahriari et al., 2013), and therefore the adsorption is hindered by the presence of competing anions, like Cl^- and SO_4^{2-}, which are present in large concentrations in the studied wastewater. On the other hand, the Mo removal percentage is high: more than 80 % of the initial amount of Mo is adsorbed when only 1 g/l of adsorbent is added. As a general conclusion, it can be stated that although adsorption from synthetic solutions showed promising results with high removal percentages at relatively low adsorbent concentrations, higher adsorbent concentrations are needed to obtain comparable removal percentages for the industrial wastewater due to the presence of interfering anions.

Conclusion

Perlite-supported magnetite is easy to synthesize and provides a better coating of magnetite on the carrier material compared to previously described zeolite-supported magnetite. It is capable of removing different oxyanions simultaneously from a synthetic solution, with removal percentages of more than 75 % for AsO_4^{3-}, CrO_4^{2-}, $MoO_4^{2-}$and $Sb(OH)_6^-$ when only 1g/l of the adsorbent was added. The removal of SeO_4^{2-} from the synthetic solution was less effective, as the oxyanion is adsorbed through weaker outer-sphere complexes than the other oxyanions. The simultaneous removal of all 5 oxyanions is optimal at pH values between 3 and 5. The removal efficiency for MoO_4^{2-} using the perlite-supported magnetite is more than 99 %, which is much higher than for commercially available adsorbents (ca. 29 – 52 %), and the maximal adsorption capacity for CrO_4^{2-} and AsO_4^{3-} removal was also superior to other coated iron oxides coated described in literature. The simultaneous removal of the 5 oxyanion forming elements from an industrial wastewater, the scrubber effluent of a waste incinerator requires higher adsorbent concentrations, as interfering anions limit the adsorption capacity for the

considered oxyanions. Good results are obtained for Mo, Sb and Se, whereas the removal percentage of As and Cr is rather low.

Acknowledgements

The authors want to thank Gina Vanbutsele en Johan Martens from the Centre for Surface Chemistry and Catalysis, KU Leuven for the BET analysis. Rieko Adriaens and Jan Elsen from the Department of Earth and Environmental Sciences, KU Leuven, are acknowledged for the XRD analysis. Siavash Darvishmanesh is acknowledged for help with the SEM analysis and Andres Van Brecht from Indaver NV for supplying the industrial wastewater.

References

Adegoke, H. I.; Adekola, F. A.; Fatoki, O. S.; Ximba, B. J. (2013) Sorptive Interaction of Oxyanions with Iron Oxides: A Review. *Pol. J. Environ. Stud.*, 22, 7-24.

Blais, J. F.; Dufresne, S.; Mercier, G. (1999) State of the art of technologies for metal removal from industrial effluents. *Revue des Sciences de l'Eau*, 12, 687-711.

Chowdhury, S. R.; Yanful, E. K. (2010) Arsenic and chromium removal by mixed magnetite-maghemite nanoparticles and the effect of phosphate on removal. *J. Environ. Manage.*, 91, 2238-2247.

Cornelis, G.; Johnson, C. A.; Van Gerven, T.; Vandecasteele, C. (2008) Leaching mechanisms of oxyanionic metalloid and metal species in alkaline solid wastes: A review. *Appl. Geochem.*, 23, 955-976.

Fendorf, S.; Eick, M. J.; Grossl, P.; Sparks, D. L. (1997) Arsenate and chromate retention mechanisms on goethite .1. Surface structure. *Environ. Sci. Technol.*, 31, 315-320.

Frau, F.; Addari, D.; Atzei, D.; Biddau, R.; Cidu, R.; Rossi, A. (2010) Influence of Major Anions on As(V) Adsorption by Synthetic 2-line Ferrihydrite. Kinetic Investigation and XPS Study of the Competitive Effect of Bicarbonate. *Water Air Soil Pollut.*, 205, 25-41.

Fukushi, K.; Sverjensky, D. A. (2007) A surface complexation model for sulfate and selenate on iron oxides consistent with spectroscopic and theoretical molecular evidence. *Geochim. Cosmochim. Acta*, 71, 1-24.

Gallios, G. P.; Vaclavikova, M. (2008) Removal of chromium (VI) from water streams: a thermodynamic study. *Environ. Chem. Lett.*, 6, 235-240.

Haitao, R.; Shaoyi, J.; Yong, L.; Songhai, W.; Yongxu, X.; Yinbao, Z. (2011) Effects of pH and Anion Species on Cr(VI) Removal by Magnetite. *Adv. Mater. Res.*, 233-235, 1055-1058.

Kanematsu, M.; Young, T. M.; Fukushi, K.; Green, P. G.; Darby, J. L. (2013) Arsenic(III, V) adsorption on a goethite-based adsorbent in the presence of major co-existing ions: Modeling competitive adsorption consistent with spectroscopic and molecular evidence. *Geochim. Cosmochim. Acta*, 106, 404-428.

Khaodhiar, S.; Azizian, M. F.; Osathaphan, K.; Nelson, P. O. (2000) Copper, chromium, and arsenic adsorption and equilibrium modeling in an iron-oxide-coated sand, background electrolyte system. *Water Air Soil Pollut.*, 119, 105-120.

Mamindy-Pajany, Y.; Hurel, C.; Marmier, N.; Roméo, M. (2011) Arsenic (V) adsorption from aqueous solution onto goethite, hematite, magnetite and zero-valent iron: Effects of pH,

concentration and reversibility. *Desalination*, 281, 93-99.

Martinez, M.; Gimenez, J.; de Pablo, J.; Rovira, M.; Duro, L. (2006) Sorption of selenium(IV) and selenium(VI) onto magnetite. *Appl. Surf. Sci.*, 252, 3767-3773.

Mayo, J. T.; Yavuz, C.; Yean, S.; Cong, L.; Shipley, H.; Yu, W.; Falkner, J.; Kan, A.; Tomson, M.; Colvin, V. L. (2007) The effect of nanocrystalline magnetite size on arsenic removal. *Sci. Technol. Adv. Mater.*, 8, 71-75.

Missana, T.; Alonso, U.; Scheinost, A. C.; Granizo, N.; Garcia-Gutierrez, M. (2009) Selenite retention by nanocrystalline magnetite: Role of adsorption, reduction and dissolution/co-precipitation processes. *Geochim. Cosmochim. Acta*, 73, 6205-6217.

Mohan, D.; Pittman, C. U. (2007) Arsenic removal from water/wastewater using adsorbents - A critical review. *J. Hazard. Mater.*, 142, 1-53.

Mostafa, M. G.; Chen, Y.-H.; Jean, J.-S.; Liu, C.-C.; Lee, Y.-C. (2011) Kinetics and mechanism of arsenate removal by nanosized iron oxide-coated perlite. *J. Hazard. Mater.*, 187, 89-95.

Mulugeta, M.; Wibetoe, G.; Engelsen, C. J.; Lund, W. (2010) Speciation analysis of As, Sb and Se in leachates of cementitious construction materials using selective solid phase extraction and ICP-MS. *Journal of Analytical Atomic Spectrometry*, 25, 169-177.

Petrova T.M., Fachikov L.; Hristov J. (2011) The magnetite as adsorbent for some hazardous species from aqueous solutions: a review. *Int. Rev. Chem. Eng.*, 3, 134-152.

Rovira, M.; de Pablo, J.; Ignasi Casas, L.; Gimenez, J.; Ciarens, F.; Martinez-Llado, X. (2006) Sorption of molybdenum(VI) on synthetic magnetite. Ghent, Belgium, 2006 12-16 September; Materials Research Society, 143-150.

Sarı, A.; Şahinoğlu, G.; Tüzen, M. (2012) Antimony(III) Adsorption from Aqueous Solution Using Raw Perlite and Mn-Modified Perlite: Equilibrium, Thermodynamic, and Kinetic Studies. *Ind. Eng. Chem. Res.*, 51, 6877-6886.

Shahriari, T.; Bidhendi, G. N.; Mehrdadi, N.; Torabian, A. Effective parameters for the adsorption of chromium (III) onto iron oxide magnetic nanoparticle. *International Journal of Environmental Science and Technology*, 1-8.

Shipley, H. J.; Yean, S.; Kan, A. T.; Tomson, M. B. (2009) Adsorption of arsenic to magnetite nanoparticles: effect of particle concentration, pH, ionic strength, and temperature. *Environ. Toxicol. Chem.*, 28, 509-515.

Vaclavikova, M.; Jakabsky, S.; Hredzak, S. (2004) Magnetic nanoscale particles as sorbents for removal of heavy metal ions. *Nanoengineered Nanofibrous Materials*. 169, 481-486.

Verbinnen, B.; Block, C.; Hannes, D.; Lievens, P.; Vaclavikova, M.; Stefusova, K.; Gallios, G.; Vandecasteele, C. (2012) Removal of Molybdate Anions from Water by Adsorption on Zeolite-Supported Magnetite. *Water Environ. Res.*, 84, 753-760.

Verbinnen B.; Block C.; Lievens P.; Van Brecht A.; Vandecasteele C. (2013) Simultaneous Removal of Molybdenum, Antimony and Selenium Oxyanions from Wastewater by Adsorption on Supported Magnetite. *Waste Biomass Valor.*, 4, 635-645.

Wang, X.; He, M.; Lin, C.; Gao, Y.; Zheng, L. (2012) Antimony(III) oxidation and antimony(V) adsorption reactions on synthetic manganite. *Chemie der Erde - Geochemistry*, 72, Supplement 4, 41-47.

Xu, N.; Christodoulatos, C.; Braida, W. (2006) Modeling the competitive effect of phosphate, sulfate, silicate, and tungstate anions on the adsorption of molybdate onto goethite. *Chemosphere*, 64, 1325-1333.

Yean, S.; Cong, L.; Yavuz, C. T.; Mayo, J. T.; Yu, W. W.; Kan, A. T.; Colvin, V. L.; Tomson, M. B. (2005) Effect of magnetite particle size on adsorption and desorption of arsenite and arsenate. *J. Mater. Res.*, 20, 3255-3264.

Yuan, P.; Fan, M. D.; Yang, D.; He, H. P.; Liu, D.; Yuan, A. H.; Zhu, J. X.; Chen, T. H. (2009) Montmorillonite-supported magnetite nanoparticles for the removal of hexavalent chromium Cr(VI) from aqueous solutions. *J. Hazard. Mater.*, 166, 821-829.

Yuan, P.; Liu, D.; Fan, M. D.; Yang, D.; Zhu, R. L.; Ge, F.; Zhu, J. X.; He, H. P. (2010) Removal of hexavalent chromium Cr(VI) from aqueous solutions by the diatomite-supported/unsupported magnetite nanoparticles. *J. Hazard. Mater.*, 173, 614-621.

4 Conclusions

4.1 Leaching of oxyanions from thermally treated waste

The main research aim for this part of the thesis was to control the formation and subsequent leaching of oxyanions during high temperature processes to increase the recycling potential. Therefore, the first objective was to develop a general framework to explain the increased Cr and Mo leaching that was observed during heating of industrial waste streams. A second objective was to identify the mechanism responsible for the subsequent decrease of leaching at more elevated temperatures. To test the correctness of both mechanisms for real industrial solid wastes, the leaching from synthetic samples was compared to that of two industrial waste streams (the sand fraction of bottom ash from MSW incineration and contaminated sludge).

From the research presented it can be concluded that elevated Cr and Mo leaching is related to the oxidation of Cr(III) and Mo(IV) to their more mobile Cr(VI) and Mo(VI) oxidation states. For Cr, this only occurs in the presence of alkali and alkaline earth salts, and for Mo this is related to the oxidation of MoS_2. Many explanations for the decrease in leaching at more elevated temperatures can be found in literature, but from our research it can be concluded that the most plausible explanation is the formation of an amorphous phase preventing Cr and Mo from leaching. The leaching behavior of Cr and Mo from the sand fraction of bottom ash and contaminated sludge as a function of heating time and temperature showed large similarities with that from synthetic samples, showing that the proposed mechanisms hold true for real situations.

Thermal treatment of solid wastes is beneficial to decrease the leaching of cation forming heavy metals like Cu, Ni, Pb and Zn. For the sand fraction of MSWI bottom ash, the leaching of both cation forming heavy metals and oxyanion forming elements is below the regulatory limits after heating at 400 °C for 30 min. At higher temperatures (at least above 700 °C), at which the leaching of Mo and Cr is decreased again, the sand fraction of bottom ash might be applied as a structured material, e.g. lightweight aggregates, for which several examples exist in literature. The knowledge gained in this thesis can also be applied in the incineration process itself. By adapting conditions like temperature, residence time and/or oxygen level in the incinerator, the ideal conditions for minimal leaching of both cation and oxyanion forming elements from the sand fraction of the bottom ash can be determined. This can be expected to lead to a better quality of the sand fraction of the bottom ash, so that it can be used in or as construction material for applications like road (sub)base, sound barriers, embankments, artificial hills,...

The use of contaminated sludge as construction material is also limited by the leached concentrations of toxic elements exceeding the limit values. Upon heating, there are some conditions for which the leaching is below the regulatory limits for all elements. By heating the material at 400 °C for 30 min, the leaching of the cation forming heavy metals Ni, Cu and Zn is lowered by destruction of the organic material. By heating the sludge for longer residence times or at higher temperatures, the leaching of Cr (and Mo, which is not yet regulated for construction applications in Flanders) starts to increase, which makes the product unsuitable for use in or as construction applications. Heating at 400 °C for 30 min suffices to control the leaching of all toxic elements, but it is doubtful whether this leads to a product that is strong enough to be used as a shaped construction

material. At this temperature, the sludge is not yet sintered and therefore the structural characteristics like compressive strength are low. Nevertheless, it can be used as filler in concrete production or as base material for road construction.

The leached concentrations of the heated sludge can also be lowered to below the regulatory limits by heating at 1100 °C for 30 min. This leads to a sintered, semi-vitrified material that can be used as (lightweight) aggregate in construction. The high temperature obviously implies higher production costs, but the aggregate also has a higher market value than when the sludge would be used as filler.

The production costs for making a structured product from the sludge could be lowered by using the knowledge gained in this thesis. It was demonstrated that by heating the sample under inert atmosphere or by adding $NH_4H_2PO_4$ as additive, the formation and subsequent leaching of Cr(VI) compounds could be avoided. Heating under inert atmosphere prevents oxidation of Cr(III), while the alkali and alkaline earth salts will preferably bind to PO_4^{3-} from $NH_4H_2PO_4$, instead of binding to Cr(III) compounds to give Cr(VI) compounds. Both methods reduce the temperature necessary to produce a structural product that meets the regulatory leaching limit values and can thus lead to an economically more feasible process. For instance the production of bricks, a process that is typically performed at temperatures around 800 °C is not possible with this sludge, as the leaching of Cr exceeds the regulatory limits by 6 – 8 times when heated in ambient atmosphere or without additives. Brick production could be possible by using the demonstrated countermeasures.

4.2 Adsorption of oxyanions from industrial wastewater

The main research aim of this part of the thesis was to remove oxyanions from industrial wastewater in order to increase the options to treat industrial wastewaters. Therefore, the first research objective was to test zeolite-supported magnetite for its removal potential for Mo, Sb and Se oxyanions, to identify the main interfering (oxy)anions and to test the adsorption from industrial wastewater. The other objective was to improve the adsorbent by using the good adsorption characteristics of zeolite-supported magnetite, but improving the coating of magnetite onto the support material, and to test this new adsorbent for its ability to adsorb oxyanions from an industrial wastewater.

The main interferences for adsorption of the oxyanions have been determined and it can be concluded that zeolite-supported magnetite is a good adsorbent for Mo(VI), Sb(III), Sb(V) and Se(IV) oxyanions, and that the adsorption of Se(VI) suffers more from the presence of interfering anions. The adsorption from industrial wastewater showed good results, especially for Mo and Sb. Perlite-supported magnetite developed in this thesis is easy to synthesize, provides a better coating of the magnetite on the support material compared to zeolite-supported magnetite and has higher adsorption capacities than commercially available adsorbents and similar adsorbents (coated iron oxides) previously described in literature. It proved to be a promising material for the removal of oxyanions from industrial wastewaters, as high removal efficiencies were obtained for Mo, Sb and Se from the scrubber effluent of an incinerator for hazardous waste.

It was shown in the literature overview that most, if not all, studies on the removal of oxyanions from waters focus on the removal of one oxyanion from a synthetic solution. When interferences were tested, this was mostly restricted to only one interfering compound. Many studies claim to have found promising adsorption materials with high adsorption capacities that can be used to treat industrial wastewaters, only based on experiments in synthetic solutions. Furthermore, many studies focus on reducing the size of the adsorbent, which can be beneficial in terms of adsorption capacity, but not in terms of practical application in columns. In this thesis, an effort was made to develop and test an adsorbent that can be used for real industrial wastewaters. By coating nanosized magnetite onto a support material, the good adsorption capacity of magnetite was preserved, while the size of the adsorbent as a whole allows its use in adsorption columns. By testing the simultaneous adsorption of multiple oxyanions and interfering anions, it was shown that interferences cannot be neglected. Mo and Sb do not suffer that much from interfering (oxy)anions present in wastewater, but the adsorption of other elements, like As, is strongly influenced by the presence of interferences. It can therefore be concluded that claims, as often been published, that an adsorbent had been developed that can be used to treat industrial wastewaters, are unrealistic, if it has not been tested properly for the considered type of wastewater. Furthermore, this thesis has shown that there is potential for coated adsorbents, as they still have high adsorption capacities and at the same time they can be used in e.g. adsorption columns.

4.3 Recommendations for future research

Due to their chemical similarity, the leaching behavior of Cr and Mo from solid residues after thermal treatment was studied in this thesis. Besides Cr and Mo, also other oxyanion forming elements can show increased concentrations in the leachate after heat treatment, but the

nature of this increase was not yet investigated. As an example, the leaching of Se from contaminated sludge heated at 400 °C is shown in Figure 4.1.

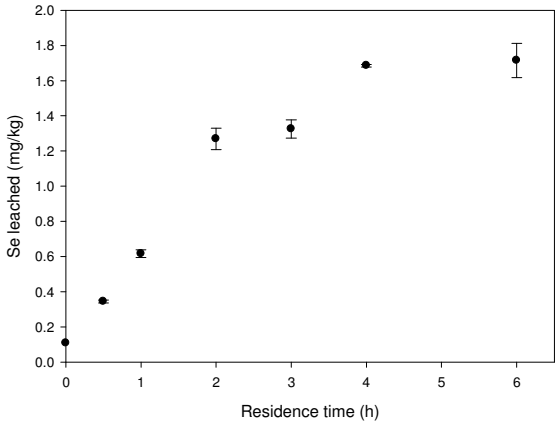

Figure 4.1: Leaching of Se from contaminated sludge heated at 400 °C for 0.5 – 6 h.

Due to the toxicity of oxyanion forming elements like As, Sb and Se, the cause of their leaching behavior (i.e. whether this is also caused by the presence of alkali and alkaline earth salts) should be investigated in order to control their leaching. Other high temperature processes where a similar elevated leaching is observed should be identified, and it should be checked whether the mechanisms for the formation and leaching of oxyanions as described in this work, hold true for these processes too.

Adsorption using perlite-supported magnetite showed good results in removing oxyanions from industrial wastewater. However, the magnetite content of the adsorbent was only 13 %, and improving this content could yield higher adsorption capacities. This could be improved by using other support materials with a higher specific surface area than perlite (0.02 m^2/g). A good coating of magnetite on

the support material stays a key parameter to decide whether a material is suitable as a host material.

A challenge for both leaching of oxyanions from thermally treated waste and adsorption of oxyanions lies in the industrial realization. Some conditions (e.g. heating for 30 min at 400 or 1100 °C) led to thermally treated products for which all leached concentrations were below the regulatory limit values. A further optimization of these conditions (e.g. a longer residence time at a lower temperature, or a lower or higher oxygen level) could optimize the economic feasibility of the process. A more detailed study on the energy consumption (not only for the heating process, but e.g. also for air pollution control in the case of contaminated sludge) could be useful to select the best conditions. Furthermore, heating under inert atmosphere or with addition of $NH_4H_2PO_4$ led to reduced Cr leaching from contaminated sludge. However, when applying this, the leaching of other elements should also be under control. In the case of bottom ash, changing the operational conditions could be beneficial for the leaching of Cr from the sand fraction, but the impact on the leaching of Cr and other elements from the sand and other fractions should also be studied.

For industrial adsorption applications, the cost of the material is important, as magnetite based materials cannot be regenerated at low cost due to the strong inner-sphere complexes that are formed between magnetite and most oxyanions. The effectiveness of adsorption using perlite-supported magnetite should also be compared to the removal efficiency and cost of coprecipitation using $FeCl_3$, as this is the method that is currently used for removal of oxyanions in the tested industrial wastewater. As the adsorption process is irreversible for most oxyanions, this causes the production of a toxic solid waste, and a good solution to dispose this waste should be found. A possible solution could be to include perlite-supported magnetite in

contaminated sludge and heat it at 1100 °C, as it was shown in this thesis that this causes the oxyanions to be immobilized. A last step to come closer to industrial realization is to test the effectiveness of perlite-supported magnetite in a continuous process.

List of publications

Articles in internationally reviewed academic journals

Verbinnen, B., Block, C., Vandecasteele, C. Adsorption of Oxyanions from Industrial Wastewater using Perlite-Supported Magnetite. Submitted to *Water Environment Research*.

Verbinnen, B., Billen, P., Vandecasteele, C. Thermal Treatment of Solid Waste in View of Recycling: Chromate and Molybdate Formation and Leaching Behavior. Submitted to *Waste Management and Research.*

Verbinnen, B., Block, C., Lievens, P., Van Brecht, A., Vandecasteele, C. (2013). Simultaneous Removal of Molybdenum, Antimony and Selenium Oxyanions from Wastewater by Adsorption on Supported Magnetite. *Waste and Biomass Valorization, 4* (3), 635-645.

Verbinnen, B., Billen, P., Van Coninckxloo, M., Vandecasteele, C. (2013). Heating Temperature Dependence of Cr(III) Oxidation in the Presence of Alkali and Alkaline Earth Salts and Subsequent Cr(VI) Leaching Behavior. *Environmental Science & Technology, 47* (11), 5858-63.

Verbinnen, B., Block, C., Hannes, D., Lievens, P., Vaclavikova, M., Stefusova, K., Gallios, G., Vandecasteele, C. (2012). Removal of Molybdate Anions from Water by Adsorption on Zeolite-Supported Magnetite. *Water Environment Research, 84* (9), 753-760.

Cruz Payan, M., Verbinnen, B., Galan, B., Coz, A., Vandecasteele, C., Viguri, J. (2012). Potential influence of CO2 release from a carbon capture storage site on release of trace metals from marine sediment. *Environmental Pollution, 162*, 29-39.

Lievens, P., Verbinnen, B., Bollaert, P., Alderweireldt, N., Mertens, G., Elsen, J., Vandecasteele, C. (2011). Study of composition change and agglomeration of flue gas cleaning residue from a fluidized bed waste incinerator. *Environmental Technology, 32* (14), 1637-1647.

Cornelis, G., Van Gerven, T., Snellings, R., Verbinnen, B., Elsen, J., Vandecasteele, C. (2011). Stability of pyrochlores in alkaline matrices: Solubility of calcium antimonate. *Applied Geochemistry, 26*, 809-817.

Papers at international scientific conferences, published in full in proceedings

Billen, P., Verbinnen, B., Villani, K., De Greef, J., Van Caneghem, J., Vandecasteele, C. (2013). Solidificiation/stabilization of MSWI residues with and without cement: a comparison. In Cossu, R. (Ed.), He, P. (Ed.), Kjeldsen, P. (Ed.), Matsufuji, Y. (Ed.), Reinhart, D. (Ed.), Stegmann, R. (Ed.), *14th International waste management and landfill symposium proceedings*. Sardinia_2013. Cagliari, Italy, 30 September - 04 October 2013 (pp. 1-8) CISA Publisher.

Verbinnen, B., Billen, P., Vandecasteele, C. (2013). Influence of heating conditions on the leaching of Cr and Mo from thermally treated wastes. *Proceedings of the 8th Conference on Sustainable Development of Energy, Water and Environment Systems, September 22-27, 2013*. Sustainable Development of Energy, Water and Environment Systems. Dubrovnik, Croatia, September 22-27, 2013 (pp. 0312/1-0312/8).

Verbinnen, B., Billen, P., Van Coninckxloo, M., Vandecasteele, C. (2012). Cr(VI) formation during thermal treatment of waste. Application to ceramic materials for recycling in construction. In Arm, M. (Ed.), Vandecasteele, C. (Ed.), Heynen, J. (Ed.), Suer, P. (Ed.), Lind, B. (Ed.), *Wascon 2012 conference proceedings*. International Conference on the Environmental and Technical Implications of Construction with Alternative Materials. Gothenburg, Sweden, May 30 - June 1, 2012 (pp. 1-8).

Billen, P., Verbinnen, B., Uccello, R., Van Coninckxloo, M., Vandecasteele, C. (2012). Cr(VI) formation and destruction during incineration of waste. In Nzihou, A. (Ed.), Castro, F. (Ed.), *The 4th international conference on engineering for waste and biomass valorization (WasteEng 2012): Vol. 2*. WasteEng 12. Porto, 10-13 September 2012 (pp. 657-662).

Verbinnen, B., Block, C., Vandecasteele, C. (2012). Adsorption of Mo, Sb and Se oxyanions from industrial wastewater using zeolite-supported magnetite. In Nzihou, A. (Ed.), Castro, F. (Ed.), *Proceedings of the the 4th international conference on engineering for waste and biomass valorization: Vol. 3*. The 4th international conference on engineering for waste and biomass valorization (WasteEng 2012). Porto, 10-13 September 2012 (pp. 880-885).

Lievens, P., Verbinnen, B., Bollaert, P., Alderweireldt, N., Mertens, G., Elsen, J., Vandecasteele, C. (2010). Study of solidification of flue gas cleaning residue from industrial waste incineration in a fluidised bed incinerator. In Giderakos, E. (Ed.), Cossu, R. (Ed.), Stegmann, R. (Ed.), *Hazardous and Industrial waste management - Proceedings*. Hazardous and Industrial waste Management. Chania, Crete, 5-8 October 2010 (pp. 189-190).

Abstracts presented at international scientific conferences, published in proceedings

Verbinnen, B., Billen, P., Vandecasteele, C. (2013). Influence of heating conditions on the leaching of heavy metals and oxyanions from thermally treated waste. The International Solid Waste Association World Congress. Vienna, Austria, 7-11 October 2013.

External reports

Verbinnen, B., Van Caneghem, J., Vandecasteele, C., Block, C., Van Hooste, H. (2010). *MIRA Achtergronddocument 2010 Industrie*, 120 pp.